University of Alberta

Proteomic analysis and the determination of the role of actin cytoskeleton remodelling in Rac-mediated neutrophil primary granule exocytosis

by

Andrea Ngar-Yee Lo

A thesis submitted to the Faculty of Graduate Studies and Research
in partial fulfillment of the requirements for the degree of

Master of Science

in

Experimental Medicine

Department of Medicine

Edmonton, Alberta

Fall 2008

Library and Archives Canada

Published Heritage Branch

395 Wellington Street
Ottawa ON K1A 0N4
Canada

Bibliothèque et Archives Canada

Direction du Patrimoine de l'édition

395, rue Wellington
Ottawa ON K1A 0N4
Canada

Your file Votre référence
ISBN: 978-0-494-47296-5
Our file Notre référence
ISBN: 978-0-494-47296-5

NOTICE:
The author has granted a non-exclusive license allowing Library and Archives Canada to reproduce, publish, archive, preserve, conserve, communicate to the public by telecommunication or on the Internet, loan, distribute and sell theses worldwide, for commercial or non-commercial purposes, in microform, paper, electronic and/or any other formats.

The author retains copyright ownership and moral rights in this thesis. Neither the thesis nor substantial extracts from it may be printed or otherwise reproduced without the author's permission.

AVIS:
L'auteur a accordé une licence non exclusive permettant à la Bibliothèque et Archives Canada de reproduire, publier, archiver, sauvegarder, conserver, transmettre au public par télécommunication ou par l'Internet, prêter, distribuer et vendre des thèses partout dans le monde, à des fins commerciales ou autres, sur support microforme, papier, électronique et/ou autres formats.

L'auteur conserve la propriété du droit d'auteur et des droits moraux qui protège cette thèse. Ni la thèse ni des extraits substantiels de celle-ci ne doivent être imprimés ou autrement reproduits sans son autorisation.

In compliance with the Canadian Privacy Act some supporting forms may have been removed from this thesis.

While these forms may be included in the document page count, their removal does not represent any loss of content from the thesis.

Conformément à la loi canadienne sur la protection de la vie privée, quelques formulaires secondaires ont été enlevés de cette thèse.

Bien que ces formulaires aient inclus dans la pagination, il n'y aura aucun contenu manquant.

Canada

University of Alberta

Library Release Form

Name of Author: Andrea Ngar-Yee Lo

Title of Thesis: Proteomic analysis and the determination of the role of actin cytoskeleton remodelling in Rac-mediated neutrophil primary granule exocytosis

Degree: Master of Science

Year this Degree Granted: 2008

Permission is hereby granted to the University of Alberta Library to reproduce single copies of this thesis and to lend or sell such copies for private, scholarly or scientific research purposes only.

The author reserves all other publication and other rights in association with the copyright in the thesis, and except as herein before provided, neither the thesis nor any substantial portion thereof may be printed or otherwise reproduced in any material form whatsoever without the author's prior written permission.

_____

Signature

University of Alberta

Faculty of Graduate Studies and Research

The undersigned certify that they have read, and recommend to the Faculty of Graduate Studies and Research for acceptance, a thesis entitled **"Proteomic analysis and the determination of the role of actin cytoskeleton remodelling in Rac2-mediated neutrophil primary granule exocytosis"** submitted by **Andrea Ngar-Yee Lo** in partial fulfillment of the requirements for the degree of **Master of Science** in **Experimental Medicine**.

_____
Dr. Paige Lacy
(Supervisor)

_____
Dr. Dean Befus
(Supervisory Committee Member)

_____
Dr. Gary Eitzen
(Supervisory Committee Member)

_____
Dr. David Brindley
(External examiner)

Date: May 31, 2008

Abstract

Neutrophils contain pre-formed anti-microbial compounds within secretory granules, but these also cause damage to neighbouring healthy tissue, especially when neutrophils are overactivated. Rac2 has been shown to regulate primary granule release and F-actin polymerization; however, its pathways remain unknown.

Using proteomic analyses, we identified 9 proteins that showed significant differences in abundance between wild-type and $Rac2^{-/-}$ murine bone marrow neutrophils. Many were actin-associated proteins, leading us to examine the role of actin in human primary granule exocytosis.

We used biochemical assays, confocal and electron microscopy to investigate the effects of various actin-altering drugs on primary granule release. We found there was a requirement for both F-actin polymerization and depolymerization in exocytosis. We also showed that NSC23766, a small molecule Rac inhibitor, blocked primary granule exocytosis and actin remodelling. Interestingly, NSC23766 did not alter superoxide release, suggesting that different GEFs may be involved in superoxide production and exocytosis.

Acknowledgements

To Gord, for everything.

"To whom I owe the leaping delight
That quickens my sense in our wakingtime
And the rhythm that governs the repose of our sleepingtime,
The breathing in unison."
- T.S. Eliot

I would like to thank my parents and my sister for their love, patience and understanding, without which any of this could be written. Mere words cannot describe my gratitude.

A special thanks to my supervisor, Dr. Paige Lacy, for her support, insight and mentorship.

I would also like to extend my appreciation to the members of my supervisory committee, Dr. Dean Befus and Dr. Gary Eitzen for their helpful comments and guidance.

To all members of the Pulmonary Research Group, thank you for your support. I am especially indebted toward Troy Mitchell, Melanie Abel and Candy Tsang for their help, but most of all, their friendship.

Table of Contents

CHAPTER I - INTRODUCTION 1

1.1. The neutrophil 1
1.1.1. Neutrophils and innate immunity *2*
1.1.2. Neutrophils and inflammation *3*
1.2. Role of neutrophils in pulmonary disease 4
1.3. Neutrophil granules 5
1.3.1. Primary (azurophilic) granules *6*
1.3.2. Secondary (specific) granules *8*
1.3.3. Tertiary granules *8*
1.3.4. Secretory vesicles *9*
1.4. Mechanisms of exocytosis 9
1.5. Role of Rho GTPases in exocytosis 10
1.5.1. Regulation of Rho GTPases *11*
1.5.2. Rac2 GEFs *11*
1.5.3. Rac2 and primary granule exocytosis *14*
1.6. Proteomic analyses 15
1.7. Role of actin cytoskeleton in exocytosis 18
1.8. Rationale for the study 19
1.9. Study objective 19

CHAPTER II - MATERIALS AND METHODS 21

2.1. 2D DIGE proteomic analysis of $Rac2^{-/-}$ murine bone marrow neutrophils 21
2.1.1. Animals *21*
2.1.2. Isolation of murine bone marrow neutrophils *21*
2.1.3. Stimulation of BMNs with CB/fMLF *22*
2.1.4. Protein sample preparation *22*
2.1.5. Labelling of BMNs with CyDye™ *23*
2.1.6. 2D gel electrophoresis *24*
2.1.7. Image acquisition and analysis of DIGE gels *24*
2.1.8. Image analysis and spot picking *25*
2.1.9. In-gel tryptic digestion, peptide extraction and mass spectrometric analysis *25*
2.1.10. Protein abundance calculations *26*
2.2. The role of actin cytoskeleton in Rac-mediated exocytosis in human neutrophils 26
2.2.1. Isolation of human peripheral blood neutrophils *26*
2.2.2. Neutrophil stimulation *27*
2.2.3. Measurement of primary granule exocytosis *28*
2.2.4. Confocal microscopy *28*
2.2.5. Rac activation assay *29*
2.2.6. Actin polymerization assay *29*
2.2.7. Measurement of O_2^- release from neutrophils *30*
2.2.8. Flow cytometry *30*
2.2.9. Electron microscopy *31*
2.2.10. Calculations and statistical analysis *32*

CHAPTER III - PROTEOMIC ANALYSIS 33

3.1. Background 33
3.1.1. Ettan DIGE *37*
3.2. Results 40
3.2.1. Differential in-gel analysis *40*
3.2.2. Biological variance analysis *43*
3.2.3. Proteins identified as being differentially expressed in Rac2 KOs *43*
3.3. Summary 56

CHAPTER IV - ROLE OF ACTIN CYTOSKELETON 59

4.1. Background 59
4.2. Results 60
4.2.1. Effects of actin drugs on primary granule exocytosis *60*
4.2.2. Morphological staining of stimulated neutrophils via actin and primary granule staining *62*
4.2.3. The Rac inhibitor NSC 23766 blocks human neutrophil Rac1 and Rac2 activation *66*
4.2.4 The Rac inhibitor NSC23766 inhibits primary granule exocytosis and actin polymerization in response to CB/fMLF and Lat B/fMLF, but not A23187 ..... *68*
4.2.5. NSC23766 inhibits CB/fMLF- and Lat B/fMLF-induced primary granule translocation as visualized via confocal microscopy *70*
4.2.6. Actin polymerization is unaffected by NSC23766 as detected by flow cytometry *74*
4.2.7. Electron microscopy *74*

CHAPTER V - DISCUSSION 82

5.1. Proteomic analysis 82
5.2. Actin cytoskeleton 85
5.3. Outcomes and future directions 89

REFERENCES 93

List of Tables

Table 1. Contents of human neutrophil granules. 7

Table 2. BVA on spots of interest from WT unstimulated versus WT stimulated BMN samples determined from the DIA software module. 44

Table 3. BVA on spots of interest from $Rac2^{-/-}$ unstimulated versus $Rac2^{-/-}$ stimulated BMN samples determined from the DIA software module. 45

Table 4. BVA on spots of interest from WT unstimulated versus $Rac2^{-/-}$ unstimulated BMN samples determined from the DIA software module. 46

Table 5. BVA on spots of interest from WT stimulated versus $Rac2^{-/-}$ stimulated BMN samples determined from the DIA software module. 47

Table 6. Proteins identified by mass spectrometry and their differences in spot abundance compared between WT unstimulated BMN and WT stimulated BMN. 49

Table 7. Proteins identified by mass spectrometry and their differences in spot abundance compared between $Rac2^{-/-}$ unstimulated BMN and $Rac2^{-/-}$ stimulated BMN. 50

Table 8. Proteins identified by mass spectrometry and their differences in spot abundance compared between WT unstimulated BMN and $Rac2^{-/-}$ unstimulated BMN. 51

Table 9. Proteins identified by mass spectrometry and their differences in spot abundance compared between WT stimulated BMN and $Rac2^{-/-}$ stimulated BMN. 52

List of Figures

Figure 1. Rac2 network pathway map. 12

Figure 2. Schematic diagram of neutrophil receptor-mediated signalling pathways in degranulation. 16

Figure 3. Sample preparation for proteomic analysis. 35

Figure 4. Diagram of Amersham Ettan DIGE 2D electrophoresis analysis. 36

Figure 5. Schematic of single gel analysis using the DeCyder DIA module. 38

Figure 6. Schematic of multi-gel analysis using the DeCyder BVA module. 39

Figure 7. Annotated gels from the DIA module of the DeCyder software. 41

Figure 8. Three dimensional histograms of spots of interest taken from the DIA software module. 42

Figure 9. Spots on a WT unstimulated BMN gel were identified as coronin and chitinase. 54

Figure 10. Scatter plots of standardized log abundance of spots of coronin and chitinase taken from the DeCyder BVA module. 55

Figure 11. Comparison of the effects of actin altering drugs on fMLF-stimulated neutrophil exocytosis. 61

Figure 12. Effect of actin altering drugs on CB/fMLF- and A23187-induced primary granule exocytosis. 63

Figure 13. Morphological analysis of stimulated neutrophils pretreated with actin altering drugs. 65

Figure 14. Detection of activated total Rac and Rac2 in stimulated neutrophils. 67

Figure 15. Effect of NSC23766 pre-treatment on neutrophil exocytosis. 69

Figure 16. Determination of actin polymerization activity of neutrophil lysates. 71

Figure 17. Effect of NSC23766 on respiratory burst. 72

Figure 18. Morphological analysis of stimulated neutrophils pretreated with NSC23766. 73

Figure 19. Mean fluorescence of F-actin in neutrophils pre-treated with NSC23766. 75

Figure 20. Electron micrographs of human neutrophils exposed to various stimulatory conditions and actin altering drugs. 76

Figure 21. Granule count of neutrophils exposed to actin altering drugs. 78

Figure 22. Electron micrographs of human neutrophils exposed to various stimulatory conditions and NSC23766. 79

Figure 23. Granule count of neutrophils exposed to NSC23766. 80

Figure 24. Conceptual model of fMLF-induced Rac2 pathway leading to actin polymerization for primary granule translocation to cell periphery. 92

List of Abbreviations

2D-DIGE	two-dimensional fluorescence difference gel electrophoresis
A23187	calcium ionophore
ANOVA	one way analysis of variance
ARDS	acute respiratory disease syndrome
BAL	bronchoalveolar lavage
BMN	bone marrow neutrophils
BP	band pass
BSA	bovine serum albumin
BVA	biological variance analysis
CB	cytochalasin B
CHAPS	3-[(3-cholamidopropyl)dimethylammonio]-1-propanesulfonate hydrate
COPD	chronic obstructive pulmonary disease
DAB	diaminobenzidine
DH	Dbl homology
DIA	differential in-gel analysis
DMSO	dimethyl sulfoxide
DTT	dithiothreitol
EDTA	ethylene diamine tetraacetic acid
ER	endoplasmic reticulum
ERK	extracellular signal-regulated kinase
FBS	fetal bovine serum

fMLF	formyl-methionine-leucine-phenylalanine
FPR	formyl peptide receptor
GAP	GTPase-activating protein
GDI	guanine nucleotide dissociation inhibitor
GDP	guanosine-5'-diphosphate
GEF	guanine nucleotide exchange factor
GST-PBD	glutathione-S-transferase p21 binding domain
GST-RBD	glutathione-S-transferase Rhotekin Rho binding domain
GTP	guanosine-5'-triphosphate
GTPγS	guanosine-5'-O-(3-thiotriphosphate)
HBSS	Hanks' balanced salt solution
HBSS-BG	Hanks' balanced salt solution with BSA and glucose
HEPES	4-(2-hydroxyethyl)-1-piperazineethanesulfonic acid
HPLC	high-performance liquid chromatography
IBD	Institute of Biomolecular Design
IEF	isoelectric focussing
IL	interleukin
$InsP_3$	inositol-1, 4, 5-triphosphate
IPG	immobilized pH gradient
JP	jasplakinolide
Lat B	latrunculin B
LC/MS/MS	liquid chromatography/mass spectrometry/mass spectrometry
LPS	lipopolysaccharide

LTF	lactoferrin
MMP-9	matrix metalloproteinase-9
MPO	myeloperoxidase
NCBI	National Centre for Biotechnology Information
NIH	National Institutes of Health
p38 MAP kinase	p38 mitogen-activated protein kinase
PBS	phosphate buffered saline
PH	pleckstrin homology
PI3K	phosphoinositol-3 kinase
PIP_3	phosphatidylinositol-(3, 4, 5)-P_3
PKC	protein kinase C
PMA	phorbol myristate acetate
Q-Tof	quadrupole time of flight
RPMI	Roswell Park Memorial Institute medium
SDS-PAGE	sodium dodecyl sulfate polyacrylamide gel electrophoresis
SEM	standard error of the mean
TMB	3, 3', 5, 5'-tetramethylbenzidine
VAMP	vesicle-associated membrane protein
WT	wild-type

CHAPTER I - Introduction

1.1. The neutrophil

Neutrophils constitute the majority of circulating blood leukocytes and play a crucial role in innate immunity by their ability to rapidly accumulate in inflamed tissue and clear infection. The main function of neutrophils – to contain and destroy invading microbial pathogens – is achieved through a succession of coordinated responses culminating in phagocytosis and killing of the pathogen. Thus, neutrophils possess a potent arsenal of cytotoxic proteins such as oxidants, proteinases and antimicrobial peptides. Furthermore, they can also release immunoregulatory cytokines and chemokines to recruit other inflammatory cells to the site of infection.

Phagocytosis involves the uptake of microorganisms into intracellular vesicles that fuse with cytoplasmic granules and form phagolysosomes which aid in the digestion of the microorganism. Formation of the phagolysosome also results in the assembly and activation of the respiratory burst NADPH oxidase at the phagolysosome membrane. The oxidase reduces oxygen (O_2) to superoxide free radicals ($\cdot O_2^-$) and releases them into the phagolysosomes where the spontaneous dismutation of two superoxide radicals produces oxygen and hydrogen peroxide (H_2O_2) (1, 2). Granular myeloperoxidase (MPO) catalyzes the oxidation of chloride ions (Cl^-) by H_2O_2 to form hypochlorous acid (HOCl), the neutrophil's most potent bactericidal product (3, 4).

Neutrophils are primarily phagocytic cells, but they can also release cytotoxic compounds into their extracellular environment and it is these toxins, when released *in vivo*, which contribute to tissue injury at sites of infection and inflammation. Neutrophils secrete these mediators through three principal mechanisms: 1) exocytosis of stored,

preformed mediators from granules; 2) release of reactive oxygen species and their by-products; and 3) the formation of lipid mediators by enzymatic actions on membrane or intracellular lipids (5).

1.1.1. Neutrophils and innate immunity

The notion that neutrophils are essential for optimal host response is firmly established as illustrated by the elevated risk of mortality seen in individuals that have depressed numbers of blood neutrophils (6). Similarly, patients with disorders of neutrophils (i.e. neutropenia) suffer from frequent and severe microbial infections, whether it be congenital, cyclic, idiopathic, autoimmune or drug-induced (7). Therefore, optimal numbers (between 40-80% of total leukocytes) of circulating blood neutrophils are necessary to prevent disease and successful microbial incursions. Indeed, neutrophil numbers become elevated in the blood and tissue in response to bacterial, fungal and protozoan infections.

Although low or absent numbers of blood neutrophils can be detrimental to human health, conversely, the overactivation of neutrophils can be fatal. Septic shock and acute respiratory distress syndrome (ARDS) are examples of disorders where extensive neutrophil degranulation occurs and host tissues become irreparably damaged. In sepsis, it is the patient's acute immune response to infection that causes most of the symptoms. There is widespread production of acute phase proteins from the liver, such as C-reactive protein, serum amyloid A, fibrinogen, mannose-binding proteins and complement components (8). These mediators affect the complement system and the coagulation pathways, which then causes damage to the vasculature and the organs (9). This results in hemodynamic consequences and organ deterioration. Even with

immediate and aggressive treatment, many patients succumb to multiple organ failure and eventually die. Likewise, ARDS progresses in a similar manner except it is initially localized to the lungs. ARDS is characterized by inflammation of the lung parenchyma as a result of injury or attack of acute illness. This leads to impaired gas exchange along with the systemic release of inflammatory mediators causing inflammation, hypoxemia and frequently resulting in multiple organ failure then death (10). Thus, homeostasis of neutrophils must be tightly regulated in order to maintain human health.

1.1.2. Neutrophils and inflammation

In normal conditions, inflammation is a protective attempt by the body to ward off impending harm from infection or injury, remove damaged tissue, heal wounds and promote recovery. Inflammation is characterized by *rubor* (redness, due to hyperemia), *tumor* (swelling, due to increased permeability to the microvasculature and leakage of protein into the interstitial space), *calor* (heat, due to enhanced blood flow and metabolic activity of inflammatory mediators), *dolor* (pain, due to changes in the perivasculature and associated nerve endings), and *function laesa* (tissue dysfunction) (11).

In most instances, inflammation is beneficial, but when massive injury, major surgery, serious infection, or chronic diseases occur, the response may be inappropriately elevated, excessively prolonged or insufficient, leading to widespread tissue damage. Neutrophils, unlike other types of inflammatory cells, respond poorly to corticosteroids, the classical treatment for inflammation. In fact, corticosteroids prolong neutrophil survival by inhibiting apoptosis (12), highlighting the need for alternative anti-inflammatory therapies based on the better understanding of the mechanisms in neutrophilic inflammation.

1.2. Role of neutrophils in pulmonary disease

The lungs have the largest marginated pool of neutrophils in the body, likely due to their sentinel role in maintaining sterility in the airways. Neutrophils are one of the first inflammatory cells recruited to the airways in response to either allergen exposure or injury, and are often found in the sputum of patients with chronic asthma (13). Although asthma is typically considered an eosinophilic disease, neutrophils may also play an important role in severe forms as there is a consistent increase of neutrophils in bronchoalveolar lavage (BAL) fluid and in both bronchial and transbronchial biopsies of patients with chronic steroid-dependent severe asthma who remain symptomatic compared to those with milder disease (14). The neutrophil has also been proposed to be a major component of inflammation in asthmatic patients with severe forms of the disease, patients who smoke, and patients with viral exacerbations (14-18).

The role of neutrophils in asthma is quite controversial and remains unclear, but its involvement in chronic obstructive pulmonary disease (COPD) is well established. COPD is characterized by airflow limitation that is not entirely reversible and associated with an abnormal inflammatory response of the lung to noxious particles or gases (19). The chronic airflow limitation is caused by narrowing and blockage of the small airways, reducing expiratory flow, such that a slow forced expiration is required to empty the lungs (20). A primary risk factor for COPD is cigarette smoking. It has been postulated that cigarette smoke induces lung macrophages and epithelial cells to release neutrophil chemokines such as interleukin-8 (IL-8). IL-8 levels have been shown to be higher in the sputum and bronchial washings of smokers compared with controls (21). Cigarette smoke also impairs phagocytosis of neutrophils by macrophages and reduces the ability

of macrophages to ingest apoptotic cells. This leads to a cascade of events that disrupt central and peripheral airways along with terminal airspaces, causing physiologic and clinical abnormalities. There are also higher numbers of neutrophils and CD8+ T lymphocytes infiltrating smooth muscle in the peripheral airways of patients with COPD compared with smokers and nonsmoking controls (22). This chronic inflammation contributes to changes in structure and contractility of airway smooth muscle, and chemokines such as IL-8 may play a role in smooth muscle proliferation and constriction (20).

1.3. Neutrophil granules

Upon stimulation, cytotoxic granule-derived compounds are released into phagosomes or into the extracellular environment. These granules can be characterized into four distinct populations: primary or azurophilic, secondary or specific, tertiary and secretory vesicles (23). Exocytic release of these granules is sensitive to different signalling mechanisms, evident in the hierarchy of release in response to increasing intracellular Ca^{2+} concentrations (24), suggesting granule-specific regulated pathways. Secretory vesicles are mobilized first, followed by tertiary granules (identified by gelatinase) which are mobilized more readily than secondary granules (identified by lactoferrin; LTF), which again are more readily exocytosed than primary granules (identified by MPO) (25). Although distinct in function and form, all granule subtypes share common structural characteristics. These include a phospholipid bilayer membrane and an intra-granular matrix containing proteins intended for exocytosis or delivery to the phagosome (26).

Neutrophil granules are formed continuously during myeloid cell differentiation in the bone marrow. They start to form at the first stage of neutrophil maturation, marked

by the transition from myeloblast to promyelocyte, and continue unabated up to the stage of segmented cells. Granules are believed to be produced by the fusion of immature transport vesicles budding off from the *trans*-Golgi network (27, 28). Vesicles bud off from the *cis*-Golgi to form storage granules at the promyelocyte stage, but interestingly also from the *trans*-Golgi at the myelocyte stage where specific granules are formed (27, 28). It has been suggested there exists a sorting apparatus that is localized in the *cis*-Golgi in promyelocytes and moves to the *trans*-Golgi network in more mature cells (23).

Granules may be sorted on the basis of their size, morphology, electron density or with reference to a given protein (28). The initial classification was based on whether the granule contained peroxidase or not (27), but granules can be further subdivided based on their intra-granular proteins. It is important to note that the development of granules is a continuum; some proteins are shared while others can serve as specific markers for a certain subset, eg. MPO, LTF and gelatinase (23). Therefore, granules are classified from a functional point of view; based on their readiness to exocytose. Table 1 shows the luminal contents of the different types of granules.

1.3.1. Primary (azurophilic) granules

Granule subtypes possess unique luminal contents and of these, primary granules contain the most potent cytolytic enzymes that aid in the elimination of pathogens. However, they also contribute extensively to host tissue damage in inflammatory states when released extracellularly. These early appearing granules were initially defined by their high concentration of MPO and their affinity for the basic dye azure A, hence their alternate name: azurophilic granules (29). Primary granules undergo limited exocytosis in response to stimulation, and they are believed to contribute primarily to the killing and

Table 1. Contents of human neutrophil granules.

Primary (azurophilic) granules)	Secondary (specific) granules	Tertiary (gelatinase) granules	Secretory vesicles
·Acid β-glycerophosphatase	·β_2-Microglobulin	·Acetyltransferase	·Plasma proteins
·Acid mucopolysaccharide	·Collagenase	·β_2-Microglobulin	
·α_1-Antitrypsin	·Cysteine-rich secretory protein-3 (specific granule protein-28)	·Cysteine-rich secretory protein-3	
·α-Mannosidase	·Gelatinase	·Gelatinase B (MMP-9)	
·Azurocidin	·Human cathelicidin protein-18	·Lysozyme	
·Bactericidal permeability increasing protein	·Histaminase		
·β-Glycerophosphatase	·Heparanase		
·β-Glucuronidase	·Lactoferrin		
·Cathepsins	·Lysozyme		
·Defensins	·Neutrophil gelatinase-associated lipocalin		
·Elastase	·Urokinase-type plasminogen activator		
·Lysozyme	·Sialidase		
·Myeloperoxidase	·Transcobalamin-1		
·N-Acetyl-β-glucosaminidase			
·Proteinase-3			
·Sialidase			
·Ubiquitin protein			

Modified from: Farschou, M., and N. Borregaard. 2003. Neutrophil granules and secretory vesicles in inflammation. *Microbes Infect* 5:1317-1327.

degradation of engulfed microorganisms that take place in the phagolysosome (30). Moreover, CD63 is a lysosomal membrane marker specific to primary granules (31). Physically, they are rather large (~0.3 μm in diameter) and electron dense (32, 33).

1.3.2. Secondary (specific) granules

Secondary granules constitute the second major subtype of neutrophil granules. Although smaller than primary granules (~0.1 μm in diameter), they outnumber primary granules by three-fold (32). They are electron-lucent and peroxidase-negative as are tertiary granules, but they are unique in their luminal contents: secondary granules are rich in bacteriostatic compounds while tertiary granules are not. Readiness in exocytosis is also unique; tertiary granules are mobilized more rapidly in response to stimuli. Lactoferrin (LTF), which has bacteriostatic activity against a broad spectrum of Gram-positive and Gram-negative bacteria, is stored mainly in secondary granules. It is bacteriostatic because it impairs bacterial growth by sequestering iron, which is essential for bacteria survival (34). CD66b is a lysosomal membrane marker specific to secondary granules in neutrophils.

1.3.3. Tertiary granules

Tertiary granules primarily serve as a reservoir of matrix-degrading enzymes and membrane receptors needed during neutrophil diapedesis (26, 35). An important marker for tertiary granules is gelatinase B, also known as matrix metalloproteinase-9 (MMP-9). It is stored in an inactive proform that undergoes proteolytic activation during exocytosis. Gelatinase B is capable of degrading structural components of the extracellular matrix and it is believed to be responsible for the destruction of vascular basement membranes and interstitial structures during neutrophil diapedesis and migration (36).

1.3.4. Secretory vesicles

The most rapidly mobilizable intracellular granules in neutrophils are the secretory vesicles. Interestingly, the only known intravesicular content of secretory vesicles is plasma proteins, which suggests that they are endocytic in origin (37). It is their membrane that is important because they are rich in receptors required at the earliest stage of the neutrophil-mediated inflammatory response (38). They are distinguished by their detergent-dependent alkaline phosphatase activity (39, 40).

1.4. Mechanisms of exocytosis

Upon receptor-mediated stimulation of neutrophils, granules are mobilized leading to docking and membrane fusion which can occur intracellularly with phagolysosomes, or extracellularly at the plasma membrane. As stated above, the different subtypes of granules are mobilized in a hierarchal manner, with secretory vesicles showing the highest propensity for exocytosis, followed by tertiary granules, secondary granules and lastly, primary granules (25). Because granules and secretory vesicles appear to be distributed randomly throughout the cytoplasm, this hierarchy must rely on mechanisms that are able to distinguish between the subsets, rather than proximity or quantitative differences. Moreover, compound exocytosis can occur within neutrophils. Compound exocytosis is defined as the fusion of two or more granules prior to their fusion with the plasma membrane (33). As such, there must exist some kind of mechanism that recognizes granule subsets as target membranes to allow for homotypic or heterotypic fusion.

The release of granule-derived mediators from neutrophils occurs by a tightly controlled receptor-coupled mechanism termed "regulated exocytosis" (5). It is thought

to take place in four discrete steps (41). The first step is granule recruitment from the cytoplasm and translocation to the target membrane which is dependent on actin cytoskeleton remodeling and microtubule assembly (42). This is followed by the second step of granule tethering and docking, leading to contact of the outer surface of the granule lipid bilayer membrane with the inner surface of the target membrane. The third step is granule priming that serves to make granules fusion-competent and ensure that they fuse rapidly, in which a reversible fusion pore develops between the granule and the target membrane. The fourth and final step, granule fusion, occurs via the creation and rapid expansion of the fusion pore, leading to total fusion of the granule membrane with the target membrane and expulsion of granular contents.

1.5. Role of Rho GTPases in exocytosis

One particular group of *ras*-related GTPases is the Rho subfamily of GTPases. The three prototypical members of the Rho GTPase subfamily are Rho, Rac, and Cdc42 (43, 44). Rho GTPases act as molecular switches and cycle between two states: an active GTP-bound state and an inactive GDP-bound state. They serve a role in regulating actin cytoskeletal rearrangement and in the release of reactive oxygen species in neutrophils (43, 45). Remodeling of the actin cytoskeleton by Rho GTPases is crucial for allowing a wide range of cellular activities to occur, including regulation of cell polarity, microtubule dynamics, vesicular transport pathways, membrane trafficking, cell growth control and development (43, 46). Evidence that Rho GTPases are critically important in cellular regulation is provided in their availability as substrates for a number of bacterial toxins, including *Clostridium difficile* Toxin B and *Clostridium sordellii* lethal toxin, which inhibit Rho GTPase function by monoglucosylation of specific residues (47, 48).

1.5.1. Regulation of Rho GTPases

Rho GTPases are controlled by three classes of regulatory proteins: GTPase-activating proteins (GAPs), guanine nucleotide dissociation inhibitors (GDIs), and guanine nucleotide exchange factors (GEFs). GAPs and GDIs negatively affect Rho GTPases by promoting the inactive GDP-bound state. GAPs catalyze the relatively slow intrinsic rate of GTP hydrolysis, while GDIs inhibit the exchange of GDP to GTP and also prevent the Rho GTPase from localizing to the plasma membrane (46). GEFs, on the other hand, enhance the rate at which GDP is exchanged for GTP, and also physically link the GTPase to specific subcellular locations where they produce an active signal (46, 49).

All Rho GEFs contain a Dbl homology-Pleckstrin homology (DH-PH) signature domain. Named after the *Dbl* oncogene, the DH domain contains the catalytic core for GDP-to-GTP activity. Dbl was first postulated to have GEF function when it was observed to have 29% sequence identity with the *Saccharomyces cerevisiae* cell division cycle protein Cdc24 (50). Genetic analysis showed that Dbl was indeed upstream of the yeast small GTP-binding protein Cdc42 in the bud assembly pathway, and biochemical analysis also showed that Dbl can release GDP from the human homolog of Cdc42 *in vitro* (50). The PH domain, on the other hand, has no catalytic activity but is important for correct GEF cellular localization as it possesses a phosphatidylinositol-(3, 4, 5)-P_3 (PIP_3) binding domain (49).

1.5.2. Rac2 GEFs

More than 35 GEFs are known to activate Rho GTPases, but only five, thus far, have been observed to interact specifically with mammalian Rac2. These are Swap70, Tiam1, Dock2/Elmo complex, Vav1 and P-Rex1 (Figure 1). Bone marrow mast cells from

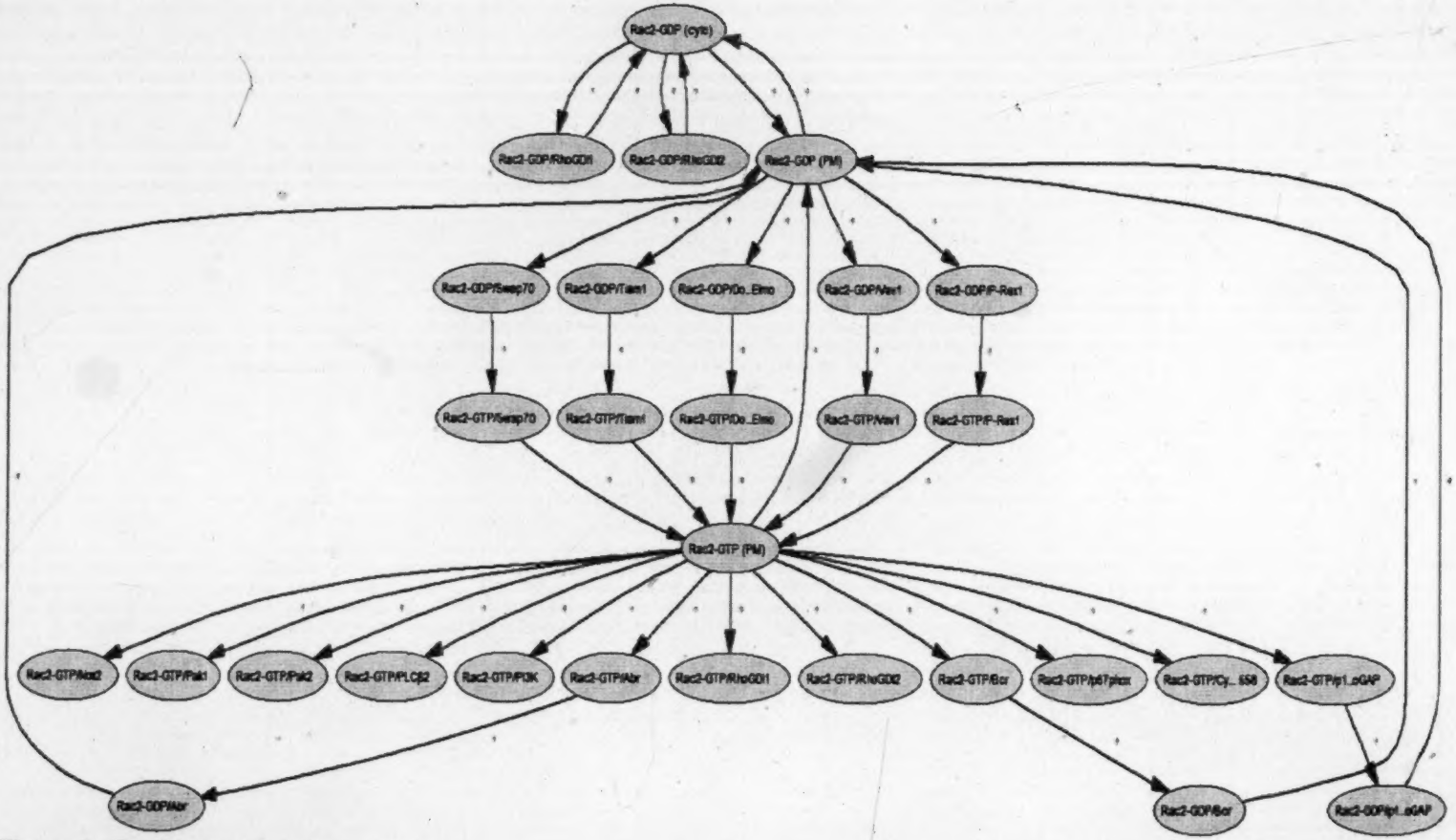

Figure 1. Rac2 network pathway map.

Rac2-GDP is inactive in the cytoplasm and is activated by GEFs into its GTP-bound state. Rac2 is also translocated to the plasma membrane by GEFs. These GEFs include SWAP70, Tiam1, DOCK2/Elmo complex, Vav1 and P-Rex1. The activation of Rac2 leads to many downstream effects. Rac2-GTP can also be inactivated by several RhoGDIs and GAPS such as Abr, Bcr and p190RhoGAP. Modified from: Diebold, B.A. and Bokoch, G.M. 2008. Rac2. *UCSD-Nature Molecule Pages*. (doi:10.1038/mp.a002002.01)

Swap70$^{-/-}$ mice show reduced FcεRI-mediated degranulation, abnormal actin rearrangement, defects in cell migration, impairment of calcium flux, abnormal translocation and activity of Akt kinase, and also improper translocation of Rac1 and Rac2 upon c-kit stimulation (51). Furthermore, the fourfold reduction in chemotaxis of Swap70$^{-/-}$ mast cells toward stem cell factor is similar to that of Rac2$^{-/-}$ mast cells (51, 52). However, Rac2 deficiency in mast cells seems to affect their function more severely than Swap70 deficiency. Sivalenka and Jessberger suggest that other GEFs of Rac may (partially) complement Swap70's function in Rac activation; or perhaps it is the coordinated action of several GEFs on Rac that is required for its full multi-factorial activation (51). Tiam1 can act as a GEF for the three Rac isoforms (Rac1, 2 and 3), but it is more specific for Rac2. Kinetic analysis showed that Tiam1-induced nucleotide exchange of Rac1 and Rac3 were equal, but the GDP dissociation from Rac2 was six-fold faster (53). The Dock2/Elmo complex has also been shown to regulate Rac2 as a GEF. Dock2$^{-/-}$ murine neutrophils show reduced Rac2 activation, defects in chemotaxis and reduction in superoxide production (54). Interestingly, while there were no actin polymerization rate abnormalities, there was poorly focussed distribution of F-actin, thus implicating a role for Dock2 in the polarized accumulation of actin in the leading edge of neutrophil cell motility (54). Likewise, Vav1$^{-/-}$ neutrophils from bone marrow or peritoneal exudates exhibit reductions in superoxide production, F-actin generation and cell motility (55). These defects only occur when the neutrophils are stimulated with fMLF and not with IL-8 or leukotriene B_4 (55). Vav1 also associates with p67^{phox} in order to activate nucleotide exchange on Rac2, which in turn enhances the interaction of Vav1 with p67^{phox}, suggesting a positive feedback loop where p67^{phox} targets Vav1-

mediated Rac activation (56). Finally, P-Rex1 has also been shown to have GEF activity for Rac2. P-Rex1 is synergistically activated by the $\beta\gamma$ subunits of heterotrimeric G proteins and phosphatidylinositol-(3, 4, 5)-P_3 (PIP_3) and is more specific for Rac2 over Rac1 activation (57, 58). In P-Rex1 deficient mouse neutrophils, fMLF-induced F-actin formation, superoxide production and cell migration rate were attenuated although degranulation was not altered (58). These processes are not affected when the neutrophils are stimulated by lipopolysaccharide (LPS) or phorbol myristate acetate (PMA), two pathways that are not Rac dependent (58).

1.5.3. Rac2 and primary granule exocytosis

Our lab has shown that Rac2, a Rho GTPase, has a crucial and selective role in degranulation from neutrophils (59). Gene deletion of Rac2 led to an exocytotic defect in neutrophils, characterized by the complete absence of primary granule MPO release from murine bone marrow neutrophils (59). Interestingly, secondary and tertiary granule exocytosis in response to a variety of stimuli was normal, indicating a selective role for Rac2 in primary granule exocytosis. $Rac2^{-/-}$ neutrophils from KO mice express normal or even elevated levels of Rac1 (60, 61), suggesting that Rac2 serves a distinct role from Rac1 in regulating translocation and exocytosis of granules. This is interesting as Rac1 and Rac2 share 92% identity in their amino acid sequences and mainly differ in the final 10 amino acids of their carboxyl termini (62). Rac1 and Rac2 also show different functions in cell movement, with Rac1 being important for directed migration and Rac2 being important for cell motility (63-65).

Our previous findings suggest that activated Rac2 promotes F-actin-induced granule translocation. $Rac2^{-/-}$ neutrophils failed to translocate primary granules to the cell

membrane during cytochalasin B (CB) and fMLF stimulation (59). This suggests that the defect in primary granule exocytosis in $Rac2^{-/-}$ cells lies in the translocation machinery required for the mobilization of granules toward the membrane for docking and fusion. This most likely requires actin polymerization, and Rac2 has been shown to induce the formation of F-actin which is required for chemotaxis (61). This may be the critical step which allows Rac2 to translocate granules to the cell membrane and direct the movement of neutrophils at the leading edge of the cell (61). Identification of downstream effectors that are responsible for regulating actin cytoskeletal remodeling will be important in identifying the pathway(s) associated with Rac2-mediated primary granule exocytosis (Figure 2).

1.6. Proteomic analyses

Two-dimensional (2D) gel electrophoresis, first described by O'Farrell (66), is based on the separation of proteins according to their charge in the first dimension by isoelectric focussing and size in the second dimension by SDS-PAGE. It is an excellent tool for protein abundance studies and the only technology available for simultaneous resolution of thousands of proteins. It has also been used as a diagnostic tool, comparing protein profiles of diseased tissue versus healthy tissue.

The application of proteomics may provide a novel method to investigate differences in stimulated and non-stimulated neutrophils, potentially enabling the discovery of inflammation-associated targets. In fact, previous studies on proteomic changes within neutrophils exposed to LPS have identified proteins involved in the innate immune response (67). Fessler *et al.* compared the genomic and proteomic profiles of

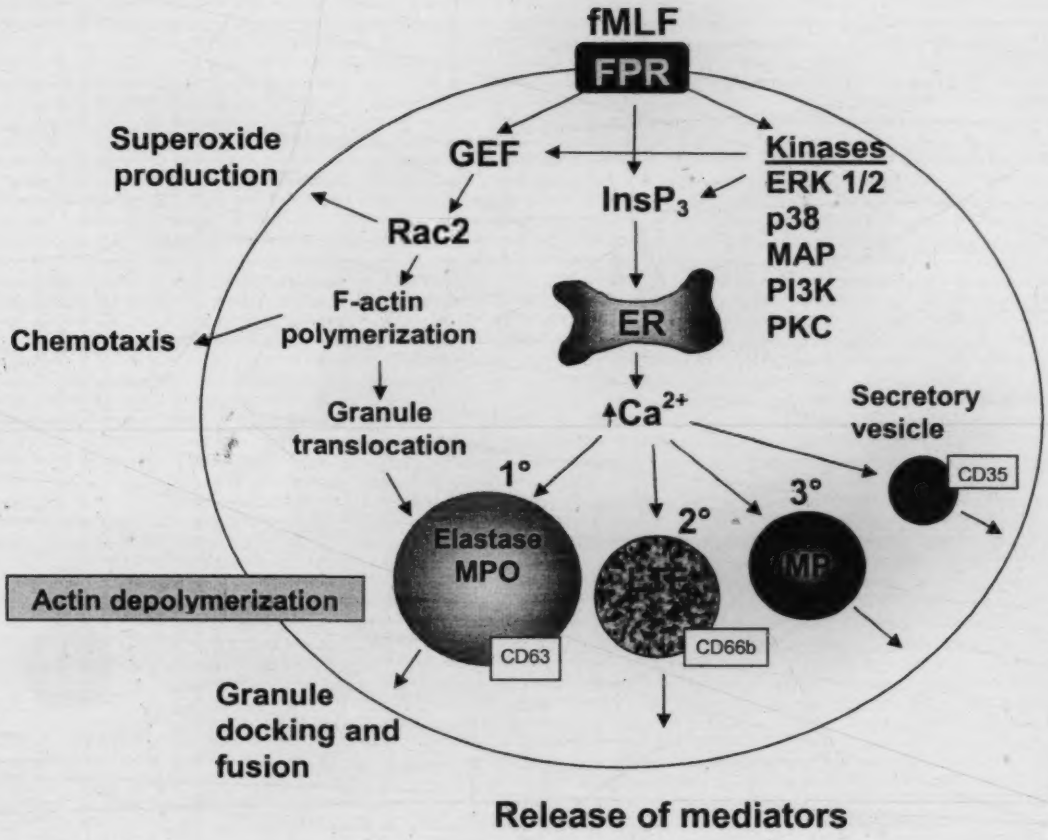

Figure 2. Schematic diagram of neutrophil receptor-mediated signalling pathways in degranulation.

When the chemotactic peptide fMLF binds formyl peptide receptor (FPR), it activates a number of pathways. The Rac2 pathway is specific to primary granule release and superoxide production, while increases in intracellular calcium affect primary, secondary, tertiary and secretory vesicles in a hierarchal manner. Several kinases are also affected although their downstream effectors have yet to be identified. ER, endoplasmic reticulum; ERK, extracellular signal-regulated kinase; fMLF, formyl-Met-Leu-Phe; GEF, guanine exchange factor; $InsP_3$, inositol-1,4,5-triphosphate; LTF, lactoferrin; MMP-9, metalloproteinase-9; MPO, myeloperoxidase; p38 MAP, p38 mitogen-activated protein; PI3K, phosphoinositol-3 kinase; PKC, protein kinase C; VAMP-7, vesicle-associated membrane protein.

Modified from: Lacy P. 2005. The role of Rho GTPases and SNARES in mediator release from granulocytes. *Pharmacol Ther* 107:358-376.

activated human neutrophils after a 4 h challenge with LPS (67). Their results showed an up-regulation of inflammatory regulators (i.e. annexin III), signalling molecules (i.e. Rab-GDP dissociation inhibitor β), several actin fragments and the proteasome β chain, and the down-regulation of various signalling proteins (i.e. Rho GTPase activating protein 1) (67).

The cytoskeleton of neutrophils plays an important role in the maintenance of chemotactic signalling, cell polarity, movement, adhesion and phagocytosis. Intracellular signal transduction occurs at cytoskeleton-stabilized membrane domains and lipid rafts which contain integral membrane proteins (68). Therefore, a study to investigate the proteomic profile of endogenous lipid rafts and proteins was done on bovine neutrophils (69). Proteomic analyses on a subset of plasma membrane skeleton proteins isolated within cholesterol-rich, detergent-resistant membrane fragments identified 19 detergent-resistant membrane proteins including fodrin, myosins, α-actinins, vimentin, F-actin binding proteins, lipid raft-associated integral membrane proteins and intracellular-dually acylated signal proteins (69). Although the difference between bovine and human neutrophils remain unclear, it is important because it shows that variation of proteomic profiles between animal and human neutrophils, and that differences between normal and pathological conditions should be further clarified to provide more tools for the further understanding of the pathophysiology of inflammatory diseases in humans.

Furthermore, proteomic analysis has been used to examine human neutrophil granules. Lominadze *et al.* determined that optimal protein identification in the granule subsets required different methods because of their physical properties and luminal components, also identified 286 proteins from primary, secondary and tertiary granule

subsets (70). By performing a comprehensive analysis of the granule subsets, they provided a basis for understanding the role of exocytosis in neutrophil biology.

1.7. Role of actin cytoskeleton in exocytosis

Actin remodeling is a prime downstream target of activated effector molecules during receptor-mediated exocytosis. The actin cytoskeleton forms a ring-like structure around the periphery in many different kinds of secretory cells (71-73). This is thought to act as a barricade against aberrant granule docking and fusion at the plasma membrane. Therefore, it is logical to presume that the actin cytoskeletal mesh must be disassembled during exocytosis (74). However, some studies in neutrophils suggest that F-actin is normally diffuse in resting neutrophils and only forms into a cortical ring upon fMLF stimulation (65, 75). Other studies also report of actin remodeling to regulate neutrophil migration (76). Chemotaxis towards sites of infection are powered by polarized F-actin formation, with the leading edge of cells showing increased levels of actin polymerization (77). Jog *et al.* showed that secretory vesicles, tertiary, secondary and primary granules associate with decreasing amounts of actin, respectively (78). Furthermore, disruption of the actin cytoskeleton by latrunculin A and cytochalasin D enhanced the rate and extent of fMLF-stimulated tertiary, secondary and primary granule exocytosis, but caused a decrease in CD35 expression for secretory vesicles after an initial increase. This differential association of actin with neutrophil granule subsets suggest that actin may differentially regulate the exocytosis of each subset, although there does not seem to any correlation with graded exocytosis. It is not yet known what the precise relationship is between actin cytoskeletal depolymerization at the cell cortex and Rac2-mediated F-actin formation presumably involved in primary granule exocytosis.

1.8. Rationale for the study

Rac2 is a Rho GTPase that has been shown by our laboratory to be essential for primary granule exocytosis and is known to regulate actin cytoskeletal dynamics (45, 46, 59, 72). Rho GTPases are also known for their role in signalling to the cytoskeleton via kinase cascades (79). Thus, we hypothesize that Rac2 gene deletion leads to aberrant regulation of signalling required for the release of primary granules in neutrophils.

Furthermore, it is well established that actin depolymerization is critical for granule exocytosis from neutrophils. However, Rac2 has been implicated in actin polymerization, leading to the formation of F-actin filaments. We also set out to determine the requirements for actin remodelling in neutrophil exocytosis.

1.9. Study objective

The first aim is a hypothesis-generating study in which we used proteomic analysis to compare receptor-mediated signalling events between WT and $Rac2^{-/-}$ neutrophils to determine alterations in downstream Rac2-dependent pathways.

The second aim is to determine the role of Rac and actin remodelling in neutrophil granule exocytosis. This was done through a comprehensive examination of the effects of actin-altering pharmacological reagents on neutrophils. Imaging was also done to visualize these effects.

My overall hypothesis is that Rac2 is required for signalling events to initiate the mobilization of primary granules to the cell membrane for exocytosis. Some of these events involve actin cytoskeleton remodelling.

These studies provide important insights into the intracellular mechanisms regulating neutrophil mediator release. By increasing our understanding of these

mechanisms, we can contribute to the knowledge base of the role of neutrophils in inflammatory diseases, including severe asthma and COPD, and this may also provide novel anti-inflammatory targets for intervention.

CHAPTER II - Materials and Methods

2.1. 2D DIGE proteomic analysis of $Rac2^{-/-}$ murine bone marrow neutrophils

2.1.1. Animals

Rac2 knockout ($Rac2^{-/-}$) mice were previously generated by targeted disruption of the *rac2* gene and were backcrossed into C57Bl/6 mice for more than 11 generations. Wild type C57Bl/6 (WT) mice were purchased from Charles River Canada (Saint-Constant, PQ). Animals were bred on site and housed under specific pathogen-free conditions and fed autoclaved food and water *ad libitum*. Mice used in these experiments were between 4-8 weeks of age. All experiments complied with the guidelines and policies of the University of Alberta's Animal Care and Use Committee and the Canadian Council on Animal Care.

2.1.2. Isolation of murine bone marrow neutrophils

Bone marrow neutrophils (BMN) were isolated from the femur and tibia of both WT and $Rac2^{-/-}$ mice as previously described (61). The bones were immersed in a solution of 10X HBSS (Invitrogen, Burlington, ON) diluted to 1X with 0.1% BSA (Sigma-Aldrich, Oakville, ON) and 1% glucose (Sigma-Aldrich; HBSS-BG), and then crushed using a mortar and pestle (Canadawide Scientific, Ottawa, ON) to liberate the bone marrow. Large debris was filtered out using a 40 μm nylon cell strainer (BD Biosciences, Mississauga, ON). The filtrate was pelleted at 300*g* for 10 min at 4°C. Percoll (GE Healthcare, Baie d'Urfe, PQ) stock solution was made by mixing 9:1 Percoll to 10X HBSS. Pelleted cells were resuspended in 45% Percoll and then layered onto successive gradients consisting of 3 ml of 81%, 2 ml of 62%, 2 ml of 55% and 2 ml of 50% Percoll in HBSS-BG and centrifuged at 600*g* for 30 min at 10°C. The cell layer between 81%

and 62% was harvested and washed twice in 10 ml of HBSS-BG by centrifugation at 300*g* for 10 min at 4°C. The cells were resuspended in 3 ml of HBSS-BG and were layered over 3 ml of Histopaque-1119 (Sigma-Aldrich), then centrifuged at 600*g* for 30 min at 10°C to remove contaminating erythrocytes. The cell layer between Histopaque and HBSS-BG was collected and washed twice in 10 ml HBSS-BG at 300*g* for 10 min at 4°C. The cells were resuspended in colour-free RPMI-1640 (Invitrogen) and counted by using Kimura stain (for differential count) and Trypan Blue (for viability). There was an average of 3 x 10^7 isolated BMN per mouse. The purity of neutrophils was between 80-85% as assessed by nuclear morphology with the remainder being mononuclear cells, and viability was ≥ 90%.

2.1.3. Stimulation of BMNs with CB/fMLF

BMNs from WT and Rac2$^{-/-}$ mice were separated into two conditions for proteomic analysis: resting and cytochalasin B (CB)/formyl-Met-Leu-Phe (fMLF)-stimulated cells. A total of 6 x 10^8 cells were used for each condition. Resting BMNs were not treated with any stimulus, but incubated at 37°C concurrently with CB/fMLF-stimulated BMNs. For CB/fMLF treatment, cells were primed with 10 μM CB for 5 min at 37°C then stimulated to degranulate with 5 μM fMLF for 15 min at 37°C. Following stimulation, cells were centrifuged at 400*g* for 5 min at 4°. The supernatant was discarded and cell pellets were flash frozen in liquid nitrogen.

2.1.4. Protein sample preparation

The following was done by the Institute of Biomolecular Design (IBD) after we sent frozen samples of unstimulated and CB/fMLF-stimulated BMN from WT and Rac2$^{-/-}$ mice to be analyzed. Protein samples were prepared as previously described (80).

Briefly, thawed cell pellets were solubilized in 0.45 ml of lysis/rehydration buffer (8 M urea, 2% (wt/v) 3-[(3-cholamidopropyl)dimethylammonio]-1-propanesulfonate hydrate (CHAPS), 1% (v/v) immobilized pH gradient (IPG) buffer (GE Healthcare) in the same pH range as the IPG strips to be used, 2 mg/ml DTT), incubated on ice for 30 min followed by a 60 min incubation in an ultrasound bath (Branson Ultrasonics, Danbury, CT) at 4ºC. They were then centrifuged at 14 000*g* for 20 s and the supernatant was loaded onto 24 cm pH 3-10 non-linear (NL) IPG strips (GE Healthcare). An internal standard was also prepared by pooling an equal amount of protein from each experimental condition, thus allowing every protein from all samples to be represented on each gel.

2.1.5. Labelling of BMNs with CyDye™

To determine the differences in protein expression between unstimulated and CB/fMLF-stimulated WT and $Rac2^{-/-}$ BMN, we performed CyDye™ two dimensional fluorescence difference gel electrophoresis (2D-DIGE; GE Healthcare). A maximum loading volume of 40 μg protein from the BMNs were labelled with 200 pmol of the amine reactive dyes Cy™3 or Cy™5 that had been freshly dissolved in anhydrous dimethyl formamide, in buffer containing 10 mM Tris-Cl, pH 8, 5 mM magnesium acetate, 8 M urea and 4% CHAPS. The pooled sample of total protein was labelled with Cy™2. This pooled sample was used as an internal standard that was run on all gels, creating an intrinsic link across all gels. Normalization to the internal standard allowed for the calculation of relative expression of the same protein across gels, which minimized the effect of gel-to-gel variation. Samples were labelled in the dark for 30 min, then terminated by adding 10 nmol lysine. An equal volume of buffer (8 M urea, 4% CHAPS, 2% (v/v) IPG buffer pH

3-10 NL and 2 mg/ml DTT) was added to each reaction. After incubation on ice for 15 min, they were vortexed, then loaded onto 24 cm isoelectric focussing (IEF) strips at a pH range of 3-10.

2.1.6. 2D gel electrophoresis

The samples were loaded via active rehydration at 20 V for 12 h. Active rehydration requires the use of an isoelectric focusing tray while passive rehydration can be done overnight in the rehydration/equilibration tray. The strips were then focussed at 8 kV until a reading of 72 kV x h was reached. Prior to SDS-PAGE, the strips were equilibrated in 15 ml equilibration buffer (50 mM Tris-Cl, pH 8.8, 6 M urea, 30% (v/v) glycerol, 2% SDS, 10 mg/ml DTT) for 15 min on a rocking platform. Strips were positioned on 13% SDS-PAGE gels and electrophoresed at 2.5 W for 30 min, followed by 100 W at 10°C until bromophenol blue dye front reached the gel bottom.

2.1.7. Image acquisition and analysis of DIGE gels

The Typhoon™ 9400 Imager (GE Healthcare) was used to visualize the CyDye™ labelled proteins. Cy™3 images were scanned using a 532 nm laser and an emission filter of 580 nm band pass (BP) 30, Cy™5 images were scanned using a 633 nm laser and an emission filter of 670 nm BP 30, and Cy™2 images were scanned using a 488 nm laser and an emission filter of 520nm BP 40 at 100 μm resolution. Images were cropped before analysis using ImageQuant V 5.2 (GE Healthcare). Image analysis was done using the cross-stain analysis mode of Progenesis Workstation v2004. To exclude background artifacts, gels were manually screened for visible anomalies such as streaks, particulates or background noise after automatic spot detection, and then matched to the annotated reference gel. One reference gel was arbitrarily selected in which all spots

were annotated with reference numbers. All other gels were compared to the reference gel.

2.1.8. Image analysis and spot picking

Gels were stained with Coomassie brilliant blue (PhastGel Blue R; GE Healthcare) for 12 h, then destained in 30% methanol, 10% acetic acid. Scanning was done on a flat bed computer scanner. Image analysis was done using Progenesis Workstation v2002.01 (Nonlinear Dynamics Ltd, Newcastle, UK). Spot picking lists were automatically generated and exported directly to the Ettan™ spot picker robot. Protein spots were excised directly from the gel and, using the circular 1.5 mm picker head and put into 96-well microtitre plates.

2.1.9. In-gel tryptic digestion, peptide extraction and mass spectrometric analysis

In-gel digestion was performed using an automated Mass PREP™ station (Waters Canada, Mississauga, ON) according to the manufacturer's protocol. Briefly, gel plugs were washed with 50 mM ammonium bicarbonate, then 50% (v/v) acetonitrile in water. This was followed with a wash in 100% acetonitrile to dehydrate the gel plugs. The gel plugs were then reduced in 10 mM DTT and alkylated by 50 mM iodoacetamide, followed by overnight digestion with trypsin in 50 mM ammonium bicarbonate (pH 8) at 37°C. Tryptic peptides were extracted using sequential steps of 1% (v/v) formic acid, 2% (v/v) acetonitrile and 50% (v/v) acetonitrile. Liquid chromatography/mass spectrometry/mass spectrometry (LC/MS/MS) on a Micromass Q-ToF-2™ mass spectrometer coupled with a Waters CapLC capillary HPLC (Waters Canada) was used to analyse peptide extracts. Peak lists were developed using Mascot Distiller (v 1.1.1.0). Smoothing was not applied, and the peak-to-noise criterion for peak picking was 2.

Centroids, or the peak's centre of mass, were calculated at peak height of 50% and charge states were calculated using the Q-ToF survey scan and peaks were de-isotoped. Protein identification from the generated MS/MS data was performed using the Mascot search engine (Mascot Daemon 2.0.1, Matrix Science, UK). Parameters used in the search include: the enzyme was specified as trypsin; one missed cleavage was allowed; precursor mass accuracy of ±0.6 Da; fragment ion mass accuracy of ±0.8 Da; fixed and variable modifications were cabamidomethyl (C) and oxidation (M) respectively; and the National Center for Biotechnology Information (NCBI) non-redundant database was searched for matches. The absolute score threshold for individual peptides was examined and only those peptides with a score threshold high enough to warrant identity were used to identify the proteins.

2.1.10. Protein abundance calculations

Protein relative abundance was calculated using the Progenesis software by normalizing the intensity signal measured for a protein spot from each experimental sample (i.e. the gel on which the protein was detected via Cy™3 or Cy™5 labelling) to the intensity signal of the pooled sample (i.e. total protein abundance via Cy™2 labelling).

2.2. The role of actin cytoskeleton in Rac-mediated exocytosis in human neutrophils

2.2.1. Isolation of human peripheral blood neutrophils

Human neutrophils were purified from peripheral blood of healthy donors in accordance with the University of Alberta Health Research Ethics Board requirements for the use of human samples. Briefly, 50-100 ml of peripheral blood was drawn from donors and sedimented in 6% dextran in RPMI-1640 for 30 min at ambient temperature. The leukocyte-rich suspension was collected, layered onto a 15 ml Ficoll-paque (GE

Healthcare) gradient and then centrifuged at room temperature at 400*g* for 30 min to separate out plasma, monocytes/lymphocytes and granulocytes/erythrocytes. After centrifugation, the plasma, monocyte/lymphocyte and Ficoll layers were discarded, and the cell pellet was resuspended in 1.5 ml of sterile deionized water for 20 s to lyse contaminating erythrocytes. Cells were quickly placed in 12 ml of RPMI-1640 containing 5 mM EDTA (Invitrogen; Buffer A) and centrifuged at room temperature at 300*g* for 5 min. The supernatant was discarded and the cell pellet was resuspended in 10 ml RPMI-1640 containing 5 mM EDTA and 2% FBS (Invitrogen). Cells were allowed to rest on ice for 1 h before experiments. Counts using Kimura stain and Trypan Blue indicated ≥ 95% purity of neutrophils and ≥ 99% viability, respectively.

2.2.2. Neutrophil stimulation

Secretion assays were carried out as previously described (59). Briefly, cells were resuspended at 1 x 10^6 cells/ml in RPMI-1640, and aliquots (50 μl) of this cell suspension was added to each well of a 96 v-well microplate (Invitrogen) already containing the respective drug to be examined in RPMI-1640 to a total well volume of 250 μl. Latrunculin B (Lat B; destabilizes F-actin; Calbiochem, San Diego, CA), jasplakinolide (JP; stabilizes F-actin; Calbiochem) and the small molecule Rac inhibitor NSC23766 (Calbiochem) were dissolved in DMSO (Sigma-Aldrich). Neutrophils were pretreated with these drugs for 15 min at 37°C prior to stimulation with 2.5 μM Ca^{2+} ionophore A23187 for 15 min at 37°C or 10 μM CB (Sigma-Aldrich) for 5 min at 37°C then 5 μM fMLF (Sigma Aldrich) for 15 min at 37°C to induce granule exocytosis. At the end of the incubation times, the v-well microplate was placed on ice to stop the reactions, and unstimulated cells were lysed by addition of an equivalent volume of RPMI-1640

containing 0.5% CHAPS (Sigma-Aldrich). The microplate was then centrifuged at 300*g* at 4°C for 6 min to pellet the cells. Supernatant was carefully removed for assay of released granule proteins.

2.2.3. Measurement of primary granule exocytosis

Myeloperoxidase (MPO), an enzyme marker for primary granules, was assayed using 3, 3', 5, 5'-tetramethylbenzidine (TMB; Sigma-Aldrich) in a colorimetric enzyme secretion assay based on a previously established technique (81). Briefly, 150 μl of TMB substrate solution was added to 50 μl of supernatant and incubated in the dark at room temperature for 15-30 min. The reaction was then terminated with 50 μl of 1 M H_2SO_4. Plates were read spectrophotometrically at 450 nm (Molecular Devices, Sunnyvale, CA). Background-corrected absorbance values were divided into the average value from an equivalent number of 0.5% CHAPS-lysed cells to give a percentage of total cellular mediators released.

2.2.4. Confocal microscopy

Neutrophils were prepared by treatment of cells in suspension with the indicated drugs for 15 min, followed by stimulation with A23187, CB/fMLF or fMLF. The suspensions were then fixed in freshly prepared 2% paraformaldehyde (Sigma-Aldrich) in 0.25 M sucrose (Sigma-Aldrich) to maintain cell integrity. Cells were adhered to poly-L-lysine coated glass slides. Cells were then permeabilized with 0.5% Triton X100 in PBS, stained with a 1:500 dilution of anti-CD63 (Serotec, Raleigh, NC) conjugated to Alexa Fluor 488 (Invitrogen) to detect primary granules. A 1:1000 dilution of rhodamine-phalloidin (Invitrogen) was used to stain for F-actin. Images were acquired on an Olympus FV1000 confocal laser scanning microscope (Olympus Canada, Markham, ON)

with a 63X/1.4 NA plan apochromat objective and processed using Fluoview software (Olympus).

2.2.5. Rac activation assay

Activated, or GTP-bound, Rac1 and Rac2 were affinity precipitated from neutrophils lysates using glutathione-S-transferase-tagged p21 binding domain of PAK (GST-PBD) immobilized on GST-affinity beads (82). Lysates were prepared from 8 x 10^6 cells by sonication in 400 μl of H-buffer (20 mM HEPES-KOH, pH 7.5, 1 mM DTT, 5 mM $MgCl_2$, 60 mM NaCl, 1% Triton X-100 + PIC: 1 μg/ml each of leupeptin, pepstatin, antipain and aprotinin, 1 mM phenylmethylsulfonyl fluoride). Cell debris was then removed by centrifugation and 300 μg of lysate was incubated with 30 μg of immobilized GST-PBD beads. These were incubated in 400 μl H-buffer for 30 min at 4°C. The bead pellet was washed four times with H-buffer and resuspended in 45 μl of Laemmli sample buffer. 15 μl of each sample was analyzed by immunoblot for Rac1 (ARC03; Cytoskeleton Inc., Denver, CO) and Rac2 (07-604; Upstate, Waltham, MA) specific antibodies. Immunoblots were detected using IRDye800 fluorescently tagged secondary antibodies (Rockland Immunochemicals, Gilbertsville, PA) and the Odyssey image analysis system (LiCor, Seattle, WA).

2.2.6. Actin polymerization assay

Actin polymerization induced from cellular activity was measured using a previously described pyrene-actin polymerization assay (83). Briefly, 12 μg of purified neutrophils lysates were lysed using 70 μl of lysis buffer (5 mM Tris-Cl, pH 8, 50 mM KCl, 0.2 mM $CaCl_2$, 0.2 mM ATP, 0.17% NP-40, 0.35 mM $MgCl_2$ + PIC). This was then mixed with 50 μl of 12 μM actin polymerization stock mixture containing 35% pyrene-labelled actin

in G-buffer (5 mM Tris-Cl, pH 8, 0.2 mM $CaCl_2$, 0.2 mM ATP) (Cytoskeleton Inc.). Fluorescence intensity readings were recorded every 18 s using a QM-4SE spectrofluorimeter (Ex 360 nm/Em 407 nm, 10 nm bandwidth, 2 s integration) with a four-position heated sample holder set to 30°C (Photon Technologies Inc., London, ON). The pyrene-actin stock mixture was equilibrated for 10 min, test samples were then added and fluorescence measurements were taken for 30 min. Actin polymerization activity (APA) was calculated from polymerization curves by determining the average rate of fluorescence intensity increase for 30 min of reaction time (84) divided by the micrograms of test sample protein (ΔFI/μg). APA values were normalized to untreated resting cells for each experiment with the APA of the lysis alone subtracted.

2.2.7. Measurement of O_2^- release from neutrophils

Production of extracellular O_2^- from neutrophils in suspension was measured using an established technique (85). Briefly, 2 x 10^6 cells were suspended in 1-ml microcuvettes containing supplemented PBS (PBS+), pH 7.4 (with 1.2 mM $MgCl_2$, 5 mM KCl, 0.5 mM $CaCl_2$, 5 mM glucose and 0.1% BSA) and 50 μM ferricytochrome *c* (Sigma-Aldrich) at room temperature. The mixture was blanked at 550 nm in a Beckman DU 640 spectrophotometer (Beckman Instruments, Mississauga, ON) before adding 10 ng/ml phorbol myristate acetate (PMA) or 5 μM fMLF to induce O_2^- production. To test the effects of Rac inactivation, 160 μM of NSC23766 was added to 2 x 10^7 cells/ml in RPMI-1640 and incubated at 37°C for 15 min before stimulation with PMA or fMLF.

2.2.8. Flow cytometry

Neutrophil samples for flow cytometry were prepared and stimulated in similar fashion to those prepared for the *in vitro* actin polymerization assay. Samples were fixed in 4%

paraformaldehyde for 30 min on ice. They were then permeabilized by incubation with 0.5% Triton-X100 in PBS and stained using a 1:500 dilution of anti-CD63 conjugated to Alexafluor-488. F-actin was detected using a 1:1000 dilution of rhodamine-phalloidin. The volume was approximately 500 µl at 10^7 cells/ml for each sample. They were then measured for differences in F-actin fluorescence and granularity via detection of anti-CD63 labelled primary granules.

2.2.9. Electron microscopy

Neutrophils were examined by electron microscopy after drug pre-treatment followed by stimulation as described previously in 2.2.2. The cells were then cooled on ice, centrifuged at 1000*g* for 1 min and fixed overnight in 2.5% glutaraldehyde, 0.1 M cacodylate, pH 7.2 at 4 ° C. Fixed cells were stained with diaminobenzidine (DAB) (5 min incubation in 2.5 mM DAB, 0.02% hydrogen peroxide, 0.1 M cacodylate, pH 7.2 at room temperature) to enhance the density of peroxidase-containing vesicles. The neutrophils were washed three times in 0.1 M cacodylate, pH 7.2, embedded in 1% ultrapure agarose and post-fixed in 0.2% aqueous osmium tetroxide for 1 h at 4°C. After serial dehydration by incubation in 60%, 80%, 95% and 100% ethanol, propylene oxide and 50% propylene oxide epon resin, the samples were embedded in epon resin. Ultra-thin sections were excised from cured resin-embedded cells, mounted on copper coated grids and stained with saturated uranyl acetate and lead citrate. The neutrophils were viewed on a Phillips 410 transmission electron microscope and images were acquired using AnalySIS camera and software.

Neutrophil EM sections were counted for granule numbers. Counts were performed in a blinded manner; that is, images were labelled as A, B, C, etc., and given to

another person unaware of the conditions. Cells that were selected for counting were those that contain multi-lobed nuclei, characteristic of polymorphonuclear neutrophils, and had a minimum section width of 7 μm (86). Since cell preparations were usually >98% pure neutrophils, there were few contaminating cells. Cells used for image acquisition and granule counting did not display nuclear shrinkage or chromatin condensation (i.e. did not appear pycnotic). Granules were counted if they possessed the following characteristics: dark grey or black membrane-bound organelles, electron-dense, peroxidase-containing (i.e. DAB-positive) structures that were not part of the nucleus, with a size ranging 0.2-0.5 μm.

2.2.10. Calculations and statistical analysis

Data was analyzed by one-way statistical analysis of variance (ANOVA) and *post-hoc* analysis was determined by Tukey's post test. The data depicted in figures are means plus or minus the standard error of the mean (± SEM).

CHAPTER III - Proteomic Analysis

3.1. Background

Neutrophil activation promotes the production and release of inflammatory mediators, up-regulation of cell surface adhesion molecules, an increase in migration, infiltration, phagocytosis and degranulation, as well as receptor modifications and signal transduction (87, 88). Neutrophils play an important role in the inflammatory process, and since other leukocyte-derived proteins have been associated with the pathogenesis of this disease, the identification of neutrophilic inflammatory biomarkers may also be useful in diagnosis and treatment. For example, the proteomic profile of macrophages taken from HIV-infected patients with cognitive impairment demonstrated that alterations in the monocyte function corresponded with the onset of HIV-1-associated dementia (89). Moreover, previous studies have used proteomic analyses to investigate proteins undergoing nitration in response to stimuli in inflammatory disease models. Aulak *et al.* identified more than 40 nitrotyrosine-immunopositive proteins, including 30 not previously identified (90). The proteins identified comprise of those related to oxidative stress, apoptosis ATP production and other metabolic functions (90).

The molecular mechanisms that regulate neutrophil exocytosis are poorly understood. Several pathways may be associated with this, including actin cytoskeleton remodelling and protein kinase activation (Figure 2). Rac2 has been previously shown to be important in the regulation of neutrophil primary granule exocytosis (59), but little is known regarding its downstream effectors and how they are perturbed. Gene deletion of Rac2 in mice leads to a loss of chemotactic ability in peripheral blood and bone marrow neutrophils, along with reduced superoxide production in response to fMLF, tumour

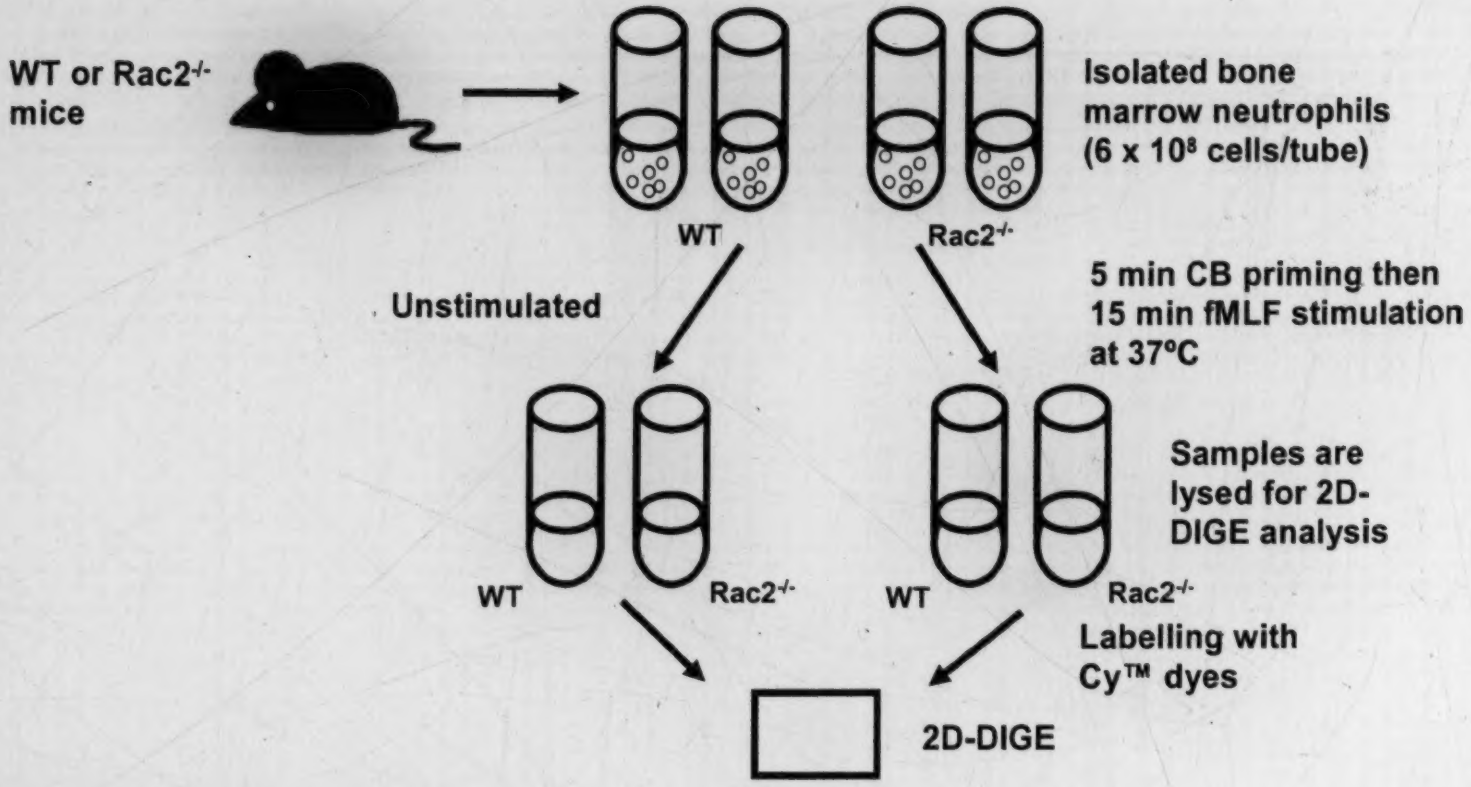

Figure 3. Sample preparation for proteomic analysis.
Bone marrow neutrophils were isolated from C57Bl/6 WT and Rac2-/- mice and separated into two conditions for proteomic analysis: unstimulated and CB/fMLF-stimulated. Unstimulated cells were not treated with anything, but were incubated at 37°C concurrently with the stimulated condition. For the CB/fMLF condition, cells were primed with 10 μM CB for 5 min then 5 μM fMLF for 15 min at 37°C. The samples were then lysed to release proteins and labelled with Cy™ dyes for 2D-DIGE anlysis.

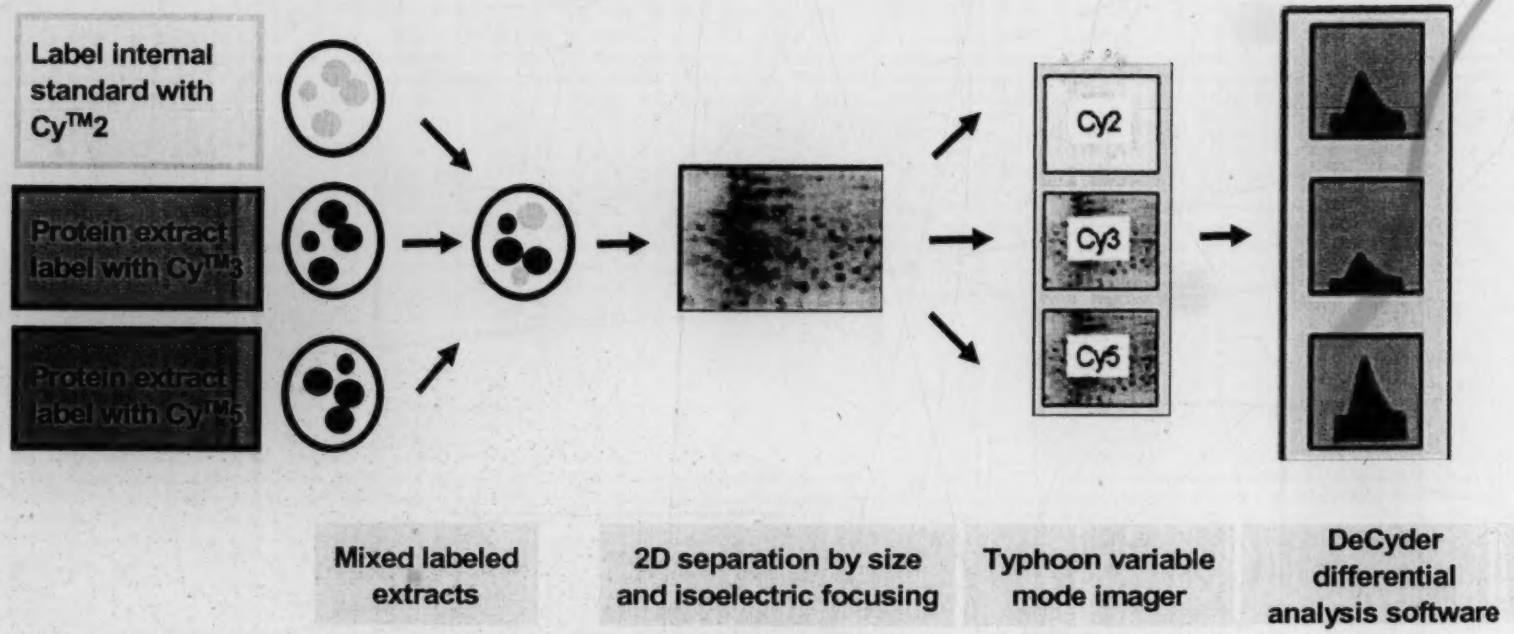

Figure 3. Diagram of Amersham Ettan DIGE 2D electrophoresis analysis.
A total of 40 μg of protein from each sample was labelled with either Cy™3 or Cy™5 dye and internal standard was labelled with Cy™2 dye. The internal standard consists of a pool taken from all the samples. These were then run on a single gel, separating them by size and isoelectric focusing. The fluorescent gel was then imaged at different wavelengths and algorithms applied using the DeCyder DIA module software to be examined for spot differences.

the samples within the experiment. This created an image that is the average of all experimental samples, with all proteins in the experiment represented. By doing so, we are able compare each protein spot to its representative within the internal standard on the same gel to produce a ratio of relative protein levels, effectively removing the system gel-to-gel variation. We were interested in spots that changed significantly in abundance between WT and $Rac2^{-/-}$ samples. Spots of interest were then identified by MS and compared to a database of known protein sequences and masses. Figures 5 and 6 shows a flowchart outlining how we characterized the proteome of BMN from unstimulated or CB/fMLF-stimulated WT or $Rac2^{-/-}$ mice using the DeCyder software. We predicted that granule proteins will decrease in abundance following stimulation by CB/fMLF, while other molecules may increase in concentration. Furthermore, these same proteins were predicted to be significantly altered in $Rac2^{-/-}$ neutrophils compared with WT cells. The purpose of this study was to generate a database of protein abundance changes in WT and $Rac2^{-/-}$ neutrophils, and to further characterize identified proteins with functional studies.

3.1.1. Ettan DIGE

The DeCyder DIA module processes images from a single gel, performs spot detection and spot quantitation. This is accomplished using algorithms to detect spots on a cumulative image derived from merging three individual images from one in-gel linked image set. The co-detection ensures that all spots are represented in all the images processed. The DIA module then quantitates spot protein abundance for each image and expresses it as a ratio, indicating changes in expression levels by direct comparison of corresponding spots. The ratio is then used for protein spot quantitation against the internal standard to allow for accurate inter-gel protein spot comparisons. This data is

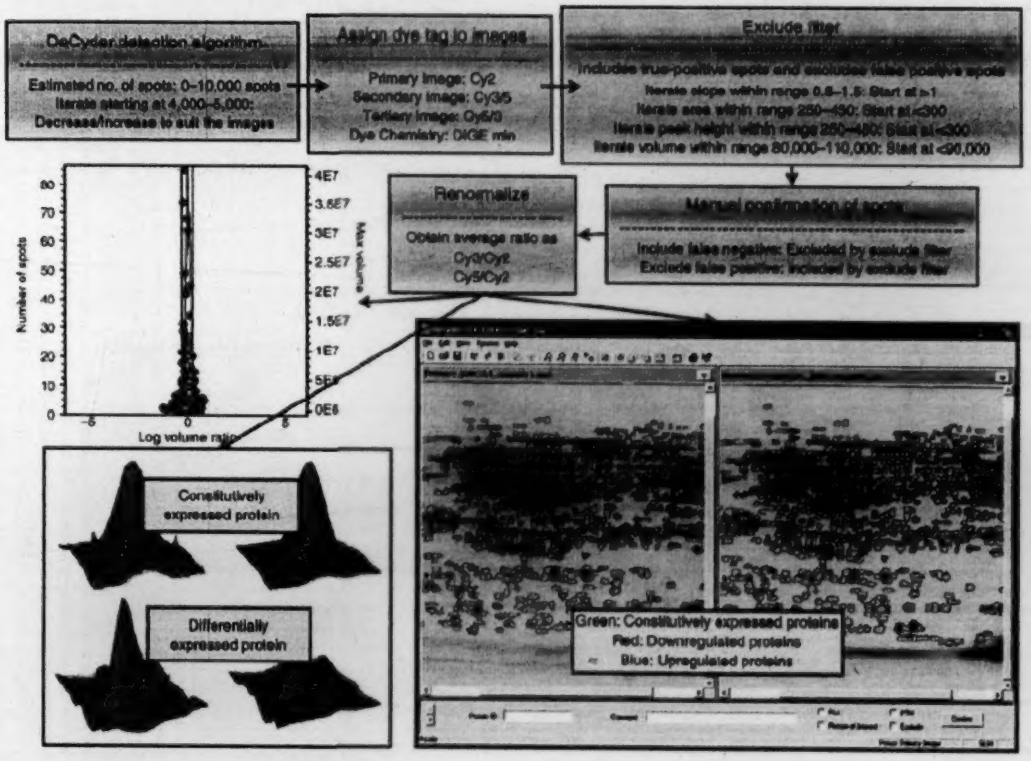
DeCyder detection algorithm
Estimated no. of spots: 0–10,000 spots
Iterate starting at 4,000–5,000:
Decrease/increase to suit the images
Assign dye tag to images
Primary image: Cy2
Secondary image: Cy3/5
Tertiary image: Cy5/3
Dye Chemistry: DIGE min
Exclude filter
Includes true-positive spots and excludes false positive spots
Iterate slope within range 0.8–1.5: Start at >1
Iterate area within range 250–450: Start at <300
Iterate peak height within range 250–450: Start at <300
Iterate volume within range 80,000–110,000: Start at <90,000
Manual confirmation of spots
Include false negative: Excluded by exclude filter
Exclude false positive: Included by exclude filter
Renormalize
Obtain average ratio as
Cy3/Cy2
Cy5/Cy2
Number of spots
Log volume ratio
Constitutively expressed protein
Differentially expressed protein
Green: Constitutively expressed proteins
Red: Downregulated proteins
Blue: Upregulated proteins

Figure 5. Schematic of single gel analysis using the DeCyder DIA module.
A single gel comprising of three images is processed for spot co-detection. The spot volumes are normalized to the normalization pool: Cy™3/Cy™2 and Cy™5/Cy™2. After normalization, Cy™3/Cy™5 volume ratios are generated.
First, DeCyder uses its detection algorithms to estimate the number of spots. Then dye tags are assigned to the images. The primary images are usually the internal standard while the secondary and tertiary images are Cy™3 or 5. To exclude artifacts such as dust, we assign parameters to the slope, area, peak height and volume of the spots. A manual confirmation of the spots comes next to ensure exclusiveness. The software then renormalizes the data based on set parameters.
Modified from: Tannu, N.S., and S.E. Henby. 2006. Two-dimensional fluorescence difference gel electrophoresis for comparative proteomics profiling. *Nat Protoc* 1: 1732-1742.

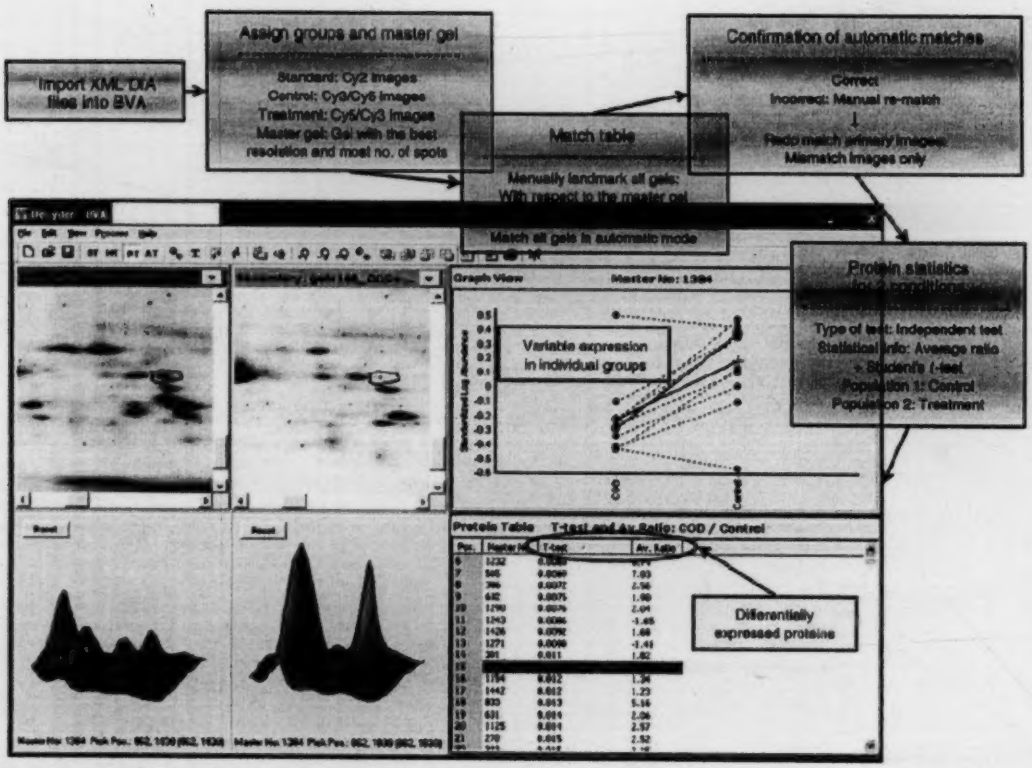
Import XML DIA files into BVA
Assign groups and master gel
Standard: Cy2 images
Control: Cy3/Cy5 images
Treatment: Cy5/Cy3 images
Master gel: Gel with the best resolution and most no. of spots
Match table
Manually landmark all gels:
With respect to the master gel
Match all gels in automatic mode
Confirmation of automatic matches
Correct
Incorrect: Manual re-match
Redo match primary images
Mismatch images only
Protein statistics
Type of test: Independent test
Statistical info: Average ratio
+ Student's t-test
Population 1: Control
Population 2: Treatment
Variable expression in individual groups
Protein Table
T-test and Av. Ratio: COD / Control
Differentially expressed protein

Figure 6. Schematic of multi-gel analysis using the DeCyder BVA module.
The BVA module allows for comparison of multiple gels. After image matching on the DIA module, the volume information is used to generate average ratios for each spot for statistical analysis (*t* test and ANOVA) to create a list of differentially regulated protein spots. The BVA module also allows for visualization of 2D and 3D images of individual spots with differential expressions as well as their within-group variability.
First, multiple XML DIA files are imported into BVA. Groups and master gels are assigned with the standard being the Cy™2 labelled images, the control and treatment gels being Cy™3 or 5, and the master gel being the one with the highest resolution and most number of spots. This is the gel where spots will be picked from. Next, we must manually landmark all the gels with respect with the master gel, or allow the software to automatically landmark for us. For our experiment, we manually landmarked and visually confirmed it. Statistical analysis was then done on the samples.
Modified from: Tannu, N.S., and S.E. Henby. 2006. Two-dimensional fluorescence difference gel electrophoresis for comparative proteomics profiling. *Nat Protoc* 1: 1732-1742.

transferred to BVA for analysis.

The DeCyder BVA module processes multiple gel images and performs gel to gel matching of spots, allowing for quantitative comparisons of protein expression across multiple gels. Images that have undergone spot detection in DIA are generated as XML files and these files, together with the original scanned image, are then used in BVA module. The images are matched to a single master image, identifying common protein spots across the gels. Statistical analysis is also done to highlight proteins that show significant abundance changes under different experimental conditions.

3.2. Results

3.2.1. Differential in-gel analysis

The initial analysis of the neutrophil proteome was carried out by subjecting whole cell lysates to Ettan DIGE analysis (see section 3.1.1 and Figures 3 - 6 for description). 2D DIGE gels were run with samples from WT unstimulated versus WT CB/fMLF-stimulated (Figure 7A), WT unstimulated versus $Rac2^{-/-}$ unstimulated (Figure 7B), $Rac2^{-/-}$ unstimulated versus $Rac2^{-/-}$ stimulated (Figure 7C), and $Rac2^{-/-}$ stimulated versus WT stimulated (Figure 7D) and directly compared. Each condition was run 3 times, for a total of 12 gels from 24 samples. The DeCyder differential in-gel analysis (DIA) software module processed single gel images by performing background subtraction, detection and quantification, in gel normalization and gel artifact removal. From this, we identified spots of interest – those that increased or decreased greater than 1.5-fold with a volume ratio of more than 1 (excluding dust or artifacts) and transferred the data to the biological variance analysis (BVA) software module for further processing. Figure 8 shows examples of 3D histograms taken from the DIA software module.

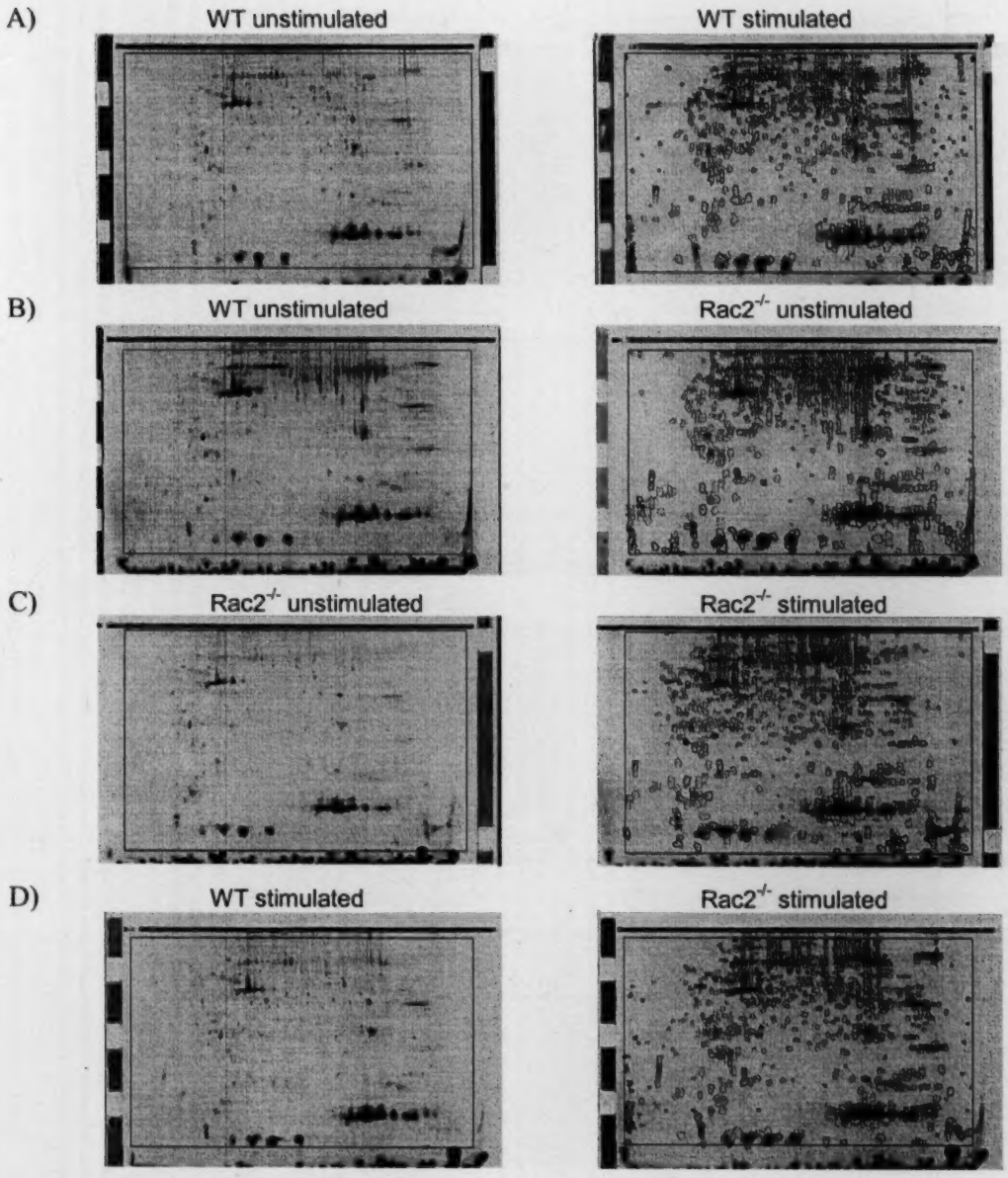

Figure 7. Annotated gels from the DIA module of the DeCyder software.
A) WT unstimulated (Cy™3 dye, left) versus WT CB/fMLF-stimulated (Cy™5 dye, right); B) WT unstimulated (Cy™3 dye, left) versus Rac2$^{-/-}$ unstimulated (Cy™5 dye, right); C) Rac2$^{-/-}$ unstimulated (Cy™3 dye, left) versus Rac2$^{-/-}$ stimulated (Cy™5 dye, right); and D) WT stimulated (Cy™3 dye, left) versus Rac2$^{-/-}$ stimulated (Cy™5 dye, right). Cells were stimulated with CB (10 μM) for 5 min, then fMLF (5 μM) for 15 min at 37°C prior to termination and lysis of sample. Red represents a decrease in spot abundance, blue represents an increase, and green represents no change.

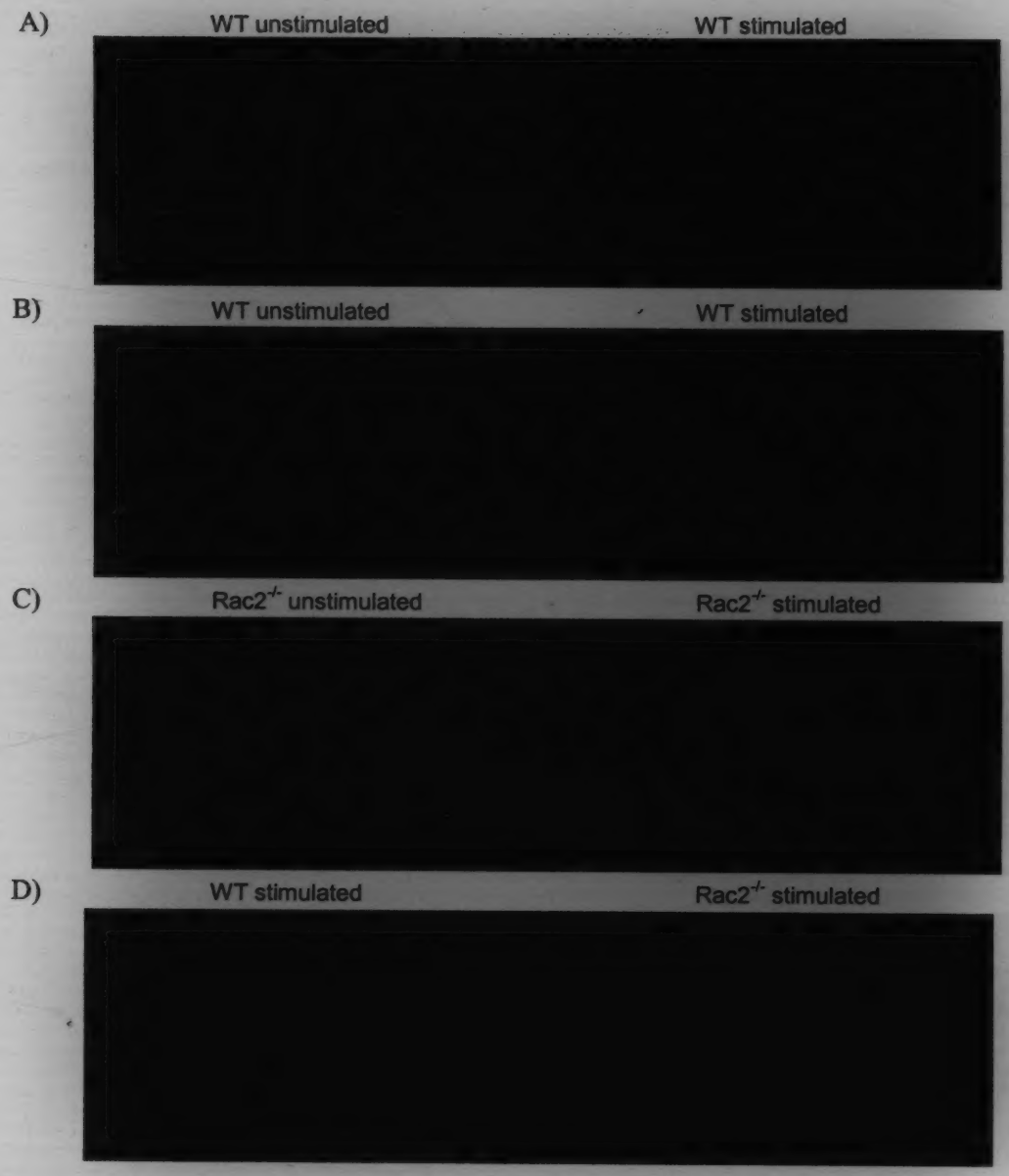

Figure 8. Three dimensional histograms of spots of interest taken from the DIA software module.

A) Spot of increased abundance in WT unstimulated compared to WT stimulated neutrophil lysates; B) spot of decreased abundance of WT unstimulated compared to WT stimulated; C) spot of increased abundance of $Rac2^{-/-}$ stimulated compared to $Rac2^{-/-}$ stimulated; and D) spot of decreased abundance of WT stimulated compared to $Rac2^{-/-}$ stimulated. This is representative of 24 samples in 12 separate gels. Each gel had 2 samples (Cy™3 and Cy™5), and a control mixture of all samples (Cy™2).

3.2.2. Biological variance analysis

The DeCyder BVA software module performed inter-gel statistical analysis to provide relative protein abundance and the first overlap of gels. Log abundance ratios were then compared between the gels using t-test and ANOVA. Using fluorescent dyes to label the proteins also allowed the use of a pooled internal standard (sample composed of equal aliquots from each condition). This approach was essential for assessing biological and experimental variance, thereby increasing the robustness of statistical analysis (93). The individual protein data from each condition (Cy™3- or Cy™5-labeled) were normalized against the Cy™2-labeled internal standard, Cy™5:Cy2™2 and Cy™3:Cy™2.

The gels were matched to a single master image and the software identified common protein spots across the gels. Tables 2 (WT unstimulated versus WT stimulated), 3 ($Rac2^{-/-}$ unstimulated versus $Rac2^{-/-}$ stimulated), 4 ($Rac2^{-/-}$ unstimulated versus $Rac2^{-/-}$ stimulated), and 5 (WT stimulated versus $Rac2^{-/-}$ stimulated) show the top 50 spots that were sorted based on their statistical significance. It was from this data that we picked spots to be identified by mass spectrometry.

3.2.3. Proteins identified as being differentially expressed in Rac2 KOs

Over 3500 spots were revealed by DIGE, from which 22 were chosen for identification by MS because they showed statistically significant differences between WT stimulated and unstimulated samples while this trend was not apparent in $Rac2^{-/-}$ samples. None of the spots chosen for sequencing correlated with Rac2, indicating that this approach was not sensitive enough to detect loss of Rac2 expression in $Rac2^{-/-}$ BMN. Indeed, no regulatory or signalling molecules (such as GTPases, kinases or phosphatases) could be

Table 2. BVA on spots of interest from WT unstimulated versus WT stimulated BMN samples determined from the DIA software module.

Master Number	Appearance	*p*-value (*t* test)	Average Ratio	*p*-value (One way ANOVA)
1018	24	2.80E-07	4.56	2.20E-10
1048	24	2.70E-06	2.62	5.30E-08
572	24	9.20E-06	2.46	5.30E-08
616	24	4.70E-05	3.41	2.60E-07
970	24	2.80E-05	3.9	2.80E-07
637	24	8.70E-06	2.75	6.60E-07
425	24	6.10E-07	-2.14	8.70E-07
965	21	9.80E-06	5.11	1.30E-06
535	18	3.10E-05	3.01	2.00E-06
1038	21	4.70E-05	3.4	2.00E-06
382	24	3.20E-05	-2.01	2.20E-06
504	24	2.70E-05	2.34	4.70E-06
312	21	0.00014	2.96	5.10E-06
888	21	5.30E-05	1.96	6.20E-06
560	21	4.50E-06	2.99	7.80E-06
1060	12	0.0013	3.52	1.20E-05
983	24	0.00011	3.48	1.50E-05
691	24	0.00053	-2.85	2.10E-05
985	24	0.0003	2.95	2.50E-05
677	24	2.80E-05	1.66	3.10E-05
971	24	0.00032	3.31	4.00E-05
1021	18	0.00044	4.15	4.30E-05
738	24	0.00093	2.24	4.30E-05
903	21	0.00058	-1.15	4.40E-05
998	21	0.0015	1.49	5.70E-05
969	24	6.60E-05	3.28	5.90E-05
220	15	0.0072	2.17	6.00E-05
957	21	0.00017	3.13	7.90E-05
999	24	0.00087	3.39	9.50E-05
854	24	8.40E-05	-1.28	0.0001
676	24	0.00033	1.7	0.00011
1037	21	0.00062	3.22	0.00013
548	21	3.00E-05	-1.55	0.00015
636	21	0.00026	3.15	0.00016
389	21	0.00062	1.94	0.00018
374	24	0.0029	-1.2	0.0002
561	21	3.80E-05	-1.7	0.00025
354	24	0.00023	-1.86	0.00025
841	21	0.001	-1.43	0.0003
234	24	0.00019	-1.26	0.00032
1162	21	0.0006	-1.35	0.00032
694	24	0.0013	1.47	0.00051
974	24	0.0003	3.08	0.00059
1010	24	0.00069	-1.59	0.00062
1039	15	0.0052	2.43	0.00062
973	12	0.0083	3.28	0.00065
567	24	0.003	-1.45	0.00093
1097	21	0.002	-1.24	0.001
603	21	0.0002	-2.96	0.0011
164	18	0.0018	-1.3	0.0013

The top 50 spots of interest were ranked in order of significance based on *p*-values from one way ANOVA. Appearance describes the amount of times the spot appeared out of 24 gels and average ratio describes the difference of the spot from the compared gel. A positive average ratio indicates an increase in relative proteins abundance, while a negative average ratio shows decreased abundance. Out of the top 50 spots, the majority of proteins increased in relative abundance (33/50) upon stimulation with CB/fMLF.

Table 3. BVA on spots of interest from Rac2$^{-/-}$ unstimulated versus Rac2$^{-/-}$ stimulated BMN samples determined from the DIA software module.

Master Number	Appearance	*p*-value (*t* test)	Average Ratio	*p*-value (One way ANOVA)
1018	24	0.00049	-1.97	2.20E-10
572	24	0.0022	-1.45	5.30E-08
1048	24	0.008	-1.4	5.30E-08
616	24	0.00037	-2.11	2.60E-07
970	24	0.0031	-1.79	2.80E-07
637	24	0.015	-1.47	6.60E-07
425	24	0.56	1.05	8.70E-07
965	21	0.016	-2.09	1.30E-06
1038	21	0.0052	-2.28	2.00E-06
535	18	0.0066	-1.88	2.00E-06
382	24	0.14	1.14	2.20E-06
504	24	0.011	-1.52	4.70E-06
312	21	0.007	-1.3	5.10E-06
888	21	0.0092	-1.58	6.20E-06
560	21	0.039	-1.52	7.80E-06
1060	12	0.0034	-1.2	1.20E-05
983	24	0.023	-2.02	1.50E-05
691	24	0.013	1.61	2.10E-05
985	24	0.0044	-2.25	2.50E-05
945	15	0.0081	-1.06	3.00E-05
677	24	0.078	-1.23	3.10E-05
981	9	ND	1.05	3.90E-05
971	24	0.0083	-2.03	4.00E-05
738	24	0.00095	-1.61	4.30E-05
1021	18	0.017	-1.99	4.30E-05
903	21	0.021	-1.24	4.40E-05
1040	24	0.0011	-1.47	4.50E-05
998	21	0.00081	-1.3	5.70E-05
969	24	0.022	-1.87	5.90E-05
220	15	0.028	-1.16	6.00E-05
957	21	0.03	-1.78	7.90E-05
999	24	0.0059	-2.34	9.50E-05
854	24	0.025	-1.17	0.0001
676	24	0.027	-1.4	0.00011
1037	21	0.055	-1.46	0.00013
548	21	0.11	1.23	0.00015
636	21	0.049	-1.9	0.00016
371	24	0.0064	-1.15	0.00016
1041	24	0.0048	-1.44	0.00017
389	21	0.085	-1.23	0.00018
374	24	0.0033	-1.14	0.0002
536	24	0.86	-1.01	0.00024
354	24	0.58	1.06	0.00025
561	21	0.85	-1.01	0.00025
1108	21	0.0013	-1.28	0.00025
841	21	ND	1	0.0003
1162	21	0.022	-1.31	0.00032
234	24	0.19	-1.07	0.00032
686	24	0.03	-1.25	0.00042
925	24	0.017	-1.41	0.00049

The top 50 spots of interest were ranked in order of significance based on *p*-values from one way ANOVA, similar to Table 2. In this case, only 5 protein spots increased in their relative abundance in CB/fMLF-stimulated BMN over unstimulated cells. The majority of the top 50 proteins decreased in relative abundance upon stimulation. The highlighted numbers indicate those spots identical to the WT top 50 values. ND = Not determined.

Table 4. BVA on spots of interest from WT unstimulated versus Rac2$^{-/-}$ unstimulated BMN samples determined from the DIA software module.

Master Number	Appearance	*p*-value (*t* test)	Average Ratio	*p*-value (One way ANOVA)
1018	24	0.042	1.2	2.20E-10
572	24	0.32	-1.06	5.30E-08
1048	24	0.69	-1.03	5.30E-08
616	24	0.039	-1.2	2.60E-07
970	24	0.54	-1.05	2.80E-07
637	24	0.0025	-1.11	6.60E-07
425	24	0.13	1.16	8.70E-07
965	21	0.93	-1.02	1.30E-06
535	18	0.66	-1.06	2.00E-06
1038	21	0.074	1.3	2.00E-06
382	24	0.26	1.09	2.20E-06
504	24	0.28	-1.1	4.70E-06
312	21	0.21	-1.19	5.10E-06
888	21	0.13	1.1	6.20E-06
560	21	0.62	-1.03	7.80E-06
1060	12	0.0094	-1.47	1.20E-05
983	24	0.55	1.17	1.50E-05
691	24	0.69	-1.09	2.10E-05
985	24	0.0085	1.28	2.50E-05
945	15	0.0013	1.35	3.00E-05
677	24	0.049	-1.22	3.10E-05
981	9	ND	-2.01	3.90E-05
971	24	0.86	-1.01	4.00E-05
738	24	0.95	-1.02	4.30E-05
1021	18	0.15	1.17	4.30E-05
903	21	0.82	1.01	4.40E-05
1040	24	0.0047	1.38	4.50E-05
998	21	0.32	1.09	5.70E-05
969	24	0.19	-1.21	5.90E-05
220	15	0.035	-1.21	6.00E-05
957	21	0.73	1.06	7.90E-05
999	24	0.031	1.37	9.50E-05
854	24	0.0015	1.3	0.0001
676	24	0.25	1.09	0.00011
1037	21	0.41	-1.14	0.00013
548	21	0.013	1.18	0.00015
636	21	0.091	-1.13	0.00016
371	24	0.04	1.1	0.00016
1041	24	0.12	1.16	0.00017
389	21	0.25	-1.12	0.00018
374	24	0.0076	1.15	0.0002
536	24	0.00067	1.68	0.00024
354	24	0.14	1.2	0.00025
561	21	0.016	1.4	0.00025
1108	21	0.0053	1.23	0.00025
841	21	0.022	1.25	0.0003
234	24	0.0032	1.19	0.00032
1162	21	0.0079	1.37	0.00032
686	24	0.016	1.19	0.00042
925	24	0.025	1.24	0.00049

The top 50 spots of interest were ranked in order of significance based on *p*-values from one way ANOVA, as described in Table 2. ND = not determined.

Table 5. BVA on spots of interest from WT stimulated versus Rac2$^{-/-}$ stimulated BMN samples determined from the DIA software module.

Master Number	Appearance	*p*-value (*t* test)	Average Ratio	*p*-value (One way ANOVA)
1018	24	9.00E-05	2.77	2.20E-10
1048	24	0.00037	1.82	5.30E-08
572	24	0.0012	1.6	5.30E-08
616	24	0.074	1.35	2.60E-07
970	24	0.0026	2.07	2.80E-07
637	24	0.011	1.69	6.60E-07
425	24	7.90E-05	-1.75	8.70E-07
965	21	0.0041	2.39	1.30E-06
535	18	0.0019	1.51	2.00E-06
1038	21	0.006	1.95	2.00E-06
382	24	0.00062	-1.61	2.20E-06
504	24	0.019	1.4	4.70E-06
312	21	0.0019	1.92	5.10E-06
888	21	0.028	1.36	6.20E-06
560	21	0.0036	1.91	7.80E-06
1060	12	0.0015	1.98	1.20E-05
983	24	0.011	2.02	1.50E-05
691	24	0.004	-1.94	2.10E-05
985	24	0.073	1.68	2.50E-05
945	15	0.0047	1.12	3.00E-05
677	24	0.15	1.11	3.10E-05
981	9	ND	-1.6	3.90E-05
971	24	0.013	1.61	4.00E-05
738	24	0.032	1.36	4.30E-05
1021	18	0.044	2.44	4.30E-05
903	21	0.00012	-1.41	4.40E-05
1040	24	0.092	1.11	4.50E-05
998	21	0.0016	1.24	5.70E-05
969	24	0.18	1.45	5.90E-05
220	15	0.0045	1.54	6.00E-05
957	21	0.032	1.86	7.90E-05
999	24	0.061	1.99	9.50E-05
854	24	0.0067	-1.16	0.0001
676	24	0.068	1.32	0.00011
1037	21	0.0098	1.93	1.30E-04
548	21	0.41	-1.07	0.00015
636	21	0.13	1.47	0.00016
371	24	0.00095	-1.28	0.00016
1041	24	0.077	1.21	0.00017
389	21	0.024	1.41	0.00018
374	24	0.0013	-1.19	0.0002
536	24	0.078	1.24	0.00024
354	24	0.0027	-1.45	0.00025
561	21	0.022	-1.23	0.00025
1108	21	0.0022	-1.22	0.00025
841	21	0.017	-1.15	3.00E-04
1162	21	0.0011	-1.3	0.00032
234	24	0.017	-1.14	0.00032
686	24	0.063	1.19	0.00042
925	24	0.088	1.22	0.00049

The top 50 spots of interest were ranked in order of significance based on *p*-values from one way ANOVA, as described in Table 2. Out of the top 50 spots, 35 proteins showed an increase in relative abundance in CB/fMLF-stimulated Rac2$^{-/-}$ BMN compared to WT stimulated cells. ND = not determined.

detected. Most of the proteins identified were cytoskeletal or housekeeping protein which makes sense since they are the most abundant and separable protein species.

The spots that were chosen to be sequenced resulted in multiple hits, but only species-specific (mouse) matches were considered. Six known proteins and three unknown proteins were identified by MS. In Table 6, the proteins are identified and sorted in descending order of WT CB/fMLF-stimulated BMN when compared to WT unstimulated BMN. In Table 7, the proteins are identified and sorted in descending order of WT CB/fMLF-stimulated BMN when compared to $Rac2^{-/-}$ unstimulated BMN. In Table 8, the proteins are identified and sorted in descending order of $Rac2^{-/-}$ unstimulated BMN when compared to WT unstimulated BMN. In Table 9, the proteins are identified and sorted in descending order of $Rac2^{-/-}$ CB/fMLF-stimulated BMN when compared to $Rac2^{-/-}$ stimulated BMN.

In all gels, the abundance of coronin showed consistent and significant changes. Chitinase also showed consistent changes and was a very abundant protein. Spot maps for these two proteins were traced back to the DeCyder BVA module. The gel showed that coronin and chitinase were of a relatively high molecular weight and had mid-range pIs (Figure 9A). From WT unstimulated to WT stimulated BMNs, coronin increased in abundance (Figure 9B) while chitinase decreased in abundance (Figure 9C). In WT stimulated compared to $Rac2^{-/-}$ stimulated BMNs, we see the converse (Figure 9D, E).

A scatter plot of abundance measurements from all gels showed that in WT and $Rac2^{-/-}$ unstimulated BMNs, coronin remained in relatively low abundance, but when stimulated with CB/fMLF, there is a large and significant increase in abundance although the increase is less pronounced in $Rac2^{-/-}$ BMNs (Figure 10A). Chitinase, on the other

Table 6. Proteins identified by mass spectrometry and their differences in spot abundance compared between WT unstimulated BMN and WT stimulated BMN.

Identity	NIH protein database accession number	WT unstim		WT stim	
		Volume (SD)	Difference	Volume (SD)	Difference
Coronin	NP_034028	0.024 (0.033)	1.000	0.084 (0.035)	3.578
GAPDH	AAU89484	0.020 (0.020)	1.000	0.035 (0.035)	1.740
HSP60	NP_034607	0.075 (0.056)	1.000	0.120 (0.116)	1.609
Chitinase	NP_075675	2.245 (1.592)	1.000	0.941 (0.741)	-2.386
Granule protein	BAB26414	0.238 (0.053)	1.000	0.086 (0.067)	-2.774
β-actin	ABL01512	0.328 (0.192)	1.000	0.111 (0.082)	-2.954
Granule protein	NP_032720	0.048 (0.019)	1.000	0.013 (0.013)	-3.685
β-actin	ABL01512	0.104 (0,068)	1.000	0.026 (0.004)	-4.025
Actin capping protein	NP_033928	0.169 (0.040)	1.000	0.037 (0.024)	-4.568
Granule protein	EDL09016	0.180 (0.223)	1.000	0.014 (0.010)	-12.423

HSP60, heat shock protein; GAPDH, glyceraldehyde 3-phosphate dehydrogenase; NIH, National Institutes of Health

Table 7. Proteins identified by mass spectrometry and their differences in spot abundance compared between $Rac2^{-/-}$ unstimulated BMN and $Rac2^{-/-}$ stimulated BMN.

Identity	NIH protein database accession number	$Rac2^{-/-}$ unstim		$Rac2^{-/-}$ stim	
		Volume (SD)	Difference	Volume (SD)	Difference
Coronin	NP_034028	0.016 (0.018)	1.000	0.044 (0.036)	2.750
GAPDH	AAU89484	0.034 (0.052)	1.000	0.052 (0.057)	1.529
HSP60	NP_034607	0.079 (0.058)	1.000	0.113 (0.092)	1.430
β-actin	ABL01512	0.076 (0.012)	1.000	0.068 (0.031)	-1.118
Chitinase	NP_075675	1.889 (1.400)	1.000	1.577 (0.815)	-1.198
Granule protein	NP_032720	0.052 (0.019)	1.000	0.039 (0.017)	-1.333
β-actin	ABL01512	0.271 (0.165)	1.000	0.201 (0.108)	-1.348
Granule protein	BAB26414	0.288 (0.078)	1.000	0.187 (0.069)	-1.540
Actin capping protein	NP_033928	0.171 (0.054)	1.000	0.105 (0.070)	-1.629
Granule protein	EDL09016	0.136 (0.156)	1.000	0.069 (0.081)	-1.971

Table 8. Proteins identified by mass spectrometry and their differences in spot abundance compared between WT unstimulated BMN and Rac2$^{-/-}$ unstimulated BMN.

Identity	NIH protein database accession number	WT unstim		Rac2$^{-/-}$ unstim	
		Volume (SD)	Difference	Volume (SD)	Difference
GAPDH	AAU89484	0.020 (0.020)	1.000	0.034 (0.052)	1.700
Granule protein	BAB26414	0.238 (0.053)	1.000	0.288 (0.078)	1.210
Granule protein	NP_032720	0.048 (0.019)	1.000	0.052 (0.019)	1.083
HSP60	NP_034607	0.075 (0.056)	1.000	0.079 (0.058)	1.053
Actin capping protein	NP_033928	0.169 (0.040)	1.000	0.171 (0.054)	1.012
Chitinase	NP_075675	2.245 (1.592)	1.000	1.889 (1.400)	-1.188
β-actin	ABL01512	0.328 (0.192)	1.000	0.271 (0.165)	-1.210
Granule protein	EDL09016	0.180 (0.223)	1.000	0.136 (0.156)	-1.324
β-actin	ABL01512	0.104 (0,068)	1.000	0.076 (0.012)	-1.368
Coronin	NP_034028	0.024 (0.033)	1.000	0.016 (0.018)	-1.500

Table 9. Proteins identified by mass spectrometry and their differences in spot abundance compared between WT stimulated BMN and Rac2$^{-/-}$ stimulated BMN.

Identity	NIH protein database accession number	WT stim		Rac2$^{-/-}$ stim	
		Volume (SD)	Difference	Volume (SD)	Difference
Granule protein	EDL09016	0.014 (0.010)	1.000	0.069 (0.081)	4.744
Granule protein	NP_032720	0.013 (0.013)	1.000	0.039 (0.017)	3.001
Actin capping protein	NP_033928	0.037 (0.024)	1.000	0.105 (0.070)	2.793
β-actin	ABL01512	0.026 (0.004)	1.000	0.068 (0.031)	2.655
Granule protein	BAB26414	0.086 (0.067)	1.000	0.187 (0.069)	2.185
β-actin	ABL01512	0.111 (0.082)	1.000	0.201 (0.108)	1.809
Chitinase	NP_075675	0.941 (0.741)	1.000	1.577 (0.815)	1.676
GAPDH	AAU89484	0.035 (0.035)	1.000	0.052 (0.057)	1.464
HSP60	NP_034607	0.120 (0.116)	1.000	0.113 (0.092)	-1.064
Coronin	NP_034028	0.084 (0.035)	1.000	0.044 (0.036)	-1.899

A)

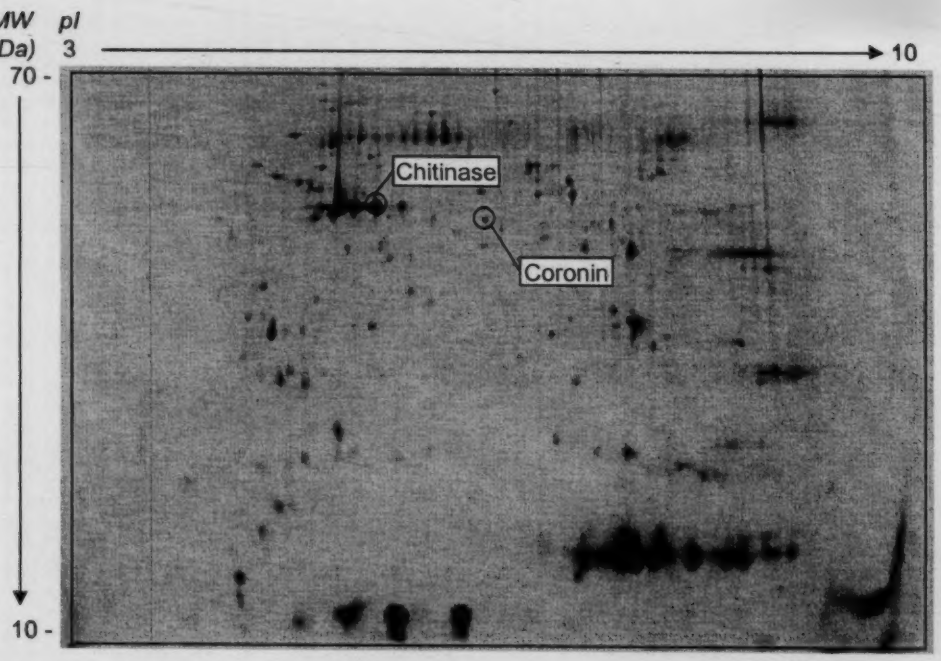
MW
(kDa)
pI
3
10
70 -
10 -
Chitinase
Coronin

B)

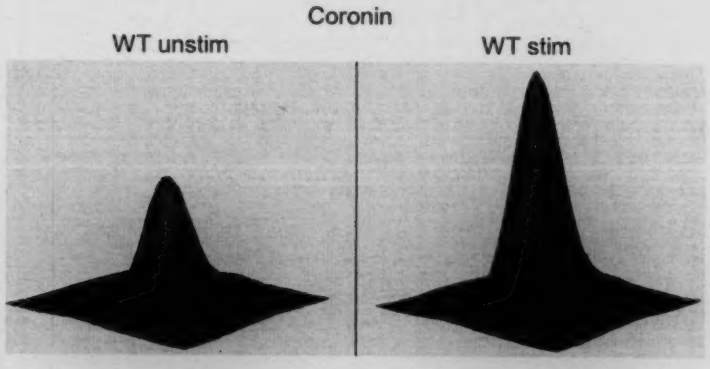
Coronin
WT unstim
WT stim

C)

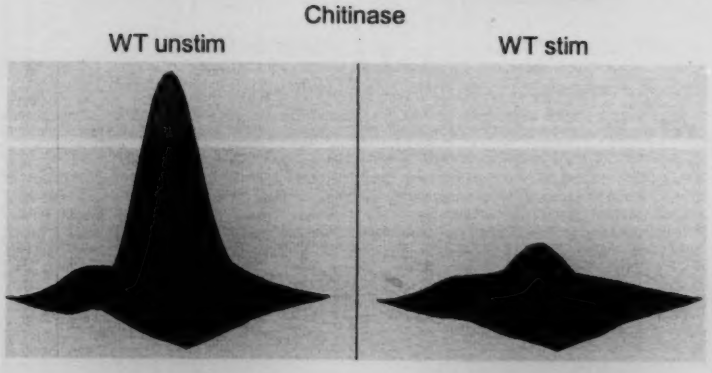
Chitinase
WT unstim
WT stim

D)

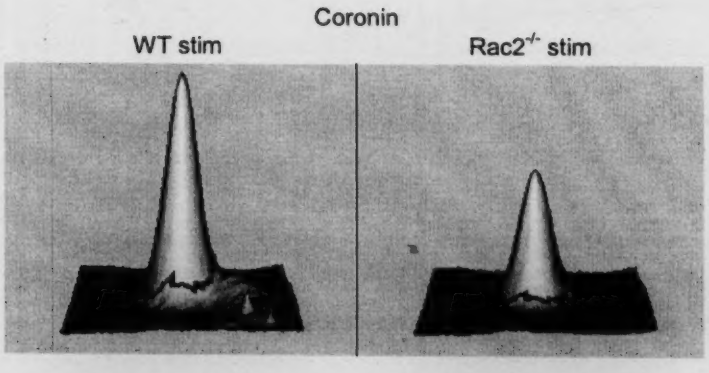

E)

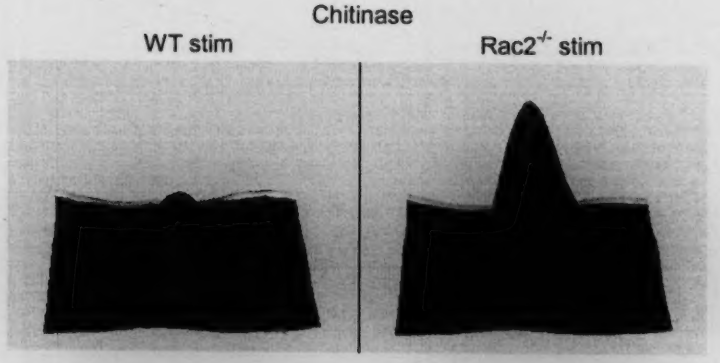

Figure 9. Spots on a WT unstimulated BMN gel were identified as coronin and chitinase.

In each gel, coronin and chitinase, as examples, were identified as discrete spots. A) An annotated gel where chitinase (MW = 52 kDa, pI = 4.84) and coronin (MW = 51 kDa, pI = 6.05) were found in positions indicated. B) 3D histogram of the spot correlating with coronin. The left panel is WT unstimulated BMN and the right is WT stimulated BMN. C) 3D histogram of the spot correlating with chitinase. The left panel is WT unstimulated BMN and the right is WT stimulated BMN. D) 3D histogram of the spot correlating with coronin. The left panel is WT stimulated BMN and the right is $Rac2^{-/-}$ stimulated BMN. E) 3D histogram of the spot correlating with chitinase. The left panel is WT stimulated BMN and the right is $Rac2^{-/-}$ stimulated BMN.

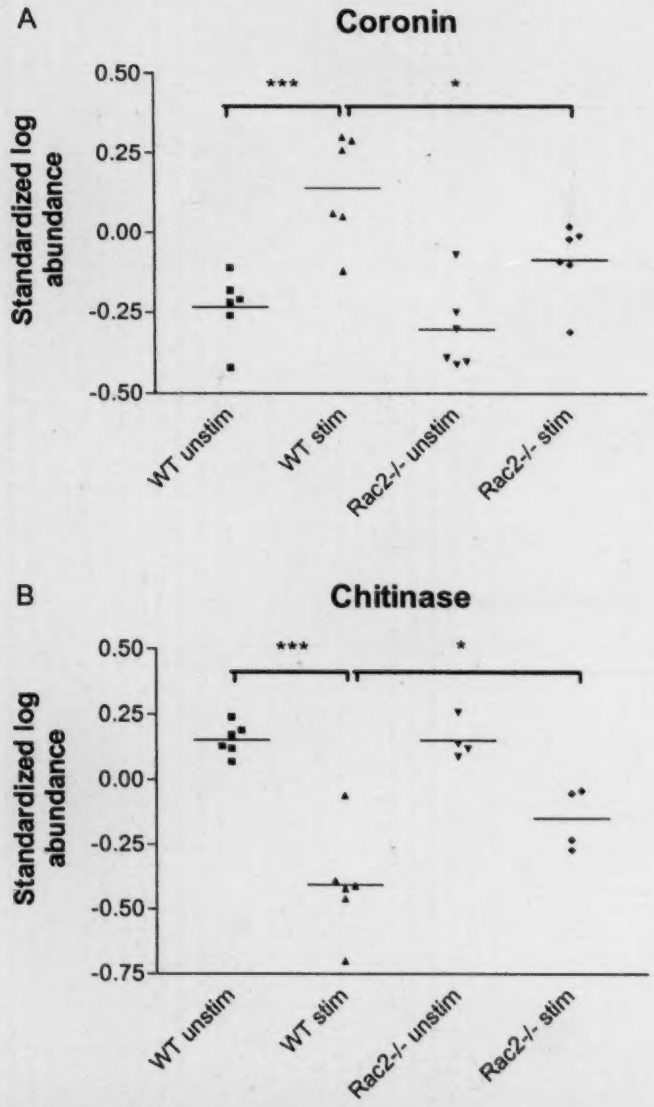

Figure 10. Scatter plots of standardized log abundance of spots of coronin and chitinase taken from the DeCyder BVA module.

Coronin and chitinase, as examples, were back traced as spots into the BVA module where the software calculated their standardized log abundance ratios. A) Coronin, in WT and $Rac2^{-/-}$ unstimulated BMN, had approximately the same abundance, but when stimulated with CB/fMLF, there was an increase in abundance. This increase in abundance was not as pronounced in the $Rac2^{-/-}$ samples as it was in the WTs. B) Chitinase, in WT and $Rac2^{-/-}$ unstimulated BMN, had approximately the same abundance, but when stimulated with CB/fMLF, there was a decrease in abundance. This decrease in abundance was not as pronounced in the $Rac2^{-/-}$ samples as it was in the WTs. Each spot represents different spots from 4-6 gels run on 3 samples (each sample is pooled from 4 mice).

hand, showed the opposite trend. In WT and Rac2$^{-/-}$ unstimulated BMNs, chitinase was in high abundance, but when stimulated with CB/fMLF, there was a decrease in abundance (Figure 10B). Again, this trend was not as pronounced in the Rac2$^{-/-}$ samples as it was in the WT samples. These differences were statistically significant.

3.3. Summary

Our findings indicate that coronin and chitinase, and other proteins listed in Tables 6 - 9, were significantly altered in their abundance in samples prepared from stimulated Rac2$^{-/-}$ and WT neutrophils. Although our analysis was sensitive enough to detect numerous changes in protein abundance (i.e. pI, molecular weight, and concentration changes), we could not determine whether they were due to specific modifications such as phosphorylation, methylation or nitration. As well, we could not correlate changes of two protein isoforms simultaneously. For example, we found that the abundance of coronin increased in wild-type samples after stimulation; however, we could not detect a corresponding decrease in abundance of another spot which would represent coronin being covalently modified. This is likely due to corresponding changes not fitting the minimal proteomic screening criteria of 1.5-fold change in abundance with statistical relevance of $p < 0.001$ by one way ANOVA.

Of particular interest was coronin which was identified as a protein which showed a more abundant isoform in WT stimulated but not WT unstimulated cells. Coronin is an actin-binding protein that is important for chemotaxis and phagocytosis (94, 95). Coronin may be an interesting protein to pursue in the elucidation of the Rac2 pathway of exocytosis because it has been implicated as a regulator of the cytoskeleton and membrane trafficking (96). Interestingly, β-actin and actin-capping proteins were also

identified. This suggests that the actin cytoskeleton, and some of its associating proteins, may play a regulatory role in neutrophil exocytosis – specifically in the Rac2 signalling cascade.

Chitinase is also interesting because it is an enzyme that degrades chitin, an abundant biopolymer that is found in the walls of fungi; the exoskeleton of crabs, shrimp, and insects; the microfilarial sheath of parasitic nematodes; and the lining of the digestive tracts of many insects (97). Chitinases are produced in large quantities by hosts defending against infections from chitin-containing organisms. Acidic mammalian chitinase is induced during TH2 inflammation through an IL-13–dependent mechanism (98). Zhu *et al.* showed that it played an important role in the pathogenesis of TH2 inflammation and IL-13 effector pathway activation and demonstrated that chitinase is expressed in an exaggerated fashion in human asthmatic tissues (98). Our data showed that chitinase was decreased in both WT and $Rac2^{-/-}$ BMNs when they were stimulated with CB/fMLF. We can infer that chitinase may be released during degranulation, resulting in a lower abundance in stimulated cells. Furthermore, its abundance is higher in stimulated $Rac2^{-/-}$ neutrophils, which falls in line with the observation that $Rac2^{-/-}$ neutrophils show less degranulation when stimulated with CB/fMLF (59). Interestingly, YKL-40, a mammalian member of the chitinase family, is found in specific granules in human neutrophils (99). To follow up on this, we should investigate the function of chitinase in relation to Rac2 in neutrophils before we can arrive at any conclusions.

A problem associated with this experimental design is that the purity of cells was 80-85%, so some of these results may not be valid because of contamination from other cells. The main contaminating cell types were immature neutrophils and monocytes. We

cannot be sure the changes in protein abundance are specific to neutrophils. Furthermore, for future experiments, it would be beneficial to analyze subcellular compartments such as purified granules, but this has an inherent problem in that granules are lost when cells degranulate which makes it difficult to compare granule proteins before and after stimulation.

In summary, we detected nine proteins (six known, three unknown) that changed in abundance between CB/fMLF-stimulated WT and $Rac2^{-/-}$ murine BMN. Our experimental design using DeCyder analysis for proteomics was not able to discriminate whether changes in protein abundance were due to modifications such as phosphorylation, methylation or nitrosylation. In addition, proteins with hydrophobic regions or low abundance were also difficult to detect using this approach – in agreement with findings from other laboratories (100). Nevertheless, the software performed statistical analysis on multiple gels, providing extensive data on spot abundance changes. Through this, we found two proteins of note – coronin and chitinase – which showed differences between WT and $Rac2^{-/-}$ neutrophils and may play a role in the Rac2-mediated primary granule pathway.

CHAPTER IV - Role of actin cytoskeleton

4.1. Background

Our proteomic data implicated a role for coronin, β-actin, and an unknown actin capping protein in exocytosis. These conclusions lead us to investigate whether actin was a key player in neutrophil granule exocytosis. Indeed, numerous studies of exocytosis in many different kinds of secretory cells have suggested a regulatory role for the actin cytoskeleton in granule translocation (42, 71, 72). Myeloid cells possess an F-actin-rich cortical region which is considered to be an impediment in preventing granule docking and fusion at the plasma membrane, the so-called "actin-barrier" hypothesis. Furthermore, F-actin exists in equilibrium with cytoplasmic G-actin. A comprehensive study of neutrophil degranulation revealed that all major granule types associated with actin (78). Indeed, primary, secondary and tertiary granule exocytosis from isolated neutrophils is enhanced through the pre-treatment of cells with CB, an actin depolymerizing drug, which supports the actin-barrier hypothesis (78). In contrast to this, other studies have shown evidence that it is rather actin polymerization that facilitates exocytosis (101-105). This suggestion seems quite plausible in neutrophils since their movement towards stimuli (i.e. a chemotactic gradient) is triggered by polarized F-actin assembly which may also drive polarized mobilization of granules on this very actin network (45, 106). Therefore, we hypothesize that actin polymerization may be needed in the cell cytoplasm to direct granules to the cell periphery, while depolymerization must occur concurrently at the cell cortex to allow for successful degranulation.

The bacterially derived secretagogue, fMLF, is a natural potent stimulus of human neutrophils, but *in vitro* stimulation of primary granule exocytosis from neutrophils

requires priming with an actin depolymerizing agent. These actin depolymerizing agents include CB, a fungal toxin which blocks barbed ends of actin filaments (107), and leads to actin meshwork disassembly, mimicking surface binding in neutrophils and enhancing fMLF-induced primary granule exocytosis (108, 109). This is a well known observation among neutrophil biologists and it suggests that primary granules require F-actin depolymerization for their extracellular secretion. We hypothesized that similar drugs which destabilize F-actin will also stimulate primary granule exocytosis when combined with fMLF, and conversely, stabilizing F-actin will have the opposite effect.

4.2. Results

4.2.1. Effects of actin drugs on primary granule exocytosis

We observed that CB, a mycotoxin that blocks addition of actin monomers to the barbed ends of actin filaments, enhanced fMLF-induced exocytosis while Lat B, a structurally unique marine toxin that acts by sequestering monomeric actin and consequently stimulates actin depolymerization (110), enhanced fMLF-induced primary granule exocytosis at much lower doses than CB (Figure 11). This finding confirms previous reports, and demonstrates that Lat B is more specific for actin than CB (110). However, at higher doses of Lat B or CB (> 10 μM), primary granule exocytosis was reduced. This suggests that partial actin depolymerization is needed for degranulation, while complete F-actin depolymerization blocks it. JP, which binds to and induces actin polymerization (111), did not stimulate exocytosis at any dose tested (Figure 11).

We next examined the effect of combinations of actin drugs on either CB/fMLF or A23187-stimulated primary granule exocytosis. Based on our data and previous literature indicating the obligatory priming step for exocytosis via actin depolymerizing

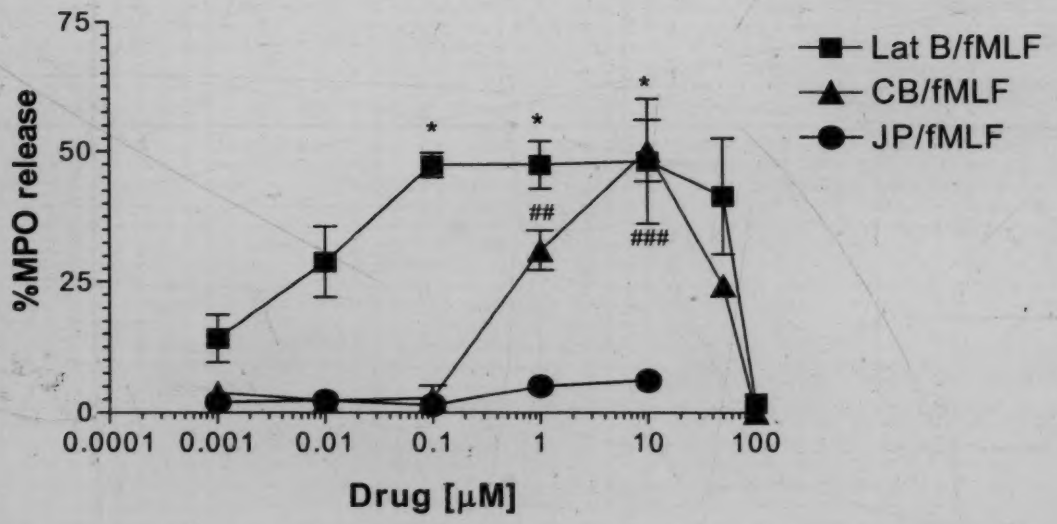

Figure 11. Comparison of the effects of actin altering drugs on fMLF-stimulated neutrophil exocytosis.

Neutrophils were preincubated with increasing concentrations of either CB, Lat B, or JP for 5 min followed by stimulation with 5 μM fMLF for 15 min at 37°C. Extracellular supernatants were collected from each condition and assayed for MPO activity. The release of MPO was calculated as a percentage of total cellular mediator activity (± SEM) from at least 3 independent experiments (except JP, where $n = 1$). Statistical significance is compared to the lowest drug dose condition. * $p < 0.05$, ** $p < 0.01$, *** $p < 0.001$. * represents Lat B/fMLF and # represents CB/fMLF.

drugs (Figure 11) (59, 108, 109), we hypothesized that further disruption of F-actin would increase primary granule exocytosis, while stabilization would suppress it. Indeed, the addition of 0.5 – 10 μM Lat B to CB/fMLF- or A23187-stimulated neutrophils further amplified MPO release (Figure 12 A, C). Lat B enhanced A23187-induced exocytosis at doses of up to 10 μM, whereas for CB/fMLF, it was only stimulatory at 0.5 μM. While these observations are statistically significant, we cannot be certain that it is not an anomaly since the graph generally follows the classic dose response curve. Be that as it may, these results can also suggest that there exists an actin depolymerization "threshold" for degranulation, and when it is exceeded, it is inhibitory to exocytosis. Treatment of neutrophils with Lat B in conjunction with CB, two drugs that promote actin destabilization, exceed the actin depolymerization threshold needed to enhance exocytosis as compared to low doses of Lat B. Stabilization of F-actin with JP reduced both CB/fMLF- and A23187-stimulated exocytosis (Figure 12 B, D), although the inhibition was not absolute. At least 20% of maximal MPO release was still observed in response to CB/fMLF, while as much as 50% of the response persisted in response to A23187 when cells were pre-treated with JP.

4.2.2. Morphological staining of stimulated neutrophils via actin and primary granule staining

We next examined human neutrophils by confocal microscopy to confirm our biochemical findings and to visualize the effects of the actin altering drugs. Neutrophil primary granules were labelled with anti-CD63 antibodies conjugated to Alexa Fluor 488, and F-actin was labelled with rhodamine-phalloidin. The cells were treated similarly to those used in the secretion assays, then fixed in suspension and adhered to poly-L-lysine

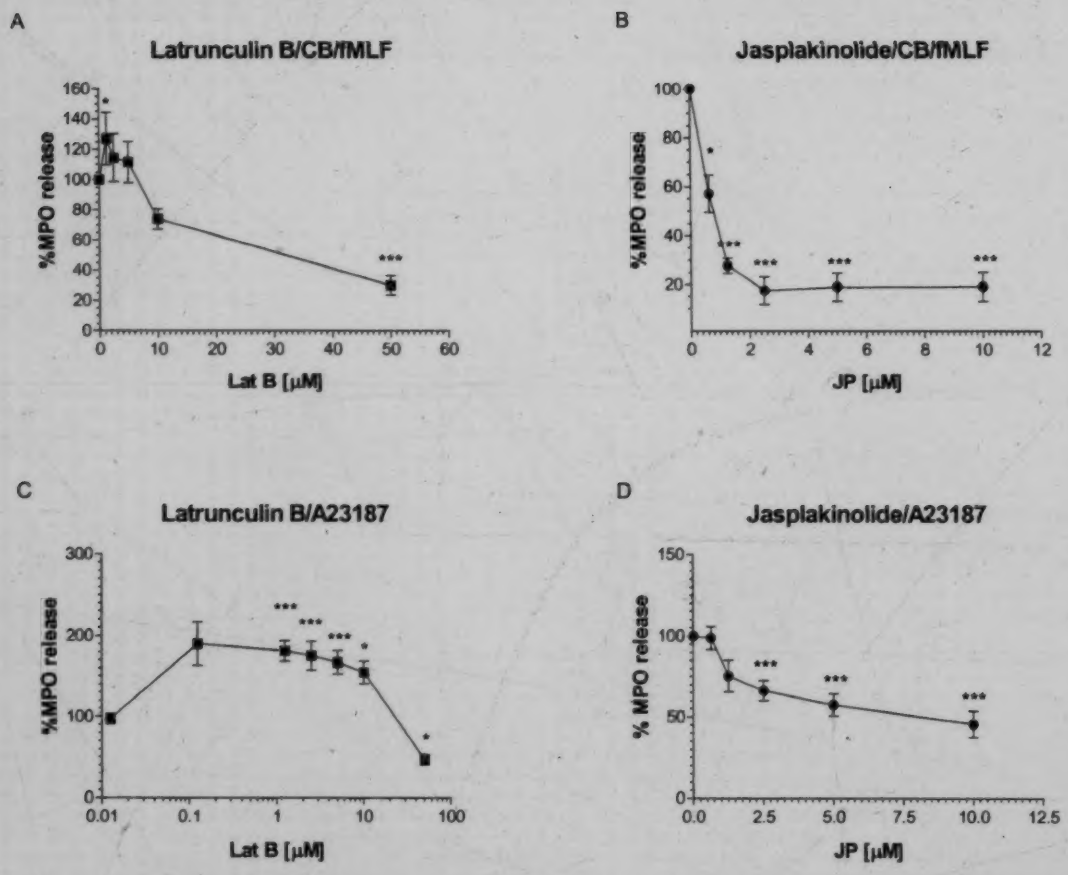

Figure 12. Effect of actin altering drugs on CB/fMLF- and A23187-induced primary granule exocytosis.
Neutrophils were preincubated with increasing concentration of either Lat B or JP for 15 min followed by stimulation with CB/fMLF or A23187 for 15 min at 37°C. Extracellular supernatants were collected from each condition and assayed for MPO activity. The release of MPO was calculated as a percentage of total cellular mediator activity (± SEM) of lysed cells and then normalized to stimulus alone for each for at least three independent experiments. Statistical significance is compared to the no drug condition.
* $p < 0.05$, ** $p < 0.01$, *** $p < 0.001$.

coated glass slides for staining. Resting neutrophils showed diffuse primary granule staining with an intact cortical ring-like structure (Figure 13). Intensity profiling (Figure 13, right column) revealed sharp peaks at the cell periphery for the rhodamine-phalloidin staining corresponding to the actin cortical ring, but relatively even distribution of CD63. When stimulated with CB/fMLF, F-actin polarization occurred along with the redistribution of primary granules to the same sites. This was evident from the colocalization of peaks on the one side of the intensity profile. Pre-treatment of the cells with JP resulted in diffuse F-actin staining and less prominent cortical actin ring. While the primary granules were also relatively diffuse, there was a detectable translocation of granules toward the cell membrane after CB/fMLF stimulation (Figure 13). This suggests that stabilization of F-actin may allow for the movement of granules to the periphery of the cell for exocytosis, but stabilization of the cortical ring hindered the final docking/fusion step required for exocytosis.

Next, we examined the morphology of the neutrophils treated with stimulatory versus inhibitory doses of Lat B in conjunction with CB/fMLF. Intriguingly, at a low dose of Lat B (1.25 μM) together with CB/fMLF, there was increased primary granule translocation to the cell periphery and reduced cytoplasmic F-actin staining in a diffuse, non-polarized state (Figure 13). At a high dose of Lat B (50 μM) together with CB/fMLF, the pattern of F-actin staining resembled the intensity profile of low Lat B and CB/fMLF. However, at high Lat B and CB/fMLF, CD63+ granule staining was distinctly enhanced throughout the cytoplasm, suggesting retention of primary granules in the neutrophil. These observations confirmed the results from the biochemical assays which showed high doses of Lat B inhibited CB/fMLF-induced primary granule exocytosis.

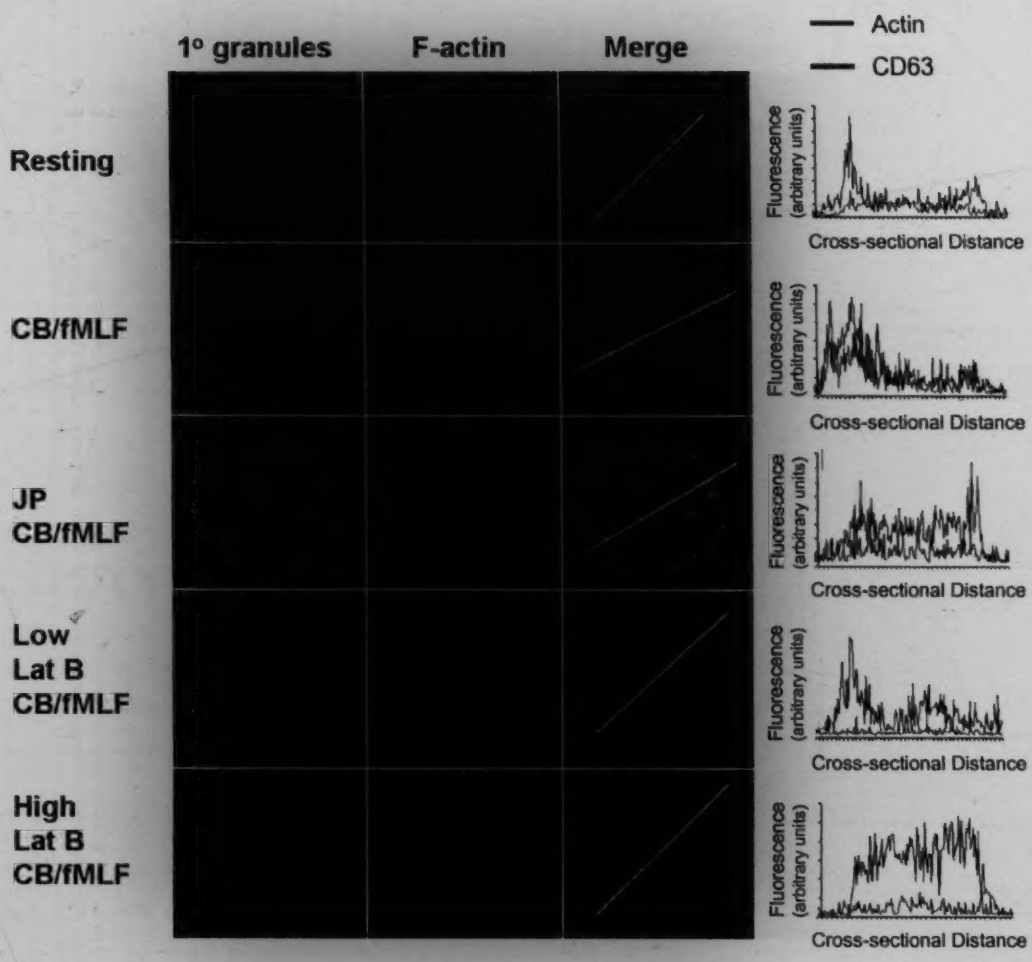

Figure 13. Morphological analysis of stimulated neutrophils pretreated with actin altering drugs.

Samples were prepared by treatment of neutrophils in suspension with either 1.25 μM (stimulatory dose) Lat B, 50 μM (inhibitory dose) Lat B or 10 μM JP for 15 min, followed by stimulation 10 μM CB 5 min/5 μM fMLF for 15 min at 37°C. Cells were fixed in 2% paraformaldehyde with 0.25 M sucrose PBS solution while still in suspension to maintain cell integrity. They were then adhered to glass slides with poly-L-lysine. Cellular F-actin was stained with rhodamine-phalloidin (*red*) and primary granules were stained with Alexa-Fluor 488-conjugated CD63 antibodies (*green*). Cross-sectional intensity profiles for F-actin (*red line*) and primary granules (*green line*) are shown on the right. Images are representative of at least 75% of cells on slides. Scale: each panel is 12 μm x 12 μm. $n = 3$.

4.2.3. The Rac inhibitor NSC 23766 blocks human neutrophil Rac1 and Rac2 activation

Our lab has previously shown that primary granule exocytosis was reduced in Rac2-/- murine bone marrow neutrophils, which was associated with a lack of primary granule translocation to the cell membrane during stimulation (59). Accordingly, we examined whether Rac regulates primary granule exocytosis by altering actin cytoskeletal dynamics in human neutrophils. NSC23766, a small molecule Rac inhibitor, has been shown to inhibit the binding of GTP to both Rac1 and Rac2, which is necessary for small G-protein activation and signalling (112, 113). NSC23766 blocks Rac function by binding to Trp56 and specifically inhibiting the binding of GEFs Trio and Tiam1 (112). However, it has yet to be determined to physically inhibit GTP binding to Rac1 and Rac2 in human neutrophils. Thus, we investigated the effects of NSC23766 on Rac activation in stimulated neutrophils. We used a pull-down assay where GST was conjugated to the Rac-binding domain of p21-activated kinase (PAK), which specifically associates with GTP-bound Rac or Cdc42 (82). Neutrophils stimulated with fMLF or CB/fMLF showed increased GTP binding to both total Rac (Figure 14A) and Rac2 (Figure 14B), but pre-treatment with NSC23766 for 15 min prior to stimulation reduced GTP binding. In contrast, the inhibitory effect of NSC23766 on GTP binding by total Rac and Rac2 was less evident in Lat B/fMLF-stimulated cells. In addition, we compared the effects of stimulation at different time intervals which showed enhanced levels of Rac-GTP in fMLF-stimulated samples at 1 min as compared to 15 min. These results indicate that the more highly specific actin depolymerization by Lat B versus CB acts to sustain Rac signalling, or elicit a positive feedback loop that countermand the inhibitory effects of

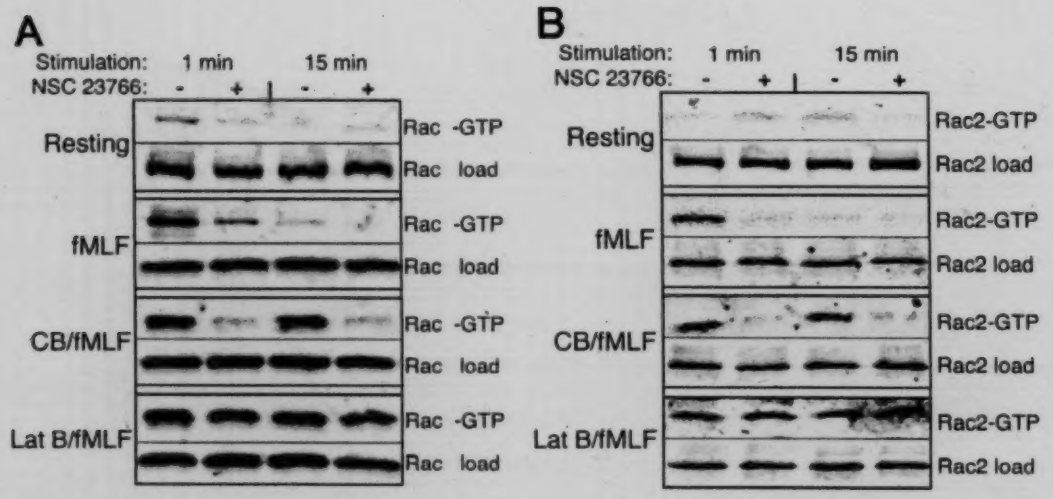

Figure 14. Detection of activated total Rac and Rac2 in stimulated neutrophils. Neutrophils were preincubated with 40 μM NSC23766 or vehicle for 15 min followed by stimulation for 1 min (left columns) or 15 min (right columns) with fMLF, CB/fMLF, or Lat B/fMLF. Control samples were not stimulated (Resting). Activated total *Rac-GTP* (A) or *Rac2-GTP* (B) was determined by incubation of 300 μg of lysates prepared from PBNs with 30 μg of GST-PBD beads (in 500 μl) and immunoblotting for total Rac and Rac2 in the bound fraction. Total *Rac load* and *Rac2 load* is immunoblot analysis of 30 μg total cell lysate. $n = 3$.

NSC23766 specifically in Lat B treated neutrophils. A23187 stimulation is not expected to increase Rac-GTP because changes in intracellular Ca^{2+} is not sufficient nor required for Rac activation (114).

4.2.4 The Rac inhibitor NSC23766 inhibits primary granule exocytosis and actin polymerization in response to CB/fMLF and Lat B/fMLF, but not A23187

To determine whether NSC23766 affects primary granule exocytosis in human neutrophils, we pre-treated cells with varying doses of NSC23766 for 15 min and then stimulated with CB/fMLF (10 μM/5 μM, respectively). This brief pre-treatment drastically reduced the secretion of primary granule MPO (Figure 15), which corresponded with inhibition of Rac activation (Figure 14). Figure 15 is normalized to the percentage of MPO release without drug as 100% but the actual percentage when stimulated with CB/fMLF or A23187 is usually approximately 60 to 80%. Inhibition was apparent at 10 μM NSC23766 and maximal at > 40 μM. Primary granule exocytosis in response to A23187 was not affected by NSC23766, even when treated with high doses (up to 160 μM). Interestingly, Lat B/fMLF-stimulated neutrophils also showed reduced MPO secretion when pre-treated with NSC23766 (Figure 15), although Rac remained activated (GTP-bound) under these conditions (Figure 14).

To associate F-actin formation with Rac activation, we examined whether inhibition of Rac using NSC23766 would affect F-actin polymerization. An *in vitro* actin polymerization assay was used; this measures the capacity of a sample to stimulate the polymerization of exogenously added pyrene-actin, which undergoes a fluorescence intensity increase when incorporated into F-actin. Neutrophil lysates prepared from fMLF or CB/fMLF stimulation and pre-treated with NSC23766 showed inhibition of F-

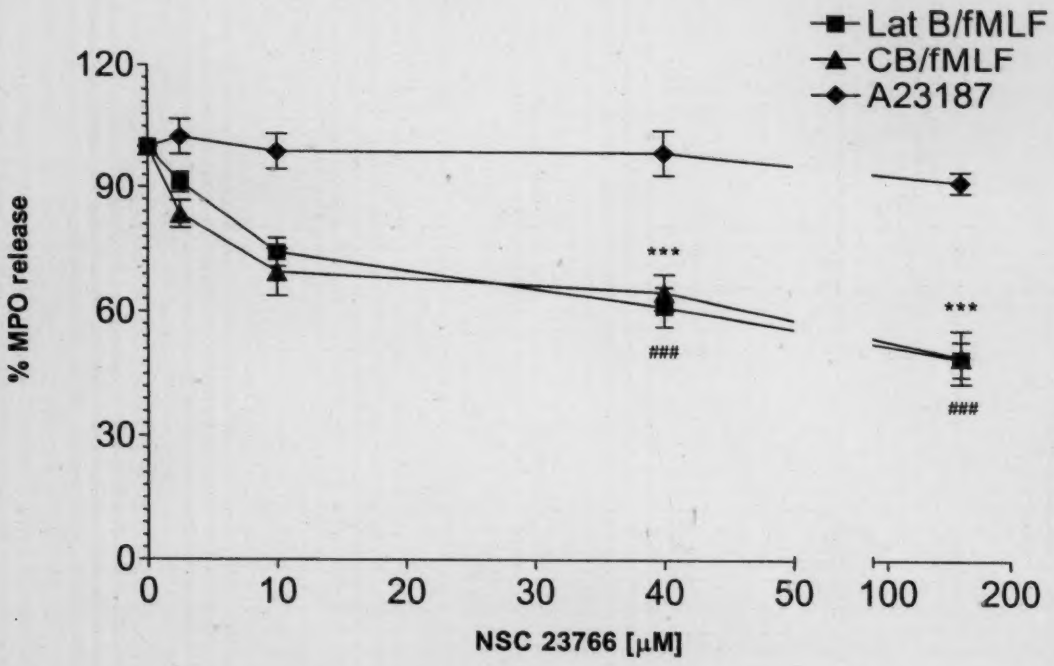

Figure 15. Effect of NSC23766 pre-treatment on neutrophil exocytosis.
Neutrophils were preincubated with increasing concentrations of NSC23766 for 15 min followed by stimulation with CB/fMLF, Lat B/fMLF or A23187 for 15 min at 37°C. Supernatants were collected from each condition and assayed for MPO activity. Release of MPO was calculated as a percentage of total cellular mediator activity (± SEM) of lysed cells and normalized to stimulus alone for at least three independent experiments. *** $p < 0.001$. * represents Lat B/fMLF and # represents CB/fMLF.

actin formation as compared to those without pre-treatment (Figure 16). However, there were negligible differences in lysates prepared from neutrophils that were stimulated with A23187.

We also investigated the effects of NSC23766 on respiratory burst induced by PMA or fMLF. Neutrophils that were pre-treated with NSC23766 for 15 min did not show any difference in O_2^- production compared to non-treated cells stimulated either with PMA (Figure 17A) or fMLF (Figure 17B). Agonists that activate G protein-coupled receptors, such as fMLF, have been shown to activate GEFs Vav1 and P-Rex1, leading to Rac activation necessary for respiratory burst (55, 115). Since NSC23766 was not able to inhibit O_2^- release from PMA-stimulated neutrophils, it can be inferred that a different GEF, such as Trio or Tiam1, may be responsible for activating Rac-mediated exocytosis of primary granules.

4.2.5. NSC23766 inhibits CB/fMLF- and Lat B/fMLF-induced primary granule translocation as visualized via confocal microscopy

Our results demonstrate that NSC23766 inhibits primary granule exocytosis in a dose dependent manner when stimulated with CB/fMLF or Lat B/fMLF. These observations were confirmed via confocal microscopy by examining neutrophils treated in the same fashion as those in the secretion assay. When stimulated with Lat B/fMLF, neutrophil primary granules translocated toward the periphery (Figure 18) which is also evident in the intensity profile as large peaks near the edge (Figure 18, right column). Unlike CB/fMLF stimulation, we did not see any significant polarization of F-actin at the cell membrane. Pre-treatment of neutrophils with NSC23766 followed by stimulation with CB/fMLF modestly reduced F-actin polarization at the cell periphery and, similar to

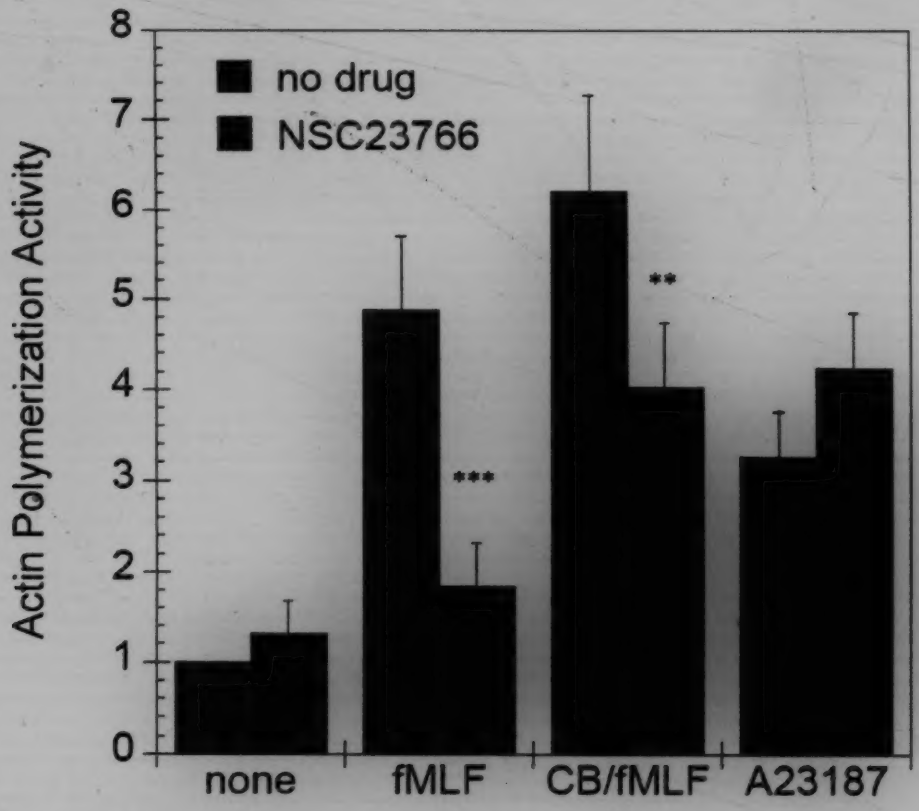

Figure 16. Determination of actin polymerization activity of neutrophil lysates. Actin polymerization stimulated by neutrophil lysates was determined by a pyrene-actin polymerization assay as described in the *Materials and Methods*, section 2.2.6. Polymerization reactions contained 5 μM pyrene-actin and 0.1 mg/ml neutrophil lysate prepared from resting cells, fMLF-, CB/fMLF- or A23187-stimulated cells. Lysates prepared from fMLF- or CB/fMLF-stimulated neutrophils showed enhanced polymerization activity (*grey bars*), which was reduced when cells were preincubated with NSC23766 (*black bars*). Shown are the average activities (± SEM) calculated from at least three independent experiments normalized to unstimulated samples (*Resting*). Statistical analysis is based on comparison to its respective condition with no NSC 23766. ** $p < 0.01$, *** $p < 0.001$.

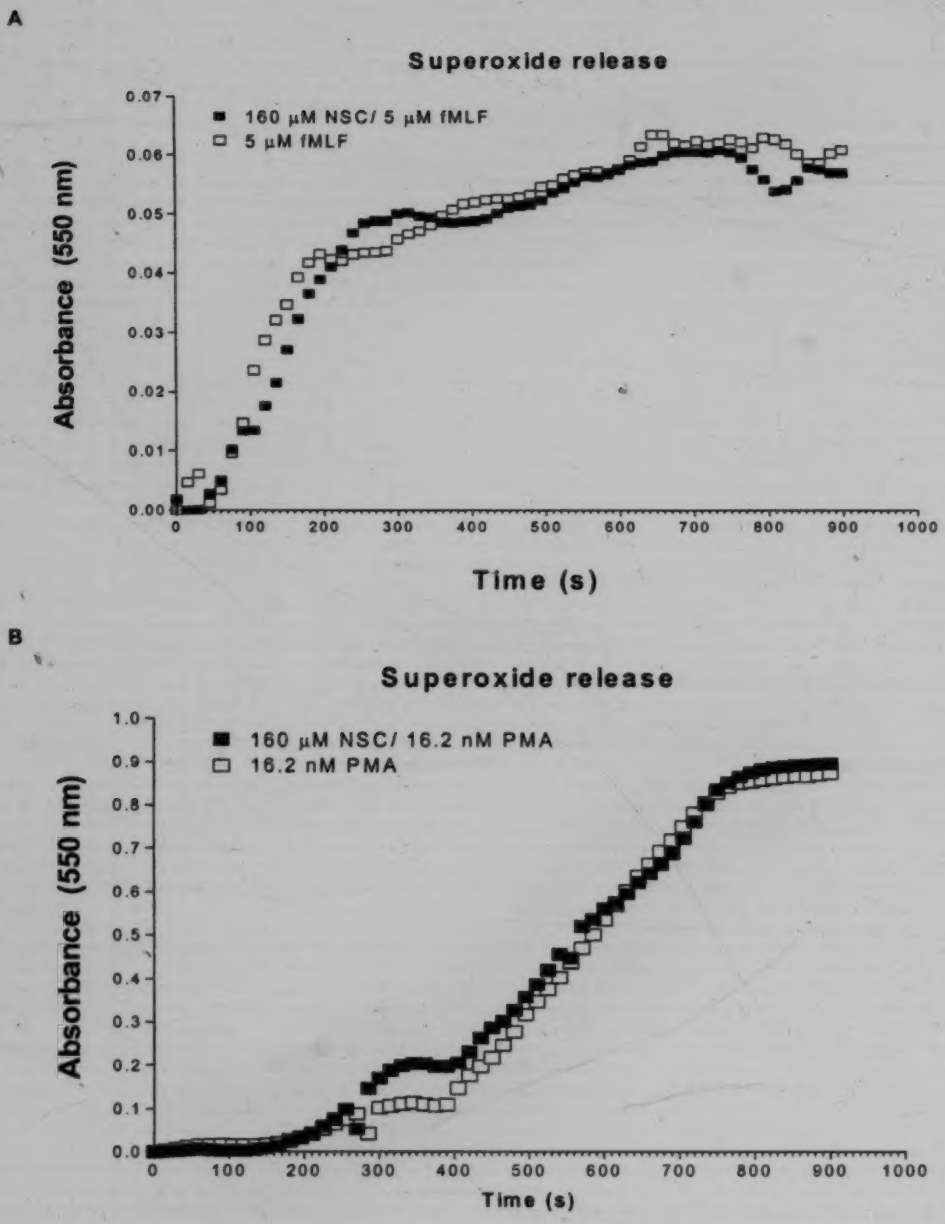

Figure 17. Effect of NSC23766 on respiratory burst.
Neutrophils (2 x 10^7/ml) were preincubated with 160 μM NSC23766 for 15 min at 37°C. Following this incubation step, 2 x 10^6 of either NSC23766 or non-treated neutrophils were suspended in 1-ml microcuvettes containing PBS+ and 50 μM ferricytochrome *c* at 25°C. The mixture was blanked at 550 nm. Stimulation of respiratory burst was achieved using either 5 μM fMLF (A) or 16.2 nM of PMA (B). Readings were collected every 15 s for a total running time of 15 min. $n = 1$.

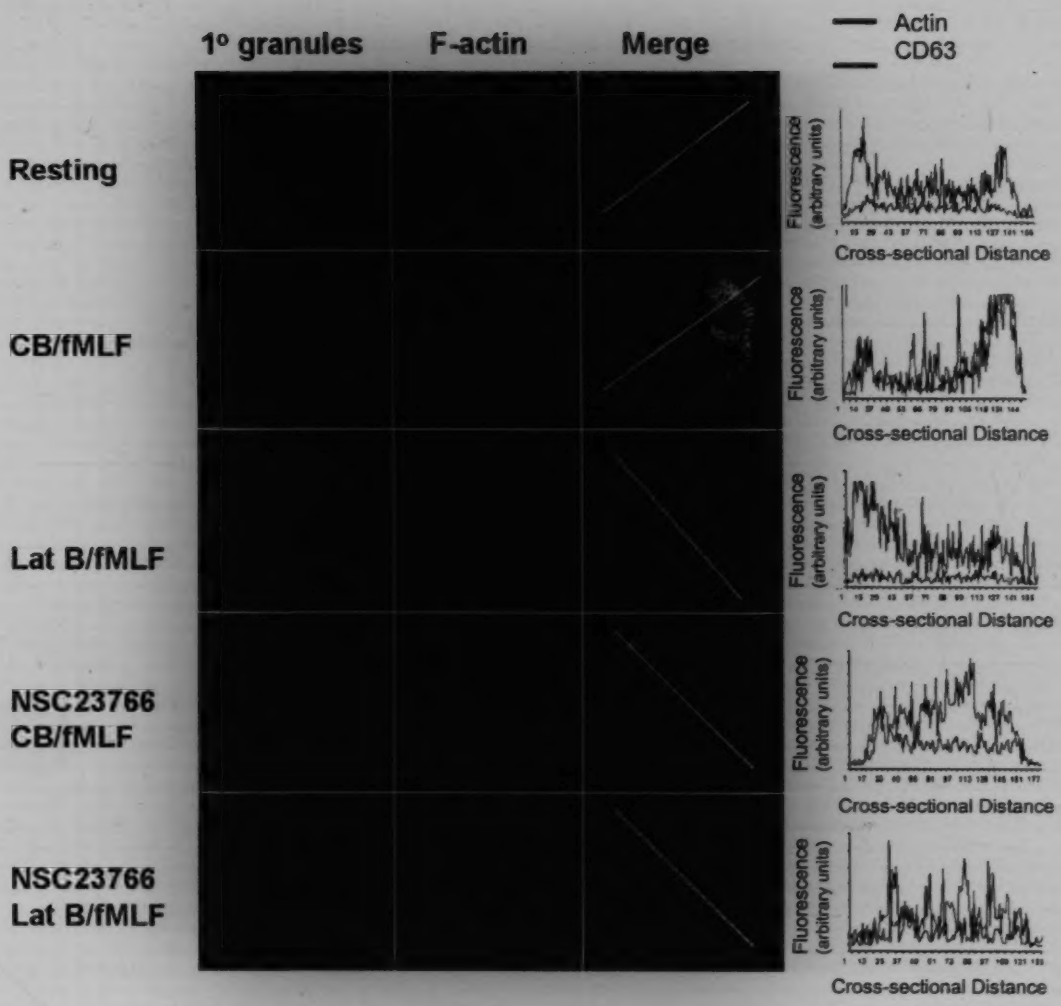

Figure 18. Morphological analysis of stimulated neutrophils pretreated with NSC23766.

Neutrophils pre-treated with NSC23766 were examined by confocal microscopy. Cells were treated in suspension with 40 μM NSC23766 (15 min), followed by stimulation with CB/fMLF or Lat B/fMLF (15 min) at 37°C. Cells were fixed in 2% paraformaldehyde with 0.25 M sucrose PBS solution while still in suspension to maintain cell integrity. They were then adhered to glass slides with poly-L-lysine. Cellular F-actin was stained with rhodamine-phalloidin (*red*) and primary granules were stained with Alexa-Fluor 488-conjugated CD63 antibodies (*green*). Cross-sectional intensity profiles for F-actin (*red line*) and primary granules (*green line*) are shown on the right. Images are representative of at least 75% of cells on slides. Scale: each panel is 12 μm x 12 μm. $n = 3$.

NSC23766 pre-treated Lat B/fMLF-stimulated neutrophils, inhibited primary granule translocation towards the cell membrane. These results suggest that NSC23766 inhibited primary granule progress from the cytoplasm to the cell periphery.

4.2.6. Actin polymerization is unaffected by NSC23766 as detected by flow cytometry

To confirm the results we observed from the *in vitro* actin polymerization assay we used stained neutrophils samples as previously described for the *in vitro* actin polymerization assay except cells were unfixed. We observed negligible differences between the various conditions which is different from the actin polymerization assay results which showed increased F-actin formation in CB/fMLF and fMLF samples, and a decreased F-actin formation in samples pre-treated with NSC23766 (Figure 19). One plausible explanation for this is the stimulation time of 15 min was too long to observe significant changes in F-actin, since these occur within 15 s of stimulation (61).

4.2.7. Electron microscopy

To support our observations from the confocal image analysis, we used EM to investigate changes in neutrophil morphology. EM provides better resolution and detail as to what was occurring with granule distribution inside the neutrophils. We stained the neutrophils with DAB to enhance the electron density of peroxidase-containing primary granules. Resting cells showed numerous vesicles evenly distributed throughout the cytoplasm (Figure 20A). When simulated with CB/fMLF, we saw fewer granules compared to resting neutrophils (Figure 20C). fMLF did not show any difference from resting (Figure 20B). Pre-treatment with JP resulted in clustering of granules in the centre of the cell but with a similar granule count to that seen in resting cells (Figure

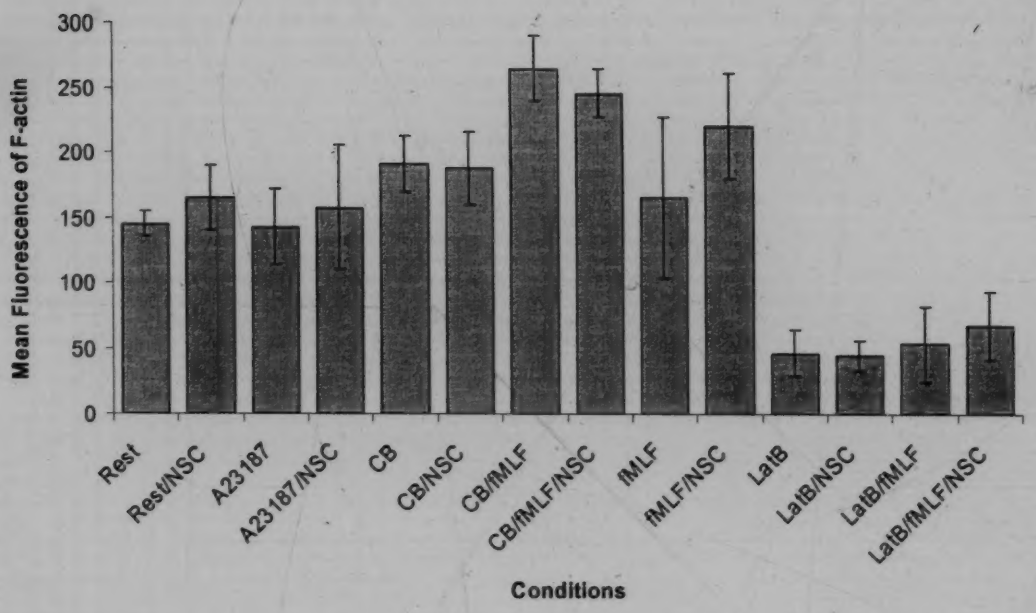

Figure 19. Mean fluorescence of F-actin in neutrophils pre-treated with NSC23766. Neutrophils were prepared in suspension with or without 40 μM of NSC 23766 for 15 min, followed by stimulation 10 μM CB (5 min)/5 μM fMLF (15 min), 10 μM Lat B (5 min)/5 μM fMLF (15 min), 2.5 μM A23187 (15 min); or 10 μM CB (5 min), 10 μM Lat B and 5 μM fMLF alone for 15 min at 37°C. Cells were then fixed in 4% paraformaldehyde for 30 min on ice. Following fixation, samples were permeabilized by incubation with 0.5% Triton-X100 in PBS and cellular F-actin was stained with rhodamine-phalloidin and primary granules were stained with Alexa-Fluor 488-conjugated CD63 antibodies. Sample volume was approximately 500 μl. This graph is a triplicate from one experiment.

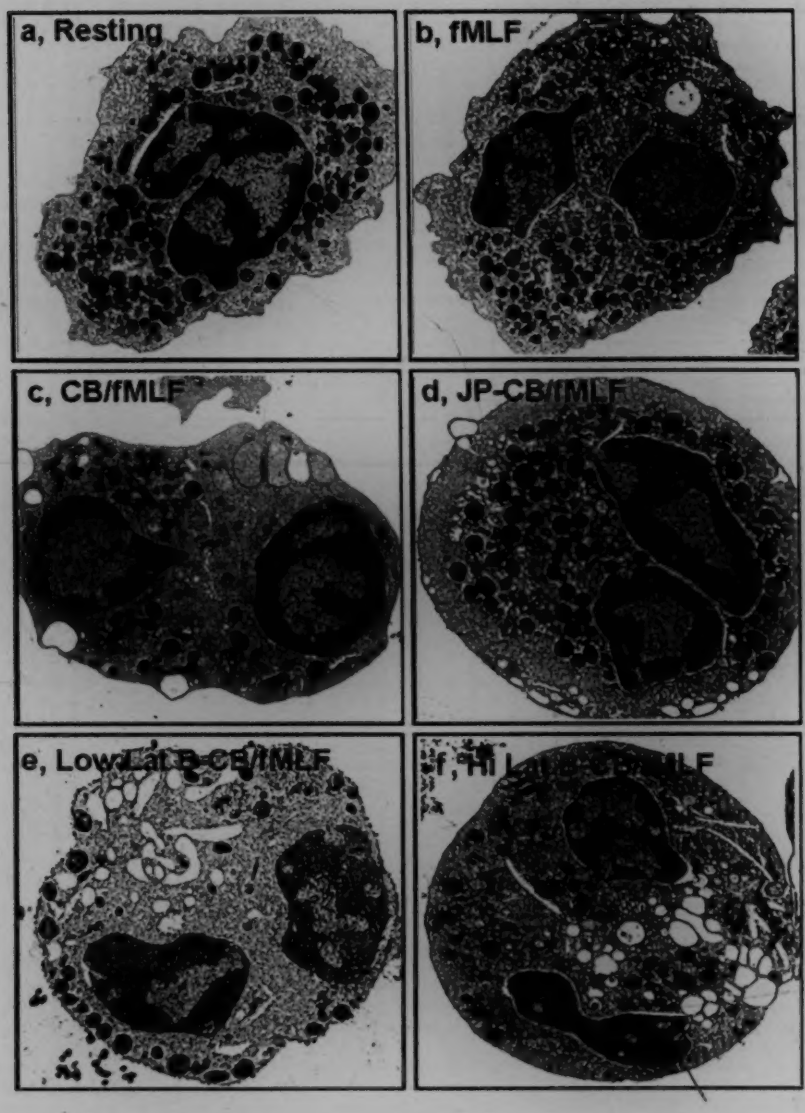

Figure 20. Electron micrographs of human neutrophils exposed to various stimulatory conditions and actin altering drugs.
Samples were prepared for EM analysis by treatment of cells at 37°C in suspension with a) no drugs; b) 5 μM fMLF (15 min); c) 10 μM CB (5 min) followed by 5 μM fMLF (15 min), hereby referred to as CB/fMLF; d) pre-incubation of 10 μM JP (15 min) followed by CB/fMLF; e) pre-incubation of 1.25 μM Lat B (15 min) followed by CB/fMLF; and f) pre-incubation of 50 μM Lat B (15 min) followed by CB/fMLF. This is representative of 90% of the cells in section and is representative of 3 separate experiments. The window size is 7 μm and magnification is 9100X.

20D). Intriguingly, at low doses of Lat B (1.25 μM) together with CB/fMLF, we see a decrease in the number of granules within the neutrophil and those that were still inside the cell were near the membrane (Figure 20E). However, high, or inhibitory, Lat B dose (50 μM) together with CB/fMLF showed similar granule count as resting cells, suggesting retention of granules in the cell (Figure 20F). These findings confirm the results from the biochemical assays where high doses of Lat B inhibited CB/fMLF-induced primary granule exocytosis and the confocal images. Figure 21 shows blinded neutrophil granule counts in graphical form.

When stimulated with Lat B/fMLF or CB/fMLF, neutrophils showed reduced granule counts compared to resting (Figure 22A, B, E). Pre-treatment of cells with NSC23766, then stimulation with CB/fMLF or Lat B/fMLF, to inhibited granule translocation since granule counts matched those seen in resting cells (Figure 22C, D). Figure 23 shows blinded neutrophil granule counts in graphical form.

Taken together, our results from EM confirm those seen in the secretion assay as well as confocal microscopy: inhibiting Rac or altering the dynamic balance of actin via stabilization (JP treatments) or conversely excessive depolymerization (with high Lat B treatments) significantly abrogates granule exocytosis.

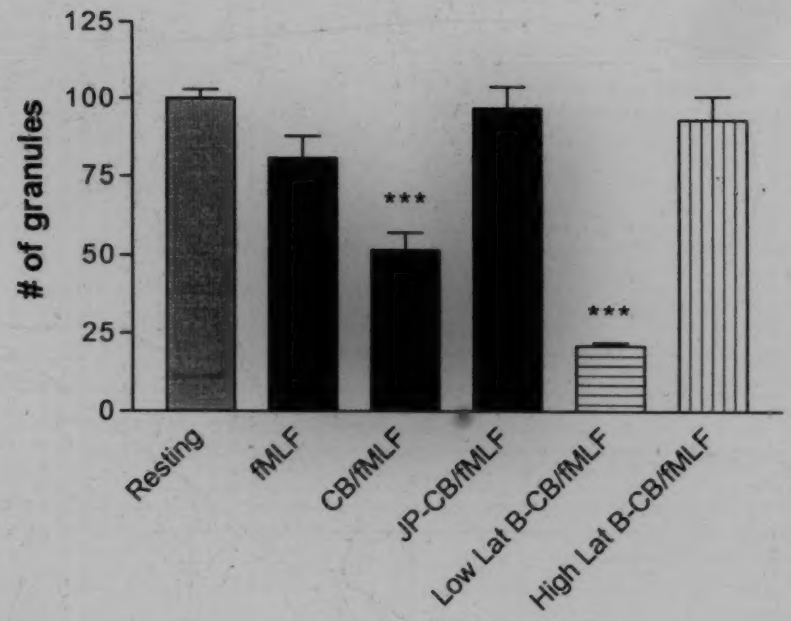

Figure 21. Granule count of neutrophils exposed to actin altering drugs.
Graphs were generated by granule count of nine separate cells that underwent that same treatment in three separate experiments. Statistically significant differences were seen in samples compared to the resting condition. *** $p < 0.001$.

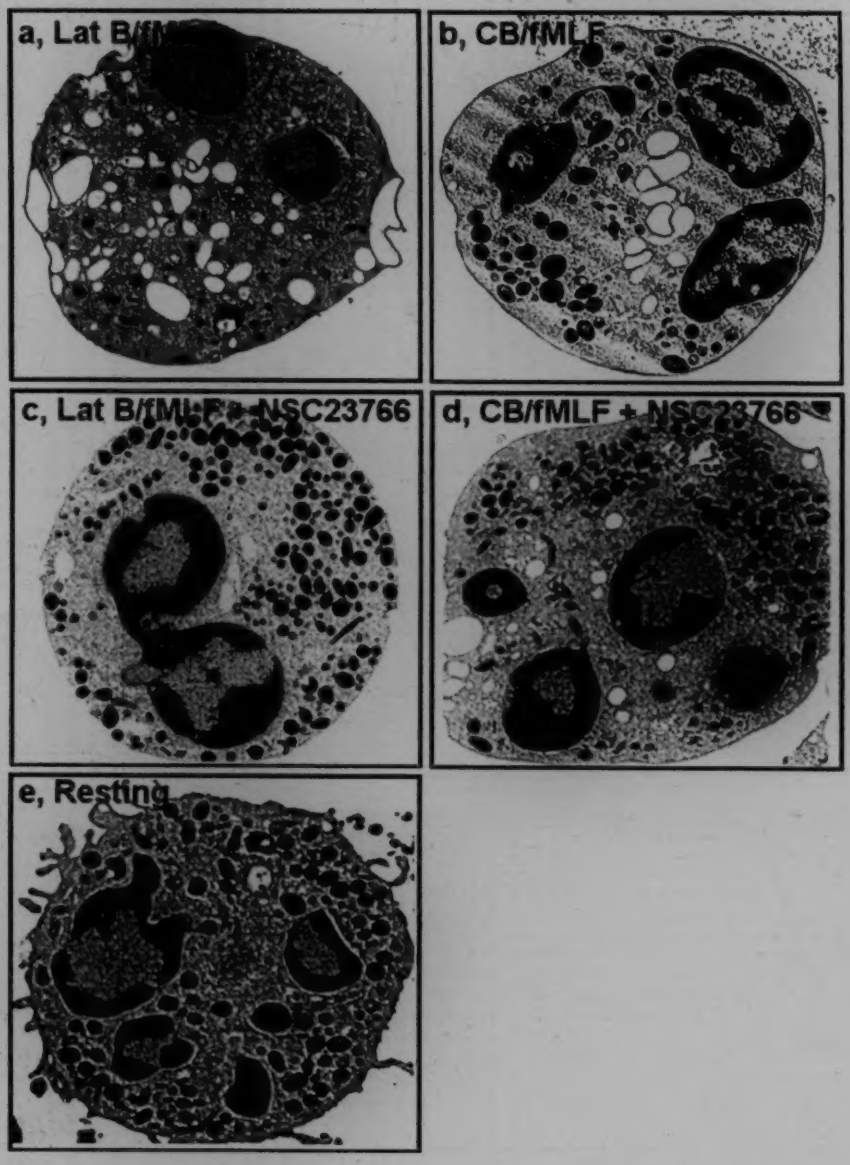

Figure 22. Electron micrographs of human neutrophils exposed to various stimulatory conditions and NSC23766.
Samples were prepared for EM analysis by stimulation with 5 μM fMLF (15 min) at 37°C with pre-treatment of cells at 37°C in suspension with a) 1.25 μM Lat B (5 min); b) 10 μM CB (5 min); c) 40 μM NSC23766 (15 min) followed by 1.25 μM Lat B (5 min); and d) 40 μM NSC23766 (15 min) followed by 10 μM CB (5 min). e) Neutrophils were not treated with any drug. This is representative of 90% of the cells in section and is representative of 3 separate experiments. The window size is 7 μm and magnification is 9100X.

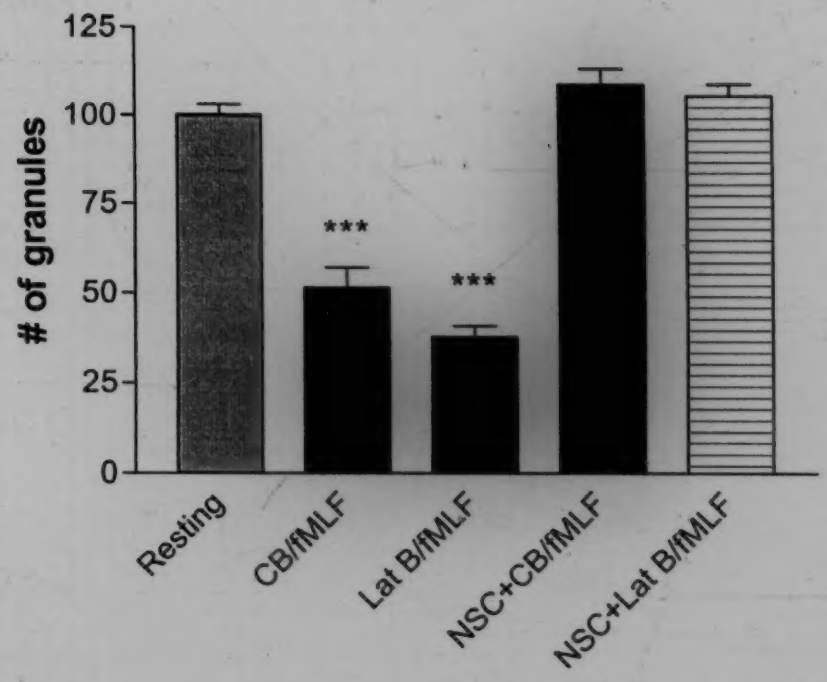

Figure 23. Granule count of neutrophils exposed to NSC23766.
Graphs were generated by granule count of nine separate cells that underwent that same treatment in three experiments. Statistically significant differences were seen in samples compared to the resting condition. *** $p < 0.001$.

4.3. Summary

We investigated the hypothesis that focal regions of actin remodelling are important for exocytosis through a comprehensive examination using pharmacological reagents that disrupt actin remodelling. Drugs that enhanced actin depolymerization stimulated exocytosis, but only at low concentrations. High doses, or combinations of depolymerization reagents, inhibited primary granule exocytosis, as did F-actin stabilization drugs at all doses tested. Confocal and electron microscopy imaging of suspended neutrophils was performed to visualize these and it showed that cortical actin was indeed remodelled. Moreover, F-actin patches were frequently seen to coincide with sites of exocytosis. We also show that NSC23766 blocks Rac activation in human neutrophils along with exocytosis and actin remodelling. However, it does not alter superoxide release, which effectively link exocytic mechanisms to Rac signalling.

The data provided by granule counting may not be statistically robust on its own since a limited number of cell sections were counted condition. Improvements to the granule count data could be made by counting a higher number of cells per experimental condition to enhance the robustness of these findings (up to a minimum of 10 cells per experiment in at least 3 separate experiments to give a total of 30 counted cells per condition). Furthermore, there may be human error in visually counting granules. To reduce this potential bias, computer software should be used to count the granules.

In summary, our results indicate that Rac plays an essential role in primary granule exocytosis via stimulation of actin polymerization to assist in granule mobilization to the cell membrane.

CHAPTER V - Discussion

5.1. Proteomic analysis

The use of proteomic technology to model systems provides unique insights into both the cellular biology of activated neutrophils and the regulation of its transduction machinery. We compared the proteomic profiles between WT unstimulated against WT CB/fMLF-stimulated, $Rac2^{-/-}$ unstimulated and $Rac2^{-/-}$ CB/fMLF-stimulated murine BMNs. Over 3500 individual spots were identified among the gels, and we attempted to establish spots of interest by rejecting those that: i) did not increase or decrease more than 1.5-fold in spot abundance, ii) had a high standard deviation when comparing replicate experiments, or iii) were present in less than two-thirds of replicate experiments. With these criteria, we narrowed our search down to 22 spots to be identified by mass spectrometry.

Most of the proteins identified were housekeeping proteins, but the finding of coronin was of significant interest. A hypothesis-generating study is one that groups and ranks data, suggesting possible relationships with other factors (i.e. generates an hypothesis). Indeed, our proteomic analysis between WT and $Rac2^{-/-}$ murine BMN created an important question: What is the role of coronin in the Rac2 pathway?

Coronin has been implicated in many actin-based processes such as cell mobility, phagocytosis and membrane trafficking (96, 116). Of the seven mammalian coronins characterized so far, most belong to the group of actin filament cross-linking and bundling proteins. Coronin-1 and -7 are mainly expressed in hematopoietic cells, coronin-5 and -6 are expressed in the brain, and coronin-2-4 are broadly expressed (96). Human neutrophils express coronin-1-4 and -7 (95).

Coronin-1 has been studied extensively in human phagocytic leukocytes and is present in cytosolic as well as cytoskeletal fractions. Macrophages and neutrophils exhibit phagocytic defects when coronin is knocked down (94, 95). Coronin is thought to act as a bridge between the actin cytoskeleton and the plasma membrane due to its membrane association (117). During phagosome formation, peripheral cytoskeleton and cytosolic coronin-1 staining is lost, and an association with the F-actin encompassing early phagocytic vacuoles can be seen (118). Dissociation of coronin-1 from the vacuole occurs along with the phosphorylation on serine residues involving PKC (118). Interestingly, the subcortical F-actin that surrounds the plasma membrane was unaffected in macrophages treated with an inhibitory coronin construct, suggesting that inhibition of coronin does not affect all actin-based processes (94).

While Rac2 has been shown to be important in neutrophil superoxide production and primary granule exocytosis, both of which require extensive actin cytoskeleton remodelling, there is a divergence in signalling pathways since PKC activation results in superoxide generation, but not in primary granule release. Given that PKC is not involved in primary granule release (119), one can assume coronin is also not involved in primary granule exocytosis. Indeed, Yan *et al* have shown that when coronin function is inhibited by transduction of a dominant-negative form of the protein, surface upregulation of CD63, a marker of primary granules, in response to cytochalasin D/fMLF or ionomycin is not affected as measured by flow cytometry when compared to control neutrophils (95). However, activation of the NADPH oxidase for superoxide production is also not affected by knocking down coronin (95). This is surprising since coronin has been previously demonstrated to associate directly with $p40^{phox}$ in a complex with $p47^{phox}$

and p67^{phox} (120). Furthermore, in neutrophils treated with PMA, a potent PKC activator, both p40^{phox} and coronin showed redistribution to perinuclear regions but this was not observed in patients with chronic granulomatosis disease lacking p47^{phox} or p67^{phox} (120). Grogan *et al* (120) suggests that the phox proteins may contribute to the regulation of the actin cytoskeleton through their interaction with coronin, although their precise role remains unknown.

The fact that the inhibition of coronin does not affect cortical actin, in macrophages, at least (94), lends credence to our conceptual model in which there exists two separate and distinct pools of actin for successful neutrophil primary granule exocytosis: the first in which Rac-mediated polymerization of actin must occur for granule translocation, and the final actin depolymerization step where the cortical actin ring must disperse for granule docking and release. One could speculate that coronin may be involved in the first step since it is decreased in both unstimulated and CB/fMLF-stimulated Rac2$^{-/-}$ BMN. On the contrary, inhibition of neutrophil coronin also does not have an effect on CD63 translocation to the cell membrane (95). In the face of such contrasting data, further experiments need to be done in order to elucidate the precise role of coronin in association with Rac2 and the actin cytoskeleton.

As with every method, there are limitations to proteomic analysis. One main problem is that we do not have a common and standard gel matrix to compare and reproducibly align protein patterns. It is very difficult to relate to the changes in expression levels on proteins on 2D gels when we can only see a tiny fraction of all proteins present. Only by using methodological manipulations such as subcellular fractionation, affinity-purification of samples or the use of zoom gels (which are used in

2D gels to cover narrow pH ranges and to give higher resolution, as well as being more sensitivity) can low abundance proteins be detected (100). Furthermore, because there is no analogous amplification step for proteins as polymerase chain reaction is for genes, proteins that are present in minute amounts are overshadowed by highly abundant proteins. These abundant proteins are usually housekeeping proteins; and in our data, we can see that this is the case. Regulatory proteins that are in low abundance, like GTPases, kinases and phosphatases, or hard to isolate proteins, like hydrophobic transmembrane receptors and basic nuclear proteins, are rarely found (100).

There are still many issues with proteomics that needs to be resolved, but the application of functional proteomics can provide researchers with a tool to investigate signal transduction networks in inflammation. By confirming the subcellular localization of proteins and their interactions, we can learn more about the functions of proteins, providing us with unprecedented opportunities to unlock the mysteries of biological processes. This may potentially enable the discovery of disease-associated targets and more effective or novel therapeutic strategies.

5.2. Actin cytoskeleton

Actin remodelling is an essential part of exocytosis (121), although specific mechanisms have yet to be understood for stimuli that elicit neutrophil exocytosis. Our results show a necessity for both actin polymerization and depolymerization in primary granule exocytosis. Low concentrations of actin depolymerizing drugs enhanced degranulation, while high concentrations or combinations of these drugs inhibited this process. Through confocal imaging of neutrophils, we observed that cortical actin was remodelled during CB/fMLF stimulation into polarized patches at the cell membrane that colocalized with

primary granules. Lat B/fMLF-stimulated cells also showed an increase in granule translocation, however, as a more potent actin destabilizer, it showed less polarization of actin to sites of granule translocation. JP, an actin stabilizing drug, was inhibitory to primary granule exocytosis at all doses tested, but interestingly, it did not completely block granule translocation. A23187-stimulated neutrophils exhibited similar responses to all the actin drug treated CB/fMLF-stimulated neutrophils, suggesting that Ca^{2+} and Rac2 signalling may share a common pathway for actin cytoskeleton remodelling for primary granule exocytosis.

There was an F-actin cortical ring in resting neutrophils, similar to that seen in resting mast cells (45), which dissipated when stimulated with CB/fMLF and more significantly, Lat B/fMLF. This is in contrast from previous studies that showed diffuse F-actin in resting neutrophils which then assembled into a cortical ring upon stimulation with fMLF (65, 75). The explanation behind this discrepancy is most likely methodological as neutrophil purification procedures, which differed in our study (used Ficoll rather than Percoll to purify), have a significant effect on morphology.

Our results show evidence that F-actin affecting drugs, either through stimulating or preventing depolymerization, inhibit neutrophil degranulation. However, we also discovered that at very low concentrations of Lat B, in conjunction with CB/fMLF, enhanced granule translocation and exocytosis. This suggests there may be a requirement for increased actin depolymerization, perhaps through the reduction of the actin polarization patch seen in CB/fMLF alone. Our results indicate there may be two pools of actin implicated in the regulation of neutrophil degranulation, especially in the case of primary granules, analogous to that observed in neuroendocrine cell exocytosis (71).

Since actin remodelling steps are necessary for chemotaxis when neutrophils encounter a chemoattractant (65), it is logical to think that actin remodelling may also facilitate polarized granule translocation and exocytosis. A shift from G-actin to F-actin would be required to expedite granule mobilization to the cell membrane. However, this idea is in direct contrast with the need for depolymerization of F-actin in order for primary granules to exocytose since depolymerizing drugs are required to achieve this in vitro (59, 108, 109). Furthermore, it is plausible that the cortical actin ring-like structure seen in resting neutrophils acts as a physical impediment which restricts random granule docking and fusion, similar to mast cells (45). There is a preferential reorganization of F-actin in neutrophils upon stimulation with CB/fMLF, and although the cortical ring-like structure dissipates when treated with CB/fMLF, F-actin was not completely converted into G-actin. However, it is difficult to arrive at conclusions regarding the role of actin in exocytosis in the presence of actin-depolymerizing drugs. Instead, it was reorganized and polarized to sites of primary granule translocation at the cell periphery. Our results suggest that fMLF activation of Rac initiates F-actin rearrangement and polarization. Lat B was much more efficacious in stimulating F-actin depolymerization as observed from our confocal images, which was also confirmed in the biochemical assays of primary granule exocytosis. This is likely due to the higher specificity that Lat B has for actin depolymerization than CB, clearly shown in our dose-response curves.

We show for the first time that the small molecule Rac inhibitor NSC23766 inhibited primary granule exocytosis in response to CB/fMLF or Lat B/fMLF stimulation. Similar to effects the gene-deletion of Rac2 in neutrophils (59), Rac may play a key role in regulation of primary granule exocytosis in human neutrophils. When we examined

Rac activation using Lat B/fMLF as a stimulus, there was prolonged Rac1- or Rac2-GTP formation when neutrophils were pre-treated with a dose of NSC23766 that inhibited degranulation. Our explanation for this is that an unknown molecule, not yet elucidated, is able to sense increases in G-actin to promote sustained activation of Rac by a GEF which is not affected by NSC23766. Currently, only the association of two Rac GEFs, Trio and Tiam1, are known to be blocked by NSC23766 while this drug has no effect on Vav1 association (112). It should be noted that we have not observed a lack of Rac-GTP formation in the presence of MPO secretion. Therefore, Rac-GTP may be necessary, but not sufficient for primary granule exocytosis, and Rac-GTP formation may be dissociated from primary granule exocytosis.

From our imaging and biochemical analyses of granule exocytosis, we showed that NSC23766 inhibited cytoplasmic F-actin polymerization, as well as primary granule translocation for subsequent exocytosis in response to CB/fMLF or Lat B/fMLF. This suggests that Rac may signal through F-actin polymerization to cause granule translocation to the cell periphery. Conversely, NSC23766 had no effect on Ca^{2+} ionophore-stimulated exocytosis, indicating that Ca^{2+} acts downstream of Rac to activate granule translocation and secretion. Previous studies have shown that Ca^{2+} signalling is very important in granule exocytosis in RBL-2H3 cells, and that Ca^{2+} levels were decreased when cells were exposed to dominant negative constructs of Rac proteins but were restored when exposed to constitutively active forms of Rac (122). Thus, it is reasonable to assume that Rac-mediated signalling, specifically Rac2 signalling in neutrophils, takes advantage of the Ca^{2+} pathway as a means of primary granule translocation and exocytosis.

In conclusion, our results highlight a possible mechanism by which Rac controls exocytosis and release of primary granule contents through favourable F-actin formation which is necessary for granule translocation to sites of exocytosis. Evidently, there is also a requirement for F-actin depolymerization within the cell cortex, which is achieved in vitro by reagents such as CB or Lat B. When neutrophils are activated in response to infection or inflammation, numerous signalling cascades are turned on, leading to the necessary depolymerization steps needed to eliminate the cortical F-actin barrier concurrently with central F-actin polymerization to enhance granule movement to the cell membrane. Our results demonstrate a role for Rac in actin-mediated granule translocation, and a dynamic process that involves constant actin remodelling rather than simple static polymerization or depolymerization. Our experimental methodology will allow us to further characterize key regulatory molecules implicated in the Rac signalling pathway. This may lead to the development of novel therapeutic strategies for the treatment of inflammatory disorders including severe asthma and COPD, among numerous others.

5.3. Outcomes and future directions

Proteomics is the global analysis of changes in the abundance of proteins in a cell. The strengths of this approach include the potential identification of new targets for disease intervention and treatment, given that most drug targets are proteins. Knowledge of protein expression patterns can contribute new insights into toxic side effects during drug screening and can guide the optimization process. Additionally, specific proteins can be identified as biomarkers for a disease, furthering the usefulness of proteomics for diagnosis and prognosis. However, protein expression can fluctuate markedly during a

course of differentiation and in response to environmental stimuli, and many proteins can exist in multiple isoforms due to alternative splicing, RNA editing, alternative promoters and post-translational modifications (123). Furthermore, there are technical challenges associated with identifying low abundance proteins. Highly abundant proteins such as cytoskeletal proteins, chaperones, endoplasmic reticulum proteins, proteasome components and matrix proteins often overwhelm the detection of regulatory proteins of low abundance like GTPases, kinases, phosphatases, hydrophobic transmembrane receptors and basic nuclear proteins (100). Nevertheless, the use of large quantities of starting material has enabled the identification of low copy numbers of proteins by DIGE analysis (124).

From our new understandings of proteomic analysis, there are some limitations that can be addressed in the future. To start, in order to identify what kind of modification the protein spot had undergone rather than just looking for changes in abundance, we can do a Western Blot on the gels with anti-phospho/methyl/nitro antibodies. Furthermore, analyzing 2D gels with whole cell lysates now seems like a "shotgun" approach. Instead, subcellular fractions of neutrophil granules may be run on 2D gels between WT and $Rac2^{-/-}$ BMNs. Additionally, in future studies, it may be prudent to go beyond protein identification and analyse protein modifications.

An alternate proteomics approach may be to use multi-dimensional protein identification technology (MudPIT). Wolters et al described an automated method for "shotgun" proteomics that could be used to test our hypothesis (125). This technique combines multi-dimensional liquid chromatography with electrospray ionization tandem MS and is analogous to DNA sequencing. It is automated and it improves the overall

analysis of proteomes by identifying proteins of all functional and physical classes. Using this method, the Yates lab identified a total of 1484 proteins, one of the largest screens to date (126). Most importantly, a dynamic ratio of 10,000 to 1 was shown between the most abundant protein and the least abundant protein. They also identified 131 proteins with 3-12 predicted transmembrane domains that may have escaped identification using conventional proteomic approaches (100, 126).

For studies of how the actin cytoskeleton regulates neutrophil exocytosis, similar experiments could be performed to determine the effects of cytoskeletal drugs on the other granule subsets (secondary, tertiary and secretory) to see whether actin alterations can also affect their exocytosis. Furthermore, since Rac2 has only been shown to be essential for primary granule exocytosis (59), it may also be interesting to examine whether Rac inhibition, using NSC23766, has any effect on exocytosis of other granule subsets.

Based on the data presented and previous literature, a simple Rac2 pathway for fMLF-stimulated neutrophil primary granule exocytosis has been proposed (Figure 24). A chemotactic peptide such as fMLF binds to a FPR, leading to PLC activation through the G_α subunit of the heterotrimeric G protein. PLC then catalyzes the cleavage of PIP_2 into IP_3 and DAG. DAG activates PKC, and PKC triggers the activation of Tiam1. Tiam1 enhances the exchange of GDP for GTP on Rac2. Rac2 activation also leads to PLC, coronin and finally, Arp2/3 complex activation. Arp2/3 causes actin polymerization which allows for granule attachment on the filament to be translocated to the cell periphery. Arp2/3 binds to the pointed end of actin, mimicking the barbed end, which has higher affinity for new monomer addition (127).

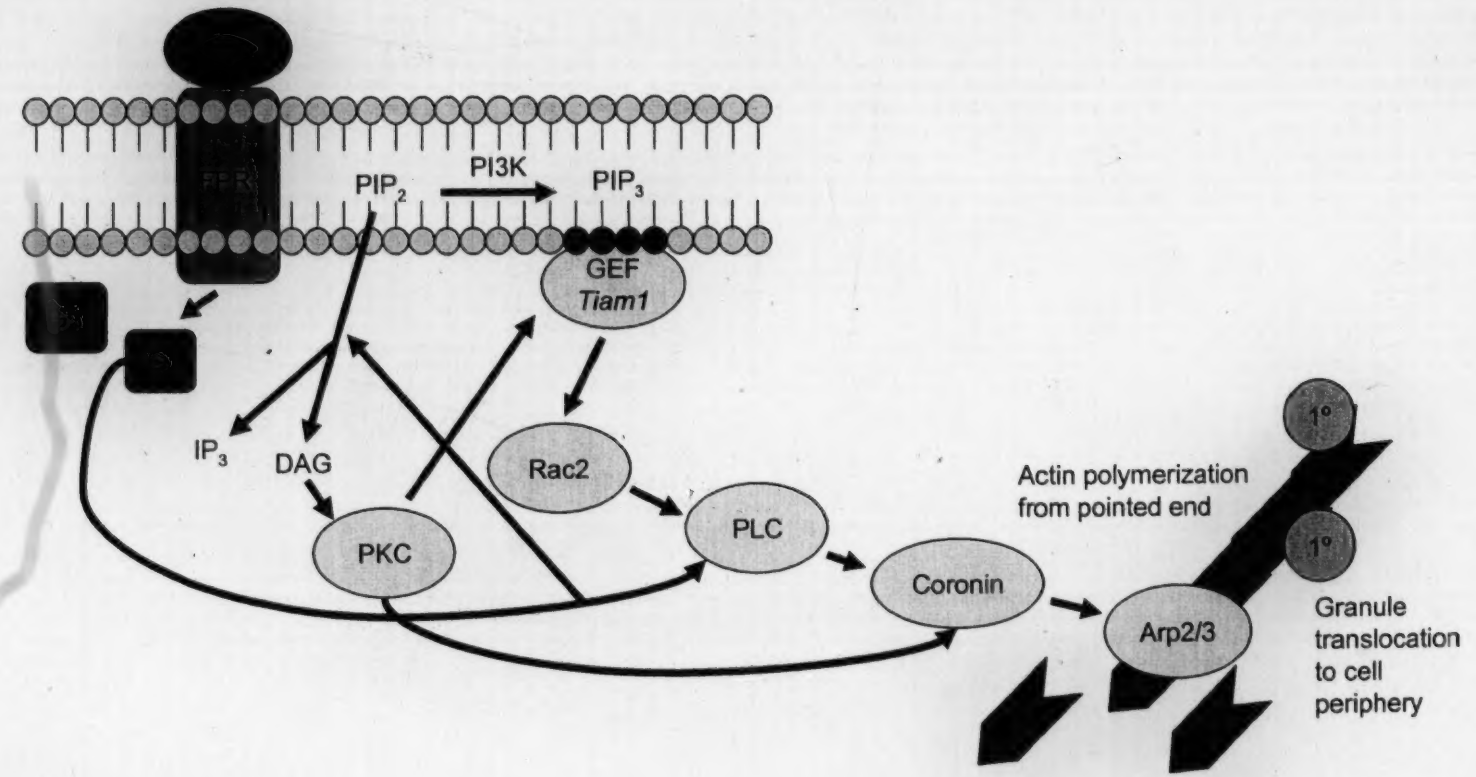

Figure 21. Conceptual model of fMLF-induced Rac2 pathway leading to actin polymerization for primary granule translocation to cell periphery.

A chemotactic peptide such as fMLF binds to FPR, leading to PLC activation through the Gα subunit of the heterotrimeric G protein. PLC catalyzes the cleavage of PIP2 into IP3 and DAG. DAG activates PKC, and PKC triggers the activation of Tiam1. Tiam1 enhances the exchange of GDP for GTP on Rac2. Rac2 activation also leads to PLC, coronin and finally Arp2/3 complex activation. Arp2/3 causes actin polymerization which allows for granule attachment on the filament to be translocated to the cell periphery.

References

1. Fialkow, L., Y. Wang, and G. P. Downey. 2007. Reactive oxygen and nitrogen species as signaling molecules regulating neutrophil function. *Free Radic Biol Med* 42:153-164.
2. Babior, B. M., J. D. Lambeth, and W. Nauseef. 2002. The neutrophil NADPH oxidase. *Arch Biochem Biophys* 397:342-344.
3. Klebanoff, S. J. 1968. Myeloperoxidase-halide-hydrogen peroxide antibacterial system. *J Bacteriol* 95:2131-2138.
4. Sheppard, F. R., M. R. Kelher, E. E. Moore, N. J. McLaughlin, A. Banerjee, and C. C. Silliman. 2005. Structural organization of the neutrophil NADPH oxidase: phosphorylation and translocation during priming and activation. *J Leukoc Biol* 78:1025-1042.
5. Lacy, P. 2005. The role of Rho GTPases and SNAREs in mediator release from granulocytes. *Pharmacol Ther* 107:358-376.
6. Schwartzberg, L. S. 2006. Neutropenia: etiology and pathogenesis. *Clin Cornerstone* 8 Suppl 5:S5-11.
7. Malech, H. L., and W. M. Nauseef. 1997. Primary inherited defects in neutrophil function: etiology and treatment. *Semin Hematol* 34:279-290.
8. Goldsby, R. A., and R. A. Goldsby. 2003. *Immunology*. W.H. Freeman, New York.
9. Dellinger, R. P., M. M. Levy, J. M. Carlet, J. Bion, M. M. Parker, R. Jaeschke, K. Reinhart, D. C. Angus, C. Brun-Buisson, R. Beale, T. Calandra, J. F. Dhainaut, H. Gerlach, M. Harvey, J. J. Marini, J. Marshall, M. Ranieri, G. Ramsay, J. Sevransky, B. T. Thompson, S. Townsend, J. S. Vender, J. L. Zimmerman, and J. L. Vincent. 2008. Surviving Sepsis Campaign: international guidelines for management of severe sepsis and septic shock: 2008. *Crit Care Med* 36:296-327.
10. Rubenfeld, G. D., and M. S. Herridge. 2007. Epidemiology and outcomes of acute lung injury. *Chest* 131:554-562.
11. Libby, P. 2007. Inflammatory mechanisms: the molecular basis of inflammation and disease. *Nutr Rev* 65:S140-146.
12. Meagher, L. C., J. M. Cousin, J. R. Seckl, and C. Haslett. 1996. Opposing effects of glucocorticoids on the rate of apoptosis in neutrophilic and eosinophilic granulocytes. *J Immunol* 156:4422-4428.
13. Little, S. A., K. J. MacLeod, G. W. Chalmers, J. G. Love, C. McSharry, and N. C. Thomson. 2002. Association of forced expiratory volume with disease duration and sputum neutrophils in chronic asthma. *Am J Med* 112:446-452.
14. Wenzel, S. E., S. J. Szefler, D. Y. Leung, S. I. Sloan, M. D. Rex, and R. J. Martin. 1997. Bronchoscopic evaluation of severe asthma. Persistent inflammation associated with high dose glucocorticoids. *Am J Respir Crit Care Med* 156:737-743.
15. Green, R. H., C. E. Brightling, G. Woltmann, D. Parker, A. J. Wardlaw, and I. D. Pavord. 2002. Analysis of induced sputum in adults with asthma: identification of subgroup with isolated sputum neutrophilia and poor response to inhaled corticosteroids. *Thorax* 57:875-879.

16. Chalmers, G. W., K. J. MacLeod, L. Thomson, S. A. Little, C. McSharry, and N. C. Thomson. 2001. Smoking and airway inflammation in patients with mild asthma. *Chest* 120:1917-1922.
17. Fahy, J. V., K. W. Kim, J. Liu, and H. A. Boushey. 1995. Prominent neutrophilic inflammation in sputum from subjects with asthma exacerbation. *J Allergy Clin Immunol* 95:843-852.
18. Norzila, M. Z., K. Fakes, R. L. Henry, J. Simpson, and P. G. Gibson. 2000. Interleukin-8 secretion and neutrophil recruitment accompanies induced sputum eosinophil activation in children with acute asthma. *Am J Respir Crit Care Med* 161:769-774.
19. Rabe, K. F., S. Hurd, A. Anzueto, P. J. Barnes, S. A. Buist, P. Calverley, Y. Fukuchi, C. Jenkins, R. Rodriguez-Roisin, C. van Weel, and J. Zielinski. 2007. Global strategy for the diagnosis, management, and prevention of chronic obstructive pulmonary disease: GOLD executive summary. *Am J Respir Crit Care Med* 176:532-555.
20. Quint, J. K., and J. A. Wedzicha. 2007. The neutrophil in chronic obstructive pulmonary disease. *J Allergy Clin Immunol* 119:1065-1071.
21. Bosken, C. H., J. Hards, K. Gatter, and J. C. Hogg. 1992. Characterization of the inflammatory reaction in the peripheral airways of cigarette smokers using immunocytochemistry. *Am Rev Respir Dis* 145:911-917.
22. Baraldo, S., G. Turato, C. Badin, E. Bazzan, B. Beghe, R. Zuin, F. Calabrese, G. Casoni, P. Maestrelli, A. Papi, L. M. Fabbri, and M. Saetta. 2004. Neutrophilic infiltration within the airway smooth muscle in patients with COPD. *Thorax* 59:308-312.
23. Borregaard, N., and J. B. Cowland. 1997. Granules of the human neutrophilic polymorphonuclear leukocyte. *Blood* 89:3503-3521.
24. Sengelov, H., L. Kjeldsen, and N. Borregaard. 1993. Control of exocytosis in early neutrophil activation. *J Immunol* 150:1535-1543.
25. Wright, D. G., D. A. Bralove, and J. I. Gallin. 1977. The differential mobilization of human neutrophil granules. Effects of phorbol myristate acetate and ionophore A23187. *Am J Pathol* 87:237-284.
26. Faurschou, M., and N. Borregaard. 2003. Neutrophil granules and secretory vesicles in inflammation. *Microbes Infect* 5:1317-1327.
27. Bainton, D. F., and M. G. Farquhar. 1966. Origin of granules in polymorphonuclear leukocytes. Two types derived from opposite faces of the Golgi complex in developing granulocytes. *J Cell Biol* 28:277-301.
28. Bainton, D. F., J. L. Ullyot, and M. G. Farquhar. 1971. The development of neutrophilic polymorphonuclear leukocytes in human bone marrow. *J Exp Med* 134:907-934.
29. Spicer, S. S., and J. H. Hardin. 1969. Ultrastructure, cytochemistry, and function of neutrophil leukocyte granules. A review. *Lab Invest* 20:488-497.
30. Joiner, K. A., T. Ganz, J. Albert, and D. Rotrosen. 1989. The opsonizing ligand on Salmonella typhimurium influences incorporation of specific, but not azurophil, granule constituents into neutrophil phagosomes. *J Cell Biol* 109:2771-2782.

31. Niessen, H. W., and A. J. Verhoeven. 1992. Differential up-regulation of specific and azurophilic granule membrane markers in electropermeabilized neutrophils. *Cell Signal* 4:501-509.
32. Nusse, O., and M. Lindau. 1988. The dynamics of exocytosis in human neutrophils. *J Cell Biol* 107:2117-2123.
33. Lollike, K., M. Lindau, J. Calafat, and N. Borregaard. 2002. Compound exocytosis of granules in human neutrophils. *J Leukoc Biol* 71:973-980.
34. Oram, J. D., and B. Reiter. 1968. Inhibition of bacteria by lactoferrin and other iron-chelating agents. *Biochim Biophys Acta* 170:351-365.
35. Mollinedo, F., M. Nakajima, A. Llorens, E. Barbosa, S. Callejo, C. Gajate, and A. Fabra. 1997. Major co-localization of the extracellular-matrix degradative enzymes heparanase and gelatinase in tertiary granules of human neutrophils. *Biochem J* 327 (Pt 3):917-923.
36. Owen, C. A., and E. J. Campbell. 1999. The cell biology of leukocyte-mediated proteolysis. *J Leukoc Biol* 65:137-150.
37. Borregaard, N., L. Kjeldsen, K. Rygaard, L. Bastholm, M. H. Nielsen, H. Sengelov, O. W. Bjerrum, and A. H. Johnsen. 1992. Stimulus-dependent secretion of plasma proteins from human neutrophils. *J Clin Invest* 90:86-96.
38. Borregaard, N., L. J. Miller, and T. A. Springer. 1987. Chemoattractant-regulated mobilization of a novel intracellular compartment in human neutrophils. *Science* 237:1204-1206.
39. DeChatelet, L. R., and M. R. Cooper. 1970. A modified procedure for the determination of leukocyte alkaline phosphatase. *Biochem Med* 4:61-68.
40. Kjeldsen, L., H. Sengelov, and N. Borregaard. 1999. Subcellular fractionation of human neutrophils on Percoll density gradients. *J Immunol Methods* 232:131-143.
41. Toonen, R. F., and M. Verhage. 2003. Vesicle trafficking: pleasure and pain from SM genes. *Trends Cell Biol* 13:177-186.
42. Burgoyne, R. D., and A. Morgan. 2003. Secretory granule exocytosis. *Physiol Rev* 83:581-632.
43. Etienne-Manneville, S., and A. Hall. 2002. Rho GTPases in cell biology. *Nature* 420:629-635.
44. Wennerberg, K., and C. J. Der. 2004. Rho-family GTPases: it's not only Rac and Rho (and I like it). *J Cell Sci* 117:1301-1312.
45. Norman, J. C., L. S. Price, A. J. Ridley, and A. Koffer. 1996. The small GTP-binding proteins, Rac and Rho, regulate cytoskeletal organization and exocytosis in mast cells by parallel pathways. *Mol Biol Cell* 7:1429-1442.
46. Van Aelst, L., and C. D'Souza-Schorey. 1997. Rho GTPases and signaling networks. *Genes Dev* 11:2295-2322.
47. Just, I., J. Selzer, M. Wilm, C. von Eichel-Streiber, M. Mann, and K. Aktories. 1995. Glucosylation of Rho proteins by Clostridium difficile toxin B. *Nature* 375:500-503.
48. Popoff, M. R., E. Chaves-Olarte, E. Lemichez, C. von Eichel-Streiber, M. Thelestam, P. Chardin, D. Cussac, B. Antonny, P. Chavrier, G. Flatau, M. Giry, J. de Gunzburg, and P. Boquet. 1996. Ras, Rap, and Rac small GTP-binding proteins are targets for Clostridium sordellii lethal toxin glucosylation. *J Biol Chem* 271:10217-10224.

49. Schmitz, A. A., E. E. Govek, B. Bottner, and L. Van Aelst. 2000. Rho GTPases: signaling, migration, and invasion. *Exp Cell Res* 261:1-12.
50. Ron, D., M. Zannini, M. Lewis, R. B. Wickner, L. T. Hunt, G. Graziani, S. R. Tronick, S. A. Aaronson, and A. Eva. 1991. A region of proto-dbl essential for its transforming activity shows sequence similarity to a yeast cell cycle gene, CDC24, and the human breakpoint cluster gene, bcr. *New Biol* 3:372-379.
51. Sivalenka, R. R., and R. Jessberger. 2004. SWAP-70 regulates c-kit-induced mast cell activation, cell-cell adhesion, and migration. *Mol Cell Biol* 24:10277-10288.
52. Yang, F. C., R. Kapur, A. J. King, W. Tao, C. Kim, J. Borneo, R. Breese, M. Marshall, M. C. Dinauer, and D. A. Williams. 2000. Rac2 stimulates Akt activation affecting BAD/Bcl-XL expression while mediating survival and actin function in primary mast cells. *Immunity* 12:557-568.
53. Haeusler, L. C., L. Blumenstein, P. Stege, R. Dvorsky, and M. R. Ahmadian. 2003. Comparative functional analysis of the Rac GTPases. *FEBS Lett* 555:556-560.
54. Kunisaki, Y., A. Nishikimi, Y. Tanaka, R. Takii, M. Noda, A. Inayoshi, K. Watanabe, F. Sanematsu, T. Sasazuki, T. Sasaki, and Y. Fukui. 2006. DOCK2 is a Rac activator that regulates motility and polarity during neutrophil chemotaxis. *J Cell Biol* 174:647-652.
55. Kim, C., C. C. Marchal, J. Penninger, and M. C. Dinauer. 2003. The hemopoietic Rho/Rac guanine nucleotide exchange factor Vav1 regulates N-formyl-methionyl-leucyl-phenylalanine-activated neutrophil functions. *J Immunol* 171:4425-4430.
56. Ming, W., S. Li, D. D. Billadeau, L. A. Quilliam, and M. C. Dinauer. 2007. The Rac effector p67phox regulates phagocyte NADPH oxidase by stimulating Vav1 guanine nucleotide exchange activity. *Mol Cell Biol* 27:312-323.
57. Welch, H. C., W. J. Coadwell, C. D. Ellson, G. J. Ferguson, S. R. Andrews, H. Erdjument-Bromage, P. Tempst, P. T. Hawkins, and L. R. Stephens. 2002. P-Rex1, a PtdIns(3,4,5)P3- and Gbetagamma-regulated guanine-nucleotide exchange factor for Rac. *Cell* 108:809-821.
58. Dong, X., Z. Mo, G. Bokoch, C. Guo, Z. Li, and D. Wu. 2005. P-Rex1 is a primary Rac2 guanine nucleotide exchange factor in mouse neutrophils. *Curr Biol* 15:1874-1879.
59. Abdel-Latif, D., M. Steward, D. L. Macdonald, G. A. Francis, M. C. Dinauer, and P. Lacy. 2004. Rac2 is critical for neutrophil primary granule exocytosis. *Blood* 104:832-839.
60. Li, S., A. Yamauchi, C. C. Marchal, J. K. Molitoris, L. A. Quilliam, and M. C. Dinauer. 2002. Chemoattractant-stimulated Rac activation in wild-type and Rac2-deficient murine neutrophils: preferential activation of Rac2 and Rac2 gene dosage effect on neutrophil functions. *J Immunol* 169:5043-5051.
61. Roberts, A. W., C. Kim, L. Zhen, J. B. Lowe, R. Kapur, B. Petryniak, A. Spaetti, J. D. Pollock, J. B. Borneo, G. B. Bradford, S. J. Atkinson, M. C. Dinauer, and D. A. Williams. 1999. Deficiency of the hematopoietic cell-specific Rho family GTPase Rac2 is characterized by abnormalities in neutrophil function and host defense. *Immunity* 10:183-196.

62. Knaus, U. G., P. G. Heyworth, T. Evans, J. T. Curnutte, and G. M. Bokoch. 1991. Regulation of phagocyte oxygen radical production by the GTP-binding protein Rac 2. *Science* 254:1512-1515.
63. Sun, C. X., G. P. Downey, F. Zhu, A. L. Koh, H. Thang, and M. Glogauer. 2004. Rac1 is the small GTPase responsible for regulating the neutrophil chemotaxis compass. *Blood* 104:3758-3765.
64. Weiss-Haljiti, C., C. Pasquali, H. Ji, C. Gillieron, C. Chabert, M. L. Curchod, E. Hirsch, A. J. Ridley, R. Hooft van Huijsduijnen, M. Camps, and C. Rommel. 2004. Involvement of phosphoinositide 3-kinase gamma, Rac, and PAK signaling in chemokine-induced macrophage migration. *J Biol Chem* 279:43273-43284.
65. Filippi, M. D., C. E. Harris, J. Meller, Y. Gu, Y. Zheng, and D. A. Williams. 2004. Localization of Rac2 via the C terminus and aspartic acid 150 specifies superoxide generation, actin polarity and chemotaxis in neutrophils. *Nat Immunol* 5:744-751.
66. O'Farrell, P. H. 1975. High resolution two-dimensional electrophoresis of proteins. *J Biol Chem* 250:4007-4021.
67. Fessler, M. B., K. C. Malcolm, M. W. Duncan, and G. S. Worthen. 2002. A genomic and proteomic analysis of activation of the human neutrophil by lipopolysaccharide and its mediation by p38 mitogen-activated protein kinase. *J Biol Chem* 277:31291-31302.
68. Jones, G. E. 2000. Cellular signaling in macrophage migration and chemotaxis. *J Leukoc Biol* 68:593-602.
69. Nebl, T., K. N. Pestonjamasp, J. D. Leszyk, J. L. Crowley, S. W. Oh, and E. J. Luna. 2002. Proteomic analysis of a detergent-resistant membrane skeleton from neutrophil plasma membranes. *J Biol Chem* 277:43399-43409.
70. Lominadze, G., D. W. Powell, G. C. Luerman, A. J. Link, R. A. Ward, and K. R. McLeish. 2005. Proteomic analysis of human neutrophil granules. *Mol Cell Proteomics* 4:1503-1521.
71. Malacombe, M., M. F. Bader, and S. Gasman. 2006. Exocytosis in neuroendocrine cells: new tasks for actin. *Biochim Biophys Acta* 1763:1175-1183.
72. Valentijn, K., J. A. Valentijn, and J. D. Jamieson. 1999. Role of actin in regulated exocytosis and compensatory membrane retrieval: insights from an old acquaintance. *Biochem Biophys Res Commun* 266:652-661.
73. Norman, J. C., L. S. Price, A. J. Ridley, A. Hall, and A. Koffer. 1994. Actin filament organization in activated mast cells is regulated by heterotrimeric and small GTP-binding proteins. *J Cell Biol* 126:1005-1015.
74. Muallem, S., K. Kwiatkowska, X. Xu, and H. L. Yin. 1995. Actin filament disassembly is a sufficient final trigger for exocytosis in nonexcitable cells. *J Cell Biol* 128:589-598.
75. Downey, G. P., E. L. Elson, B. Schwab, 3rd, S. C. Erzurum, S. K. Young, and G. S. Worthen. 1991. Biophysical properties and microfilament assembly in neutrophils: modulation by cyclic AMP. *J Cell Biol* 114:1179-1190.
76. Affolter, M., and C. J. Weijer. 2005. Signaling to cytoskeletal dynamics during chemotaxis. *Dev Cell* 9:19-34.
77. Xu, J., F. Wang, A. Van Keymeulen, P. Herzmark, A. Straight, K. Kelly, Y. Takuwa, N. Sugimoto, T. Mitchison, and H. R. Bourne. 2003. Divergent signals

and cytoskeletal assemblies regulate self-organizing polarity in neutrophils. *Cell* 114:201-214.

78. Jog, N. R., M. J. Rane, G. Lominadze, G. C. Luerman, R. A. Ward, and K. R. McLeish. 2007. The actin cytoskeleton regulates exocytosis of all neutrophil granule subsets. *Am J Physiol Cell Physiol* 292:C1690-1700.
79. Bokoch, G. M. 2005. Regulation of innate immunity by Rho GTPases. *Trends Cell Biol* 15:163-171.
80. Lopez-Campistrous, A., P. Semchuk, L. Burke, T. Palmer-Stone, S. J. Brokx, G. Broderick, D. Bottorff, S. Bolch, J. H. Weiner, and M. J. Ellison. 2005. Localization, annotation, and comparison of the Escherichia coli K-12 proteome under two states of growth. *Mol Cell Proteomics* 4:1205-1209.
81. Lacy, P., S. Mahmudi-Azer, B. Bablitz, S. C. Hagen, J. R. Velazquez, S. F. Man, and R. Moqbel. 1999. Rapid mobilization of intracellularly stored RANTES in response to interferon-gamma in human eosinophils. *Blood* 94:23-32.
82. Benard, V., B. P. Bohl, and G. M. Bokoch. 1999. Characterization of rac and cdc42 activation in chemoattractant-stimulated human neutrophils using a novel assay for active GTPases. *J Biol Chem* 274:13198-13204.
83. Cooper, J. A., and T. D. Pollard. 1982. Methods to measure actin polymerization. *Methods Enzymol* 85 Pt B:182-210.
84. Isgandarova, S., L. Jones, D. Forsberg, A. Loncar, J. Dawson, K. Tedrick, and G. Eitzen. 2007. Stimulation of actin polymerization by vacuoles via Cdc42p-dependent signaling. *J Biol Chem* 282:30466-30475.
85. Lacy, P., D. Abdel-Latif, M. Steward, S. Musat-Marcu, S. F. Man, and R. Moqbel. 2003. Divergence of mechanisms regulating respiratory burst in blood and sputum eosinophils and neutrophils from atopic subjects. *J Immunol* 170:2670-2679.
86. Worthen, G. S., B. Schwab, 3rd, E. L. Elson, and G. P. Downey. 1989. Mechanics of stimulated neutrophils: cell stiffening induces retention in capillaries. *Science* 245:183-186.
87. Seely, A. J., J. L. Pascual, and N. V. Christou. 2003. Science review: Cell membrane expression (connectivity) regulates neutrophil delivery, function and clearance. *Crit Care* 7:291-307.
88. Logan, M. R., S. O. Odemuyiwa, and R. Moqbel. 2003. Understanding exocytosis in immune and inflammatory cells: the molecular basis of mediator secretion. *J Allergy Clin Immunol* 111:923-932; quiz 933.
89. Luo, X., K. A. Carlson, V. Wojna, R. Mayo, T. M. Biskup, J. Stoner, J. Anderson, H. E. Gendelman, and L. M. Melendez. 2003. Macrophage proteomic fingerprinting predicts HIV-1-associated cognitive impairment. *Neurology* 60:1931-1937.
90. Aulak, K. S., M. Miyagi, L. Yan, K. A. West, D. Massillon, J. W. Crabb, and D. J. Stuehr. 2001. Proteomic method identifies proteins nitrated in vivo during inflammatory challenge. *Proc Natl Acad Sci U S A* 98:12056-12061.
91. Kim, C., and M. C. Dinauer. 2001. Rac2 is an essential regulator of neutrophil nicotinamide adenine dinucleotide phosphate oxidase activation in response to specific signaling pathways. *J Immunol* 166:1223-1232.

92. Bentwood, B. J., and P. M. Henson. 1980. The sequential release of granule constitutents from human neutrophils. *J Immunol* 124:855-862.
93. Tannu, N. S., and S. E. Hemby. 2006. Two-dimensional fluorescence difference gel electrophoresis for comparative proteomics profiling. *Nat Protoc* 1:1732-1742.
94. Yan, M., R. F. Collins, S. Grinstein, and W. S. Trimble. 2005. Coronin-1 function is required for phagosome formation. *Mol Biol Cell* 16:3077-3087.
95. Yan, M., C. Di Ciano-Oliveira, S. Grinstein, and W. S. Trimble. 2007. Coronin function is required for chemotaxis and phagocytosis in human neutrophils. *J Immunol* 178:5769-5778.
96. Rybakin, V., and C. S. Clemen. 2005. Coronin proteins as multifunctional regulators of the cytoskeleton and membrane trafficking. *Bioessays* 27:625-632.
97. Merzendorfer, H., and L. Zimoch. 2003. Chitin metabolism in insects: structure, function and regulation of chitin synthases and chitinases. *J Exp Biol* 206:4393-4412.
98. Zhu, Z., T. Zheng, R. J. Homer, Y. K. Kim, N. Y. Chen, L. Cohn, Q. Hamid, and J. A. Elias. 2004. Acidic mammalian chitinase in asthmatic Th2 inflammation and IL-13 pathway activation. *Science* 304:1678-1682.
99. Volck, B., P. A. Price, J. S. Johansen, O. Sorensen, T. L. Benfield, H. J. Nielsen, J. Calafat, and N. Borregaard. 1998. YKL-40, a mammalian member of the chitinase family, is a matrix protein of specific granules in human neutrophils. *Proc Assoc Am Physicians* 110:351-360.
100. Huber, L. A. 2003. Is proteomics heading in the wrong direction? *Nat Rev Mol Cell Biol* 4:74-80.
101. Lang, T., I. Wacker, I. Wunderlich, A. Rohrbach, G. Giese, T. Soldati, and W. Almers. 2000. Role of actin cortex in the subplasmalemmal transport of secretory granules in PC-12 cells. *Biophys J* 78:2863-2877.
102. Jahraus, A., M. Egeberg, B. Hinner, A. Habermann, E. Sackman, A. Pralle, H. Faulstich, V. Rybin, H. Defacque, and G. Griffiths. 2001. ATP-dependent membrane assembly of F-actin facilitates membrane fusion. *Mol Biol Cell* 12:155-170.
103. Eitzen, G., L. Wang, N. Thorngren, and W. Wickner. 2002. Remodeling of organelle-bound actin is required for yeast vacuole fusion. *J Cell Biol* 158:669-679.
104. Gasman, S., S. Chasserot-Golaz, M. Malacombe, M. Way, and M. F. Bader. 2004. Regulated exocytosis in neuroendocrine cells: a role for subplasmalemmal Cdc42/N-WASP-induced actin filaments. *Mol Biol Cell* 15:520-531.
105. Yu, H. Y., and W. M. Bement. 2007. Control of local actin assembly by membrane fusion-dependent compartment mixing. *Nat Cell Biol* 9:149-159.
106. Glogauer, M., J. Hartwig, and T. Stossel. 2000. Two pathways through Cdc42 couple the N-formyl receptor to actin nucleation in permeabilized human neutrophils. *J Cell Biol* 150:785-796.
107. Cooper, J. A. 1987. Effects of cytochalasin and phalloidin on actin. *J Cell Biol* 105:1473-1478.
108. Showell, H. J., R. J. Freer, S. H. Zigmond, E. Schiffmann, S. Aswanikumar, B. Corcoran, and E. L. Becker. 1976. The structure-activity relations of synthetic

peptides as chemotactic factors and inducers of lysosomal secretion for neutrophils. *J Exp Med* 143:1154-1169.

109. Henson, P. M., B. Zanolari, N. A. Schwartzman, and S. R. Hong. 1978. Intracellular control of human neutrophil secretion. I. C5a-induced stimulus-specific desensitization and the effects of cytochalasin B. *J Immunol* 121:851-855.
110. Spector, I., N. R. Shochet, D. Blasberger, and Y. Kashman. 1989. Latrunculins--novel marine macrolides that disrupt microfilament organization and affect cell growth: I. Comparison with cytochalasin D. *Cell Motil Cytoskeleton* 13:127-144.
111. Bubb, M. R., A. M. Senderowicz, E. A. Sausville, K. L. Duncan, and E. D. Korn. 1994. Jasplakinolide, a cytotoxic natural product, induces actin polymerization and competitively inhibits the binding of phalloidin to F-actin. *J Biol Chem* 269:14869-14871.
112. Gao, Y., J. B. Dickerson, F. Guo, J. Zheng, and Y. Zheng. 2004. Rational design and characterization of a Rac GTPase-specific small molecule inhibitor. *Proc Natl Acad Sci U S A* 101:7618-7623.
113. Cancelas, J. A., A. W. Lee, R. Prabhakar, K. F. Stringer, Y. Zheng, and D. A. Williams. 2005. Rac GTPases differentially integrate signals regulating hematopoietic stem cell localization. *Nat Med* 11:886-891.
114. Geijsen, N., S. van Delft, J. A. Raaijmakers, J. W. Lammers, J. G. Collard, L. Koenderman, and P. J. Coffer. 1999. Regulation of p21rac activation in human neutrophils. *Blood* 94:1121-1130.
115. Welch, H. C., A. M. Condliffe, L. J. Milne, G. J. Ferguson, K. Hill, L. M. Webb, K. Okkenhaug, W. J. Coadwell, S. R. Andrews, M. Thelen, G. E. Jones, P. T. Hawkins, and L. R. Stephens. 2005. P-Rex1 regulates neutrophil function. *Curr Biol* 15:1867-1873.
116. Uetrecht, A. C., and J. E. Bear. 2006. Coronins: the return of the crown. *Trends Cell Biol* 16:421-426.
117. Gatfield, J., I. Albrecht, B. Zanolari, M. O. Steinmetz, and J. Pieters. 2005. Association of the leukocyte plasma membrane with the actin cytoskeleton through coiled coil-mediated trimeric coronin 1 molecules. *Mol Biol Cell* 16:2786-2798.
118. Itoh, S., K. Suzuki, J. Nishihata, M. Iwasa, T. Oku, S. Nakajin, W. M. Nauseef, and S. Toyoshima. 2002. The role of protein kinase C in the transient association of p57, a coronin family actin-binding protein, with phagosomes. *Biol Pharm Bull* 25:837-844.
119. Abdel-Latif, D., M. Steward, and P. Lacy. 2005. Neutrophil primary granule release and maximal superoxide generation depend on Rac2 in a common signalling pathway. *Can J Physiol Pharmacol* 83:69-75.
120. Grogan, A., E. Reeves, N. Keep, F. Wientjes, N. F. Totty, A. L. Burlingame, J. J. Hsuan, and A. W. Segal. 1997. Cytosolic phox proteins interact with and regulate the assembly of coronin in neutrophils. *J Cell Sci* 110 (Pt 24):3071-3081.
121. Rizoli, S. B., O. D. Rotstein, J. Parodo, M. J. Phillips, and A. Kapus. 2000. Hypertonic inhibition of exocytosis in neutrophils: central role for osmotic actin skeleton remodeling. *Am J Physiol Cell Physiol* 279:C619-633.
122. Hong-Geller, E., D. Holowka, R. P. Siraganian, B. Baird, and R. A. Cerione. 2001. Activated Cdc42/Rac reconstitutes Fcepsilon RI-mediated Ca2+

mobilization and degranulation in mutant RBL mast cells. *Proc Natl Acad Sci U S A* 98:1154-1159.

123. Godovac-Zimmermann, J., O. Kleiner, L. R. Brown, and A. K. Drukier. 2005. Perspectives in spicing up proteomics with splicing. *Proteomics* 5:699-709.
124. Gygi, S. P., G. L. Corthals, Y. Zhang, Y. Rochon, and R. Aebersold. 2000. Evaluation of two-dimensional gel electrophoresis-based proteome analysis technology. *Proc Natl Acad Sci U S A* 97:9390-9395.
125. Wolters, D. A., M. P. Washburn, and J. R. Yates, 3rd. 2001. An automated multidimensional protein identification technology for shotgun proteomics. *Anal Chem* 73:5683-5690.
126. Washburn, M. P., D. Wolters, and J. R. Yates, 3rd. 2001. Large-scale analysis of the yeast proteome by multidimensional protein identification technology. *Nat Biotechnol* 19:242-247.
127. Pollard, T. D., and C. C. Beltzner. 2002. Structure and function of the Arp2/3 complex. *Curr Opin Struct Biol* 12:768-774.